KU LEUVEN

ARENBERG DOCTORAL SCHOOL
Faculty of Engineering Science

Short and Long Term Optimal Operation and Robustness Analysis of a Hybrid Ground Coupled Heat Pump System with Model Predictive Control

Stefan Antonov

Supervisor:
Prof. dr. ir. Lieve Helsen

Dissertation presented in partial fulfillment
of the requirements for the degree
of Doctor of Engineering Science (PhD):
Mechanical Engineering

July 2016

Short and Long Term Optimal Operation and Robustness Analysis of a Hybrid Ground Coupled Heat Pump System with Model Predictive Control

Stefan ANTONOV

Examination committee:
Prof. dr. ir. Hugo Hens, chair
Prof. dr. ir. Lieve Helsen, supervisor
Prof. dr. ir. Goele Pipeleers
Prof. dr. ir. Joris De Schutter
Prof. dr. Jeffrey Spitler
(Oklahoma, USA)
Prof. dr. Gerd Vandersteen
(Brussels, Belgium)
Dr. Signhild Gehlin
(Lund, Sweden)

Dissertation presented in partial fulfillment of the requirements for the degree of Doctor of Engineering Science (PhD): Mechanical Engineering

July 2016

"Every instance of patience
is sooner or later awarded."
Pavel Antonov

Preface

People are most important in life, in my opinion!

Some might expect that the long paragraphs follow, yet in that PhD text, mentioning all people involved in all these past years, person by person, with few-words-summaries of why the author acknowledges them. Well, that's almost true. I acknowledge you because this is my PhD text and all of you are part of my life, for good or for better ☺, and I would like to have your names here each next time I open this book myself and eventually when you open it too ☺.

I have spent six great years on my doctoral program and I am grateful for three main reasons: for the things you have done for me, for the things we have done together and for all things I had the chance to learn about people, about life, about the world,... as well as about hybrid ground coupled heat pump systems, optimization based control and robustness 😄, since I learned that while spending six years in a valuable environment of good, smart, and bright people.

First, I would gladly like to thank my supervisor. Lieve, I am grateful for your unique liberal supervision approach. Supervising tightly gives more guarantee for success but less opportunity for self development. I am very happy I had the chance to be supervised liberally. There were periods where I questioned my chance for success but I also had the chance to find the way and to reach success while developing myself. Such approach I find strategic on the long-term in both work related and life related aspects. You provided a supervision with a general attitude to life, which includes accent on work and respects that there is more to life as well. I am grateful for your understanding in personal occasions of good or bad, for your support and for sharing joy. Thank you for your analytical and constructive approach to situations and problems! You are the person who showed me what "suggestions for improvements" are, instead of "corrections", and showed me that this new for me term is not only a diplomatically smoothened version, but has a constructive and positive meaning. Thank you for motivating me, for your important, honest and constructive

feedback many times, for your detailed and constructive reviews of scientific texts and for your consistent and timely emailing! Thank you for providing me the opportunity to be part of your research group!

Honest gratitude I also express to all members of my Examination committee. Thank you all for evaluating my dissertation with attention and dedication! I highly appreciated your detailed feedback and further discussions, which I found meaningful, to the point, constructive and enriching my dissertation. I am grateful for your input and I really enjoyed applying your suggestions for improvement.

In the course of my research I passed through difficult periods. Prof. Moritz Diehl, Prof. Goele Pipeleers, and Prof. Tine Baelmans, the fruitful discussions with you during those times were of great value and determinant importance. Thank you for your expertise and contribution!

While doing research on heat pump systems I was often motivated by the examples of Prof. Wim Boydens for implementations in practice. Wim, thank you for your friendly attitude, for the inspiring conversations during conferences and for organizing the seminar on the occasion of my preliminary defense!

I would like to acknowledge the institutions funding my doctoral program. My research work is framed within the research project entitled "Black-box model based predictive control of ground coupled heat-pump systems", funded by the Research Foundation Flanders (FWO); the follow-up being funded by the KU Leuven, Department of Mechanical Engineering, Division of Applied Mechanics and Energy Conversion.

I have now the pleasure to look back in time and recall for a moment what has happened during the last six years in the department besides doing research and to whom I should send the credits for a large variety of collected memories. Dear colleagues and friends from KU Leuven, thank you for... let me see:

Ruben and Nico, for guiding my first steps in the TME society and for being my ultimate example for a high level of perfection in practical and technical issues like writing scientific texts or preparing vector graphics! Ruben, thanks also for your performance on several pleasant concerts, for being a good friend who cares, and for showing me what is good whiskey 😎! Clara, for introducing me to The SySi society and to our wonderful research field! Btw, still some borefield mysteries to unveil 😄. Griet Monteyne, for looking over my time domain challenges from a frequency domain point of view! Asim, Vladimir, Sara, Peng Wu and Eric Zhong, for the nice bicycle trips, so I discovered Flanders for the first time! Frederic Rogiers, for several nice chats about things of life! Tijs, for always giving examples how to ask good questions! Jan Hoogmartens, for showing me how difficult tasks at work can be tackled calm,

straightforward and efficiently! Maarten Sourbron, for discovering together with what amount to appreciate the service in Canadian bars! Mats, for being the most enthusiastic SySi to understand fine details about my robustness research! Anouk, for sharing a recipe for an easy to make and delicious chocomousse cake! Shijie, for being a loyal student in my driving classes! Frederic Cuypers, Jan Timmermans, Yannic, Tom, for cheering up the gang during noisy LAN parties! Jay, for appreciating the fact that everybody is allowed to read the menu! Cornelia, Emre, Asim and Jay, for hilarious Optec retreat dinner chats! Daniël, for pranking me that successfully that in the end you made me unconsciously prank myself, while thinking that you are again going to prank me! Juliana, for regularly taking care of the flora in our office, so that I re-potted all the baby-plants of the results of your effort, so now it is a jungle there! Roel, voor het met mij meestal in het Nederlands te spreken! Wouter, for showing me how extremely difficult tasks at work can be tackled absolutely calmly in deep details and endless productivity! Joachim, for showing me speed-of-light multiplexing of several software tools while working with them simultaneously! Lieven, for being a very vivid officemate for a while and for encouraging me in the middle of my thesis writing phase! Darin, for the super cool chance to have a Bulgarian office mate in Belgium! Bart Saerens, for teaching me how to burn even less fuel while driving! Maarten Vanierschot, for your hints and tips about jogging! Jeroen, Joris Gillis and Daniël, for the crazy time spent on organizing our edition of the TME Weekend! Joris, thanks also for a memorable kayaking in somewhat more rapid rivers in Wallonie! Maarten Blomaert, thanks that it has never been boring around you! Vahid! Good friend of mine! (Written in golden ink!) Thanks for your joyful mood, for discussing things of life many times and for always sharing the left or right half of a chair at TME treats! Arnaut, for showing me the fastest way ever to get awarded with The SySi Cup! Edorta, for raising our state of charge with delicious cheese, meat and wine from your home! Joris Codde, for the chats on psychology, our common hobby! Ercan, for optimally giving me optimal advices in so many optimal control problems! Bram, for playing brilliant music at the concerts of his orchestra! Geert, for taking care for Pux'n'Kux and for your humor! Damien, for discovering America together by air, by land, and by sea! Dieter! Alma time! We leave at 12 ☺! You have a meal on me to thank you for your initiative for all the lunch invitations! Filip, for a nice motorbike trip around nearest Wallonie! Kenneth and Kenneth, thanks for being great examples for decisive, influential, and successful Belgian men! Andreas, for frequently opening the window to ventilate our six-desk office! Bart Peremans, for accepting to take over my office green thumb responsibility for caring for the office plants! Sarah, for showing me how to use two machines for making one coffee! Igor, for the variety of Balkan-inspired joyful chats and for giving me the opportunity to practice jump-starting diesel engines! Nicolas, for being the plasma expert who

is actively following the thermal systems in buildings! Dries, Kristel, Sepide, Kris, Pieter, Muhannad, Dejian and Niels, for your company in the cafeteria for mind resetting towards further work! Sarah, Bart Peremans, Thomas, Paul, Mathias, Xu, Yang, and Liang, for organizing my ultimate TME Weekend with crazy kayaking! Thanasi, Wim, Gorje, Noe and Vahid, for unforgettable fun time while the moon was shining over the center of Leuven! Heidi, Laura and Anna, for having fun together, so we inspired all the colleagues join a flash mob for Juliana! Mathew, for showing me how to pronounce "Arkansas"! Max, for your smiling social attitude and delicious cheese and wine! Keivan, for impressing me with taking good photographs! Laurens and Dries, for the fun time together with all colleagues when we pumped up the jam on a newcomers reception! Dora, for all the chats on a cup of tee, sharing things of life and research! Sergio, for teaching my first DJ class! Ione, Andrea, Lucie and Enea, for rocking the karaoke in Oudemarkt! Simona, for your nice company at all three places: the department, the city center and the dance floor! Maria, for your cheerful friendliness y para el español que hemos hablado en la universidad! Vule, for the entertaining chats about astronomy and things of science(fiction)! Mari-Mo, for often passing by to invite me in the group for lunch! Axel and Sofie, for all the smiling conversations in the breaks and for exchanging birthday treat invitations! Jelena, for sharing extreme sport dreams which either came true or queue up in the ToDo! Christina, for your relaxing company at lunch in Alma! Ruben Baetens, for being such a good goal keeper that I never dared to strike a gitpush!

Thanks to The SySi's for all scientific and sportive activities we've had together! Thanks to all members of the TME Wednesday lunch group, the TFSO lunch group, and the PMA-BMe-CIB lunch group for always waiting for me to slowly finish my meal at Alma! Thanks to the Happy Hour organizing team and to the Happy Hour drinking team for all the funny Friday evenings!

Doing research in TME wouldn't have been as perspective and enriching if not being governed by the diverse and valuable professorship in the division. Dear professors, thank you for your efforts and dedication! Alessia, thank you for your friendliness! Erik Delarue, for being my ultimate example for an always widely smiling person with positive attitude to life and substantial efficiency at work! Johan, for your consistent presence and critical questions at division meetings! Tine, for your examples for fast thinking and overwhelming energy for efficient work! William, for your examples for principles and discipline, and your awesome speeches at TME Christmas parties and New Year's happenings.

Two great persons I also have respected very much; however, I wasn't as fast with my PhD as to be able to acknowledge them during their lifetime. I am proud that I knew them. I will remember the great mind of Eric Van den Bulck and the remarkable spirit of Theo Van der Waeteren!

Valérie, Marina, Lieve Notré, Karin, Anja, Regine, Carine, Marijke, Kathleen, Elise and Frieda, thank you all for processing the administration always with readiness and smile! Valérie, also thanks for your cool movie advises; Frieda, for trusting me to be the TME mailman for two weeks; and Lieve Notré, for all the extra broodjes! Ivo en Hans, veel bedankt voor al jullie zalige grapjes en toffe barbecue's! Jan and Ronny, thank you for your hard work on the software, for keeping the system up and running and for rapidly processing all tickets! Jan, I also really enjoyed your unique humor and contribution to barbecues!

Writing a thesis has never been such a pleasure when it comes to the software tools used and has never reached such nice results as when writing in LaTeX. Though, this approach might be tough sometimes. Thanks to the developers of the KU Leuven PhD LaTeX template, who made this process so easy!

I would also like to acknowledge the people from four services, who rarely receive the desired appreciation for their efforts, whereas doing a PhD in KU Leuven is much facilitated by them. People from the Acco team, the Alma team, the Velo team and the Cleaning team, thank you for providing your services!

Besides work there is free time. And it better be like that or there is something wrong at work. I rather took a while for my PhD but I am happy I never stopped living during that time and I spent it full value. Here follows who was there to share all these moments of joy.

About seven years ago I was far from ready to take on my own such important initiative like beginning a doctoral program. That changed for good thanks to Denitza. Deni, I really don't believe I would have ever started my PhD without your positive influence. Supporting each other I certainly became confident to do that. I am grateful for having been together with you for long before and long after starting this great and challenging journey in science and world. Thank you for your company while meeting new people and discovering new cultures, places and experiences! Thank you for constantly giving me your examples for initiative, braveness and curiosity to challenge almost everything! Thank you *For all good times* !

All good times include also countless unforgettable stories with my closest friends in Leuven. If the cobble stones in downtown Leuven were able to speak, they would tell all these stories because if you come down to the river bet you gonna find some people who live...

Ivo, Eli, Mitko, Eva, Deni, Yana, Hrisi, Daro, Stoyan, Vesko, Jochen, Velina, Sasho, Nastya, Ceco, Vera, Cveti, Misho, Ceco Ivanov, Cveta, Vihren, Zvezden, Pepi, Mitko Petrov, Boyan, Vanya, Svetlyo, Ani, Nadya and more, my gratitude for the fun together is indescribable, so I wouldn't even try. I would only mention colorful shots, chocolate duners, silvery voices singing, folklore dance lessons, impressive knowledge on napkins, crowdy barbecues, energetic volleyball playing, chats on philosophy or politics, tasty lukanka, mindless rock'n'roll dancing, high trampoline jumping, explosive creativity, artistic nail polish, random motorbike trips, vivid guitar playing, tasty cigars, smoky whiskey, and whatever else keeping the smiles on our faces. Any doubt which of the above highlights are related to which person 😜? Then I would gladly clarify each time you ask me on a beer 🙂. Or on a shot 🙂. Or on a cocktail 😄. Or on a whiskey with a cigar 😎. Or on an ice cream 😇.

A dozen of fun people researching in Gasthuisberg were often main actors in the above listed innocent activities. Thanks all of you for spicing the friendship and the party atmosphere!

A couple of years ago I started discovering the numerous advantages and the great pleasure of social dancing. This new hobby of mine gave me a lot of positive energy. During dancing I have never thought of any problem, struggle, worry, and I never felt stress or pressure. On the contrary, I met wonderful people, created many great memories and discovered the euphoria of the Bulgarian horo's, the thrill of the Swing dances and the beauty of the Latino dances. I want to thank three big teams of dancers who were there to be part of that. Thanks to all people from the Bulgarian folklore dance club "Horo à Bruxelles", from the KU Leuven Swing-Rock classes and from "LeuvenSalsa!"

Moving to Belgium six years ago, I left all my friends to wait for me at home. Cani & Valya, Nedi & Borko, I surely wasn't the best PhD student but thanks to you I am the Best man. Twice! Thank you for creating nice reasons for me and Deni, the Made of honor (Twice!), to travel more to home and abroad, so we have spent unforgettable time together! Sasho, wrong estimation my friend: my doctorate has cost twelve times eating Shkembe chorba, instead of eight, as we planned! And I still owe you many of them! Nasso, hold on man! Soon there will be finally 660 cc more noise in the hills of home land. Plami, I've lost the count of all track laps and beer cans that I've skipped, but I'll make it up for that! All my high school buddies, volleyball and ski friends home, thanks for keeping me in your minds and now welcoming me back!

From what I have learned about people and life, I am completely sure that I should be really happy with having a great loving family! And I certainly am!

Mamo & Tate, for the sake of being self-dependent I didn't give you many opportunities to support me during my doctoral program. Despite that intention of mine, you anyway found many ways to support me and among them I mostly value your constant and consistent alertness to be aware of how I am doing and whether things are going all right. Anyhow, I am mostly grateful to you for something else that was happening before I started my PhD. Thank you for all those twenty five years of raising me, teaching me the best manners, giving me the most important skills and motivating me to study, learn, and develop myself, so that I was able to reach the point to begin my doctoral program and find out how to complete it!

Nikola, Sofi & Dido, there is no scientific degree which can get as valuable for six years as what you two have done during that time. My warm and kind appreciation, and all the best ahead! I wish to be closer to you in the future!

Lelo, have a look at page 118, there is yet another integral to read (7.30), really! A special one, though. Not only is it discrete. I wrote it, can you believe that?

My so kind grandparents baba Lena, baba Sofi & dyado Lyubo! Thank you for your fairy-tales in my childhood, your wise advises in my boyhood and your interest in my deeds later. Also for all your gifts selected with attention, for gathering the whole family at celebrations, and for the tasty food many times! Proudly having my name Stefan, I really wish I could have addressed hereby all these things to my other grandfather as well, from whom I have it! Nevertheless, I believe he already knew I will reach this point when he wished me good luck for his last time on my way to Sweden.

Cousins and relatives, past years I have been very quiet to you but frequently recalling all joyful and loud gatherings. I believe there is now quite some material collected by everybody in the meanwhile, which can add a nice flavor at future reunions.

Near the end of my research struggles some magic has led me to the right place at the right time and it has led someone else there as well. And we met each other with Stefana. Stef, you were there along the entire final year of my PhD. A small part of what I am grateful that you gave me was your warmth, care, attention, understanding, courage, support and hope which have created the harmony during that hard period. Deeply in my mind I'll keep believing there's something in you that is not from this planet and I hope someday you will show me that other world. I am grateful to your parents for bringing you to this world and to your family for all they did for you to be so endowed. For all the rest you have done for me and you keep doing I wish I can thank you every day!

For six long years I had many colleagues and I made many friends. There exists a statistical probability that I have occasionally skipped acknowledging some of you. In any undesired occurrence of such a critical incident I kindly ask the affected to indicate my mistake, so that together we can further diminish the consequences in a collaboration for experimentally determining the volumetric concentration of ethanol in internationally appreciated liquid substances 😇. But before, please let me share what I did about hybrid ground coupled heat pump systems, optimization based control and robustness...

Stefan

Abstract

In the strive against climate change the reduction of anthropogenic greenhouse gas emissions is a key factor. The building sector is the largest consumer of primary energy which comes mainly from burning fossil fuels. The main share of buildings energy demand is represented by space heating and cooling. For this reason, improving buildings heating and cooling systems efficiency is one of the most effective ways towards sustainability.

Ground Coupled Heat Pump (GCHP) systems in the majority of cases are the most efficient systems for heating and cooling of buildings. However, the high installation cost and the associated long payback period for such systems prevent them from being widely installed. Introducing Hybrid Ground Coupled Heat Pump (HyGCHP) systems in combination with Model Predictive Control (MPC) substantially reduces this drawback.

The aim of this doctoral research is to find the optimal control strategy for a considered HyGCHP system with MPC and to guarantee its robustness to uncertainties.

For the purpose of this work an integrated dynamic model of the HyGCHP system is composed, based on models of the system components—building, Borehole Heat Exchanger (BHE), primary heating and cooling devices (heat pump and ground coupled passive cooling heat exchanger) and supplementary devices (gas boiler and air coupled active chiller). The system operation is controlled by means of an optimization problem including short-term objectives—achieving desired thermal comfort by minimized system operation cost. The optimization problem is solved for a time horizon of one year with imposing cyclic boundary conditions on the ground node temperatures to incorporate long-term objectives—thermal balance of the ground for unbalanced heating and cooling loads—integrated with the short-term objectives.

The optimization problem is also solved for shorter time horizon and without cyclic boundary conditions with two intentions: (1) to see in what conditions

the long-term optimal operation profile can be reproduced with a more realistic short-term control strategy; (2) to analyze whether in the long-term optimal solution the ground is exploited for Seasonal Underground Thermal Energy Storage (SUTES) or as a heat source/sink.

Robustness analysis for state estimation uncertainty in the case of a HyGCHP system is performed for the most commonly used short-term MPC strategy for heating and cooling systems in buildings (prediction horizon of one day, sampling time of one hour and control horizon of one time step). For that purpose an existing off-line method for robustness analysis is reproduced and clarified, then extended and applied to the HyGCHP system with MPC.

This dissertation presents the integrated short-and-long-term optimization approach to analyze HyGCHP system operation, the short-term MPC strategy to reproduce the long-term optimal system operation profiles, and the extended robustness analysis method applied to the HyGCHP system with state estimation uncertainty in the MPC.

The results show that the integrated short-and-long-term optimal operation profile with cyclic ground temperatures compensates the cooling dominated loads by annually mean ground node temperatures higher than the undisturbed ground temperature. The cooling dominated loads are mostly covered by passive cooling up to hitting the upper bound on the outlet BHE fluid temperature. The remaining peak cooling loads are covered by the chiller. On the short term a weekly optimal strategy reproduces the long-term optimal annual profiles. For a single BHE this leads to the conclusion that because of high thermal dissipation the ground is not used as a thermal storage medium on the long term but as a heat source/sink on the short term. For the investigated borefield this conclusion changes. For realistically low ground thermal conductivity the optimal system operation includes using the borefield as a seasonal thermal storage medium on the annual term.

The results for maximum allowed state estimation uncertainty computed with the robustness analysis method correspond to the performed HyGCHP system simulations with MPC. In conclusion, the method gives a reliable estimation of the maximum allowed state estimation uncertainty for guaranteed robustness.

Improving HyGCHP systems with MPC can continue in two directions. First, towards investigating the SUTES ability of systems with other borefield drilling configurations: More compact borefields of more BHEs are expected to more efficiently operate as seasonal thermal energy storage mediums. This would enable SUTES in cases with higher ground thermal conductivities, which is an opportunity of wider HyGCHP system applications. Second, the efficient implementation of optimal SUTES in short-term MPC is an important direction.

The improved exposition of the robustness analysis method and the developed subsidiary method for application of the robustness analysis to the investigated HyGCHP system with MPC represent a fast offline computation to check and guarantee system robustness to state estimation uncertainty. The developed framework enables determining key boundary conditions for further system design and control, like temperature estimation accuracy, model accuracy, and MPC prediction horizon length. HyGCHP systems of the type presented in this dissertation which are characterized by bounded uncertainties can be controlled by conventional MPC provided that the level of the incorporated uncertainties is not higher than the guaranteed level computed using the presented method.

Beknopte samenvatting

In de strijd tegen de klimaatsverandering is het verminderen van antropogene broeikasgassen essentieel. De gebouwensector vertegenwoordigt het hoogste primair energiegebruik, voornamelijk gevoed door fossiele brandstoffen. Het grootste deel van de energievraag in gebouwen gaat naar verwarmen en koelen. Om deze reden is het verbeteren van de efficiëntie in verwarming- en koelsystemen een van de meest effectieve paden naar duurzaamheid.

Grondgekoppelde warmtepomp (GGWP) systemen in de meeste gevallen zijn de meest efficiënte systemen voor verwarming en koeling. Echter, de hoge investeringskost en bijhorende lange terugbetalingstermijn verhinderen een wijdverspreide installatie van deze systemen. Het introduceren van hybride grondgekoppelde warmtepomp (HyGGWP) systemen in combinatie met modelgebaseerde voorspellende regeling (MPC) vermindert dit nadeel aanzienlijk.

Het doel van dit doctoraat is een optimale regelstrategie te vinden voor een bepaald HyGGWP systeem met MPC en om de robuustheid van deze regelaar aan te tonen tegenover onzekerheden.

Met dit doel voor ogen is een geïntegreerd dynamisch model samengesteld van HyGGWP systemen, gebaseerd op modellen van de verschillende componenten: gebouw, boorputwarmtewisselaar (BHE), primaire verwarming- en koelsystemen (warmtepomp en passieve koeling via BHE) en supplementaire systemen (gasketel en actieve koeler). De aansturing van het systeem gebeurt door middel van een optimalisatieprobleem met objectieven op korte termijn tot het verkrijgen van thermisch comfort aan een minimale operationele kost. Het optimalisatieprobleem wordt opgelost voor een termijn van één jaar met cyclische randvoorwaarden op de bodemtemperatuur om het lange termijn objectief (thermische balans van de bodem voor ongebalanceerde last) te integreren met deze korte termijn doelstellingen.

Het optimalisatieprobleem wordt ook opgelost voor kortere termijnen, zonder

cyclische randvoorwaarde, met twee doelen voor ogen: (1) identificeren onder welke condities het lange termijn objectief gereproduceerd kan worden met een meer realistische korte termijn strategie; (2) analyseren of de lange termijn optimale oplossing inzet op thermische seizoensopslag (SUTES) of eerder op warmtedissipatie.

De robuustheid tegenover onzekerheid op de toestandsschatting in het geval van een HyGGWP wordt geanalyseerd voor de meest gebruikelijke korte termijn MPC strategie voor verwarming- en koelsystemen in gebouwen (voorspellingshorizon van één dag, tijdstap van één uur en controlehorizon van één uur). Hiertoe wordt de bestaande offline methode voor robuustheidsanalyse gereproduceerd en verduidelijkt, om uiteindelijk uitgebreid en toegepast te worden op het HyGGWP systeem met MPC.

Dit doctoraat presenteert de geïntegreerde korte en lange termijn optimalisatieaanpak voor HyGGWP operationele systeemanalyse, de korte termijn MPC strategie om de lange termijn optimale profielen te reproduceren en een uitgebreide robuustheidsanalyse toegepast op de HyGGWP met onzekerheid op de toestandsschatting in de MPC.

De resultaten tonen aan dat het geïntegreerde korte en lange termijn operationeel profiel met cyclische randvoorwaarden compenseert voor de koeling-gedomineerde last, door de jaarlijks gemiddelde bodemtemperatuur te verhogen. Deze koellasten worden meestal gedekt door passieve koeling tot de bovenste grens voor de uitlaattemperatuur van het boorveld bereikt wordt. De overblijvende piek in koelvraag wordt gedekt via de actieve koeler. Op korte termijn wordt dit gereproduceerd door een wekelijkse optimale regelstrategie. Voor een enkele BHE leidt dit tot de conclusie dat, door de hoge warmtedissipatie, de bodem niet gebruikt wordt voor lange termijnopslag maar eerder als warmtedissipator op korte termijn. Voor het bestudeerde boorveld (bestaande uit meerdere boorputten) wordt een ander resultaat bekomen: voor realistisch lage thermische geleidbaarheid van de grond maakt de optimale systeemregeling op jaarlijkse basis gebruik van het boorveld als seizoensopslag.

De resultaten voor de maximaal toegelaten onzekerheid op de toestandsschatting bekomen met de robuustheidsanalyse komen overeen met de uitgevoerde simulaties van de HyGGWP met MPC. De methode geeft een betrouwbare schatting van de maximaal toegestane onzekerheid op de toestandsschatting voor een gegarandeerde robuustheid.

Het verbeteren van HyGGWP met MPC kan verdergezet worden in twee richtingen. Ten eerste kan de SUTES mogelijkheid met andere boorveldconfiguraties onderzocht worden. Meer compacte boorvelden met meer BHEs worden verwacht te leiden tot een efficiëntere uitbating als thermische seizoensopslag.

Dit zou SUTES ook uitbreiden tot toepassingen met een hogere thermische bodemgeleidbaarheid, wat op zijn beurt een opportuniteit is voor een bredere inzetbaarheid van HyGGWP systemen. Ten tweede vormt de efficiënte implementatie van optimale SUTES in korte termijn MPC strategieën een belangrijke onderzoeksrichting.

De verheldering van de robuustheidsanalysemethode en de bijhorende aanpak voor het bestudeerde HyGGWP systeem met MPC vormen een snelle offline berekening die toelaat de robuustheid tegenover onzekerheid op toestandsschatting te controleren en te garanderen. Het ontwikkelde kader laat toe de belangrijkste randvoorwaarden te bepalen voor ontwerp en regeling: nauwkeurigheid van temperatuurschatting, modelnauwkeurigheid en voorspellingshorizon van de MPC. HyGGWP systemen met beperkte onzekerheden kunnen robuust geregeld worden via een traditionele MPC wanneer deze onzekerheden niet hoger zijn dan een gegarandeerd niveau dat bepaald wordt via de voorgestelde robuustheidsanalysemethode.

Abbreviations

ANN	artificial neural network
BHE	borehole heat exchanger
CC	cooling curve
CCA	concrete core activation
CH	chiller
COP	coefficient of performance
CS	cold storing in the ground by rejecting heat to the ambient air
EER	energy efficiency ratio
ESC	extremum seeking control
GB	gas boiler
GCHP	ground coupled heat pump
HC	heating curve
HP	heat pump
HVAC	heating, ventilation and air-conditioning
HyGCHP	hybrid ground coupled heat pump
LMI	linear matrix inequality
LP	linear programming
MIMO	multiple input—multiple output
MPC	model predictive control
NLP	non-linear programming
NMPC	non-linear model predictive control

PC	passive cooling
QP	quadratic programming
RBC	rule-based control
RC	resistor-capacitor
SALTO	short and long term optimization
SISO	single input—single output
SPF	seasonal performance factor
SUTES	seasonal underground thermal energy storage

List of Symbols

A, B, C, D	state space model matrices
COP_{HP}	heat pump coefficient of performance
C_j	thermal capacity at borefield model node j
EER_{CH}	chiller energy efficiency ratio
$EER_{CH,critical}$	fictive chiller critical energy efficiency ratio
$EER_{CH,m}$	fictive chiller modified energy efficiency ratio
F_b	borefield loads scaling factor for integrating building model and borefield model
F_l	building loads scaling factor for integrating building model and BHE/borefield model
F_p	price representation factor for modifying the objective function
G	general purpose matrix
H_i	matrix representing in matrix form the objective function along a time horizon of length i
I	identity matrix
$J(\cdot)$	optimization objective function
K	general purpose matrix
L	general purpose matrix
M	subsidiary matrix allowing formulation of a lower bound of a particular objective function

N	prediction horizon length
P_0	terminal states weighting factor matrix
P_{CH}	chiller compressor electrical power
P_{HP}	heat pump compressor electrical power
P_{PC}	passive cooling circulation pump electrical power
Q	states weighting factor matrix
$\dot{Q}_{BF}$	thermal power of heat rejection to the borefield
$\dot{Q}_{BHE}$	thermal power of heat extraction from the BHE
$\dot{Q}_{Building}$	total thermal power of delivering heat to CCA
$\dot{Q}_{CH}$	active chiller cooling power
$\dot{Q}_{GB}$	gas boiler heating power
$\dot{Q}_{Ground}$	total thermal power of heat extraction from the ground
$\dot{Q}_{HP}$	heat pump heating power
$\dot{Q}'_{HP}$	heat pump power of heat extraction from source
$\dot{Q}_{INT}$	thermal power of internal heating gains
$\dot{Q}_{PC}$	passive cooling power
$\dot{Q}_{Primary,Gas}$	gas boiler power of primary energy use from fuel
$\dot{Q}_{SOL}$	thermal power of solar radiation gains
Q_i	matrix forming H_i, related to states weighting factors
R	inputs weighting factor matrix
$\mathbb{R}^d$	set of all real numbers of dimension d
R_i	matrix forming H_i, related to inputs weighting factors
R_j	thermal resistance at borefield model node j
R_p	modified inputs weighting factor matrix when switching from (7.26) to (7.30)
R_{th}	thermal resistance between supply water and CCA

T_{AMB}	ambient air temperature
$T_{BF,Out}$	borefield outlet fluid temperature
T_{CC}	concrete core temperature
$T_{Fluid,Mean}$	BHE mean fluid temperature
$T_{Fluid,Out}$	BHE outlet fluid temperature
$T_{F,Out,max}$	BHE maximal outlet fluid temperature
T_{GR}	undisturbed ground temperature
T_{VS}	ventilation supply temperature
T_{WI}	inside wall temperature
T_{WO}	outside wall temperature
T_{WS}	supply water temperature
$T_{WS,PC}$	temperature of passive cooling heat exchanger outlet fluid before entering chiller for further cooling
T_Z	zone air temperature
T_i	matrix forming H_i, related to state space model simulation
T_j	ground temperature at node j
T_{max}	upper thermal comfort bound acting on T_Z
T_{min}	lower thermal comfort bound acting on T_Z
U_i	objective function upper bound
V_j	state selection matrix
a	state estimation uncertainty
c_{el}	electricity price
c_{gas}	gas price
c_p	specific heat
$c_u(u(k))$	input constraints function
$f(\cdot)$	general purpose function

$g(\cdot)$	general purpose function
$h(\cdot)$	general purpose function
i	general purpose index
j	general purpose index
k	discrete time
l	dimension of model outputs vector
m	dimension of model inputs vector
$\dot{m}$	fluid mass flow rate
n	dimension of model states vector
p	general purpose vector
q	general purpose vector
r	general purpose index
t_s	sampling time
u	common notation for model inputs
v	general purpose vector
x	common notation for model states
$\hat{x}$	common notation for model states estimates
x^{sp}	model state setpoint
y	common notation for model outputs
z	general function argument
α_i	positive multipliers allowing feasibility of the LMI robustness condition
β_j	positive multipliers allowing feasibility of the LMI robustness condition
ΔT_{CS}	temperature difference across heat exchanger for cold storing in the ground by rejecting heat to the ambient air
ΔT_{PCHE}	temperature difference across passive cooling heat exchanger

ϵ	objective function decrease formulating robustness
ε	deviation of T_Z outside the thermal comfort bounds
η_{CS}	efficiency of heat exchanger for underground cold storing
η_{GB}	gas boiler efficiency
η_{PC}	passive cooling efficiency
λ	ground thermal conductivity
μ_j	positive multipliers allowing feasibility of the LMI robustness condition
$\Phi_{[i,j]}$	matrix formulating states-inputs vector along steps $k \in [i, j]$
Φ_j	matrix shifting with one step the states-inputs vector
Π_0	analogue to Π_1 for the case of the added extra step with horizon $i = 1$.
$\hat{\Pi}^M$	matrix formulating the lower bound of a particular objective function, see M
Π_i	matrix, which, based on objective function upper bound, formulates the inputs set containing the optimal inputs for time horizon of length i
$\hat{\Pi}_i$	analogue to Π_i when considering extended states-inputs vector and only accounting the estimated states
$\bar{\Pi}_i$	analogue to Π_i when considering extended states-inputs vector and only accounting the true states
$\hat{\Pi}_s$	matrix formulating the robustness criterion of objective function decrease
Ψ_j	matrix formulating the state estimation uncertainty model
τ_i	positive multipliers allowing feasibility of the LMI robustness condition

Contents

List of Figures

List of Tables

Chapter 1

Introduction

This chapter introduces the research presented in the current dissertation from a more general point of view to facilitate easier understanding by a broader audience and motivate the focus and goals. Introduction to more technical matter is provided locally at the start of the corresponding chapters. In the text below the context is sketched, to which the presented research is related. General introduction to heating and cooling systems in buildings is provided, and the related control methods are outlined. Gradually the motivation for the performed research is stated, followed by a description of the research approach and focus. An overview of the dissertation text finalizes this introductory chapter.

1.1 Context

Nature is known to be characterized by principles of balance and evolution, whereas humans, although being considered as part of nature, are mainly found to be permanently striving for progress and revolutionary development. Humans are rarely satisfied with their status. Instead, humans are satisfied with improving their status. Moreover, nowadays humans tend to strive even for an increasing rate of improvement, meaning that humans are satisfied with progressing exponentially (Bostrom, 2006; Kurzweil, 2004). So humans strive for more, generate more, produce more, pollute more and consequently it becomes inevitable to take responsible measures upon encountering the limitations of the surrounding environment—the Earth.

Among several factors limiting the exponential development of the civilization is the amount of anthropogenic CO_2 emissions which the Earth's atmosphere can tolerate without initiating a dramatic climate change. Anthropogenic CO_2 emissions are mainly caused by burning fossil fuels which represent above 80% of the energy sources for covering the world's energy demand (IEA, 2015). Reducing CO_2 emissions is directly related to increasing the energetic efficiency of the used technology besides using less C-intensive fuels or renewable energy sources. Governmental policies translate these incentives into directives (e.g. Energy Efficiency Directive (EU, 2012), Renewable Energy Directive (EU, 2009), etc.) and specific cost regulation mechanisms. Therefore, optimizing a technology's operation cost is related to optimizing technology's energetic efficiency, however the two concepts do not always correspond to the same environmental result depending on the effectiveness of cost-regulation mechanisms.

According to recent evaluations 40% of the primary energy use in Europe (GBPN, 2013), as well as in the USA (Hilliard et al., 2015) is addressed to the building sector. Indoor space heating and cooling has the largest share of this energy use for both commercial and residential buildings. This motivates the improvement of heating and cooling systems in buildings as one of the most substantial contributions to CO_2 emissions reduction.

1.2 Heating and cooling systems in buildings

Heating and cooling systems in buildings consist of three main parts: energy source/sink (electricity, fuel, heat storage medium, athmosphere, ground, lake, etc.); production system (installations which convert energy from the source to heat/cold and/or change the temperature of a heat carrier fluid, and distribute the heat/cold); and emission/absorption system (which delivers (or extracts) heat to (or from) the building).

Heat/cold production systems in buildings could be classified in three main groups based on the way of delivering heat/cold: (1) energy conversion based; (2) heat pumping based; (3) using "free" heat (waste heat, solar energy collection).

Energy conversion based heat production systems represent the least efficient way of heating. Examples are electrical heaters, local fuel fired boilers and old fashioned district heating (distributing hot steam produced into centralized fossil fuel plants). Modern 4^{th} generation district heating networks integrate low-temperature heat, cold, renewable energy sources, waste heat and multiple heat/cold injection points in the network. In the best case a modern condensing gas boiler could reach about 95% efficiency of converting fuel chemical energy into heat. Since electrical power plants have an average efficiency of about 40%

for converting primary energy (from fossil fuels) into electricity, the use of an electrical heater in the best case could not be even a half as efficient way to deliver heat from primary energy than using a modern gas boiler.

Heat pumping differs conceptually because a heat pump is a thermodynamical device which transfers heat from a medium with a lower temperature to a medium with a higher temperature by consuming electrical power. For example an air conditioner in heating mode (which is called a heat pump) could replace 2 parts of heat from the ambient air into the heated building by using 1 part of electrical energy to drive that process, which part during the process is converted to heat and also delivered to the building. Therefore 3 parts of heat are delivered to the building by using 1 part of electrical energy. The ratio of the thermal power of heating to the electrical power of consumption is called Coefficient of Performance (COP) of the heat pump and equals 3 in that case. Thus, compared to an electrical heater, a heat pump could be 3 times more efficient for delivering heat by consuming electricity. If the source medium of the heat pump is the ground the COP could reach the value of 6 in the heating season.

The third type of heat production systems in buildings is based on recycling of waste heat (e.g. from production processes) or collecting solar energy (e.g. by using solar collectors). Such systems require minimal costs for running the corresponding devices, whereas the heat is considered free. However, these systems have limited practical application due to topological or meteorological reasons.

Cold production systems in buildings could be classified in three main groups based on the way of rejecting building heat to an outdoor medium: (1) heat transfer based; (2) heat pumping based; (3) adsorption and absorption based.

Examples of the direct heat transfer based group are systems using cooling towers (combination of convective heat transfer and latent heat transfer—evaporation) and systems using passive heat exchangers to reject heat to mediums with lower temperature (underground soil, underground stored snow). For the case of a ground coupled passive cooling heat exchanger, the ratio of the thermal power of heat extraction from the building to the consumed electrical power could reach 12 in the cooling season.

Heat pumping based cooling systems (chillers, air conditioners) are similar to the heat pumping based heating systems, however, the electrical energy used is added to the medium of heat rejection, thus lost. The ratio of the thermal power of heat extraction from the building to the electrical power of consumption is called Energy Efficiency Ratio (EER). The EER of an air coupled chiller could reach the value of 4 in the cooling season.

Adsorption and absorption cooling systems are more complicated installations using external heat and hygroscopic effects to cool down air.

At building side it is also important what the type of the installed heat emission/absorption system is. Examples are: air based systems, radiators, ventiloconvectors, floor heating/cooling and Thermally Activated Building Systems (TABS). A type of TABS is Concrete Core Activation (CCA). CCA differs from floor heating/cooling in the construction characteristic that water circulation tubes are embedded in the deep structure of the concrete slab, instead of being incorporated in the surface layer on top of a thermal insulation base. This implies a much higher thermal inertia of the CCA system, which represents a thermal energy storage potential, giving opportunity for local heating/cooling load shifting during the day and electricity consumption peak shaving for increased system flexibility and more efficient operation. Because of their relatively large surface CCA and floor heating/cooling systems are ideally suited for low temperature heating and high temperature cooling, which allows higher flexibility and efficiency of the heat/cold production units.

Ground Coupled Heat Pump (GCHP) systems, also called Geothermal heat pump systems, extract and inject heat from and to the ground by means of vertical Borehole Heat Exchangers (BHEs). This way, the ground can be exploited as a heat source/sink or as a seasonal thermal energy storage medium, increasing the system performance in both heating and cooling regime.

Combining Geothermal heat pump systems with TABS form the so called GEOTABS concept (Helsen, 2016) and represent one of the most efficient heating and cooling systems for buildings. The high efficiency of the heating and cooling systems within the GEOTABS concept originates from three important system characteristics: (1) source temperature, (2) heat/cold emission system temperature, (3) and heat/cold emission system thermal inertia. In winter the ground is a heat source at a higher temperature compared to the ambient air and in summer it is a cold source with a lower temperature compared to the ambient air. These conditions contribute to a high COP of the heat pump and allows direct/passive cooling (very high efficiency). Due to TABS larger surface area compared to other heat/cold emission systems, TABS require lower temperature for heating and higher temperature for cooling. These conditions further contribute to a high COP of the heat pump and applicability of direct/passive cooling. The high thermal inertia of TABS represents a potential for thermal energy storage at building level, which offers flexibility in control aspect. With these characteristics GEOTABS represents the perfect match of all system components. Challenges for the achievement of GEOTABS' high efficiency potential are the optimal components integration and system control.

Either a single BHE can be used or a borefield of several BHEs installed

according to different drilling pattern designs. The major difference between a BHE and a borefield is that the BHEs within a borefield thermally interact with each other, which decreases the dissipation of heat between the borefield and the surrounding ground.

Hybrid Ground Coupled Heat Pump (HyGCHP) systems introduce a combination of heating/cooling production installations in order to increase system flexibility and decrease initial system installation costs by smaller sizing of the borefield. In the presented dissertation a HyGCHP design is considered, which combines primary heating and cooling devices (heat pump and ground coupled passive cooling heat exchanger) and supplementary heating and cooling devices (gas boiler and air coupled chiller). The primary devices are highly efficient, however, not capable of covering peak heating/cooling loads since this requires larger BHE designs, which are very expensive. For that reason the cheaper supplementary heating and cooling devices are additionally installed at much lower initial price, which can cover peak loads, however operating at lower efficiencies. The best strategy of controlling a flexible HyGCHP system is then crucial for competitive overall system efficiency and minimal operation cost.

1.3 Control of heating and cooling systems in buildings.

Control of heating and cooling systems in buildings follows the general development in control engineering reflected by practical implications for convenience of the installed heating and cooling systems. The diversity of the heating and cooling systems in buildings starts from On-Off control, developing through feedback and Rule-Based Control (RBC), reaching Model Predictive Control (MPC). In control theory a control system consists of a controller, which controls a plant (in the present case—the building). The controller acts by providing control inputs to the plant in order to achieve a certain quality of plant's control variable (for example room air temperature).

On-Off control is the simplest and most intuitive feedback control method, for which a control variable (e.g. room temperature) is kept around a setpoint by switching the heater on (or the cooler off) when the variable is below the setpoint, and switching the heater off (or the cooler on) when the variable is above the setpoint. In case of fast system dynamics high frequency oscillations will occur, which frequency is decreased by introducing hysteresis—a gap around the setpoint between different switch-on and switch-off points of the control variable. For very slow systems inverse hysteresis is applied—flipping the switch-on and the switch-off points. This control method is very easy to implement,

very stable and reliable, however resulting in non-smooth control variable profiles and not exploiting key characteristics of system flexibility.

Proportional feedback control (P-control) incorporates information about the dominating plant's dynamics. This results in a control input varying in a certain range from minimum to maximum. Additions to the P-controller also exist: PI-control (added integrative action for removing steady state offset), PID-control (added differential action to adapt the control action to the rate of deviation of the control variable). These controllers calculate the control input based on an error signal—the difference between the setpoint and the current control variable value. The error signal is passed to the controller's internal dynamic model, which computes the control input to compensate the error of the control variable. P-controllers result in a smooth profile of the control variable and more efficient system control performance. However they are still not exploiting all flexibilities of the plant, they need tuning and are not suited for hybrid systems.

In buildings, heating and cooling system performance in the case of a simple room temperature setpoint can be substantially improved by introducing the concept of variable setpoint temperature of the water supplied to the heat emission/absorption system. The idea is to compensate heat/cold loss from the building to the surroundings by adapting the supply water temperature setpoint to the ambient air temperature. This represents the so called Heating Curve (HC) and Cooling Curve (CC) method. The supply water temperature setpoint is a function of the running mean ambient air temperature for the past several days. Using HC/CC in combination with either On-Off, or P-control results in a substantial increase in system efficiency and indoor thermal comfort.

Perhaps the simplest way to control HyGCHP systems is to use RBC. Such approach is easy to implement for multi-scenario control strategy of a system comprising several heating/cooling devices. However, the composition of the number of exact rules to switch on and off or to proportionally control a particular device or a combination of such represents a difficulty. Basically there is no practical limitation on the number of implemented rules to compose a control strategy. The approach depends on the designer's know-how, creativity and skills to translate control performance of systems controlled with other techniques into rules for easy implementation. Drawback of this control method is that it comprises many parameters to tune and always results in a sub-optimal system performance.

MPC represents one of the ultimate control system types implemented also in building heating and cooling systems. The control method is based on incorporation of a dynamic model of the control plant (e.g. building) used to predict performance along future time horizons. Then mathematical

optimization methods are used to compute the solution to the control inputs such that the control variable follows an optimal trajectory. Major benefit of MPC is that the optimization problem is solved satisfying constraints on the control inputs, control variables (plant outputs) and states of the controller dynamic model. The solution is obtained such that an objective function is minimized (maximized), which can incorporate various or even multiple criteria for energy efficiency, cost efficiency, thermal comfort, etc. Satisfying constraints allows integration of several plant components models into an integrated plant model. In buildings, introducing MPC as an alternative to the conventional HC/CC based control of GCHP systems control methods has a potential for 20–40% cost savings and simultaneously better thermal comfort (Verhelst, 2012).

There exist two distinctive types of MPC approaches: regulation MPC and setpoint tracking MPC. In control theory the term "regulation" refers to control which acts to move all plant states to zero and to track the zero level. Unlike regulation, "Setpoint tracking" refers to control which sets selected plant states to their defined setpoints and tracks these setpoints. Since the mathematical optimization framework within MPC provides flexibility in determining the exact formulation, a variety of customized MPC approaches exists.

One of the practical issues of dynamic model based control methods is introducing uncertainty when re-initializing the model states at each control time step. In order to compute optimal control inputs to the plant for the next time step, in the underlying MPC optimization problem initial conditions for the model states should be provided according to the true values of the corresponding variables in the real plant. These corresponding true values are found either by measurement or by state estimation (in case a state cannot be measured methods exist to estimate the state value based on other measured plant states and outputs and the considered dynamic plant model). However state measurement and state estimation suffer from errors in practice and cause uncertain initialization of the controller model.

An important quality of a dynamic model based control method is robustness to uncertainties. A control system is robust if it retains satisfactory performance in the presence of bounded uncertainties. In the case of MPC two main approaches exist for dealing with uncertainty: robust MPC and robustness analysis of MPC. Robust MPC is a direct, explicit, online approach in which the new control inputs are computed based on incorporating information about the uncertainty within the optimization problem at each time step. On the contrary, robustness analysis is an indirect, implicit, off-line approach for evaluating a given MPC optimization formulation in order to conclude and guarantee the robustness of the system with MPC up to a given level of uncertainty.

1.4 Motivation

In most European countries office buildings require both heating and cooling to maintain the requested thermal comfort throughout the entire year. However, the building heating and cooling loads are usually not in balance. The question arises how to optimally operate the HyGCHP system such that a long-term sustainable ground storage operation is guaranteed, while thermal comfort is guaranteed at the lowest cost.

Optimizing the control of HyGCHP systems requires consideration of the building dynamics, to maintain thermal comfort, and the BHE dynamics, to evaluate the available heat extraction/injection capacity and to exploit seasonal underground thermal energy storage. For the implementation of MPC the question arises whether the optimization horizon should cover the inter-seasonal time scale to achieve optimal system operation.

Recent research on optimal control of GCHP focuses either on the short-term objectives (i.e. thermal comfort and short-term energy cost, making abstraction of the ground storage dynamics), or on the long-term objectives (i.e. ground thermal balance and annual energy cost, making abstraction of the building dynamics). However, both time scales are important. How they should be treated in the MPC framework is a question to be investigated.

For the investigated HyGCHP system with MPC, state estimation and disturbance prediction are highly uncertain, moreover, the system performance is highly sensitive to errors at these points. It has become popular to design control systems which perform explicit computations to assure robustness (e.g. min-max Robust MPC) but this framework is computationally demanding, therefore, not widely applied. The alternative approach of performing robustness analysis of an MPC controlled system is generally avoided due to complicated theoretical formulations, implicitness and conservativeness of the approach.

1.5 Objective

The main objective of this dissertation is to optimize the operation of HyGCHP systems on both short and long term using MPC with proven robustness. This allows a relevant contribution to increased energy efficiency and share of renewable energy sources in the building sector, on its turn leading to lower CO_2 emissions. The detailed objectives of this dissertation are outlined in Section 3.4 after presenting the state of the art in HyGCHP systems.

1.6 Contributions

An innovative methodology is developed, which allows optimization of the control strategy for HyGCHP systems. The methodology is applied to a particular case of HyGCHP system for different system parameters.

Optimization based control strategy is presented which combines the short- and the long-term objectives in a HyGCHP system. An optimization approach is developed, which integrates the thermal dynamics of both the building and the ground storage volume to find the characteristics of the optimal heating and cooling duties distribution over the heating/cooling devices in order to achieve annually periodic ground temperatures behavior while satisfying thermal comfort requirements with minimal system operation cost.

The optimal system operation, found by solving the optimization problem for a prediction horizon of one year, is compared to the operation obtained using MPC with a receding horizon of one week to conclude for the requirements to be set on a practically realistic control system which performs optimally on the multi-annual operation time scale.

In order to obtain a guarantee for the robustness of the investigated HyGCHP system with MPC, an existing framework for robustness analysis is reproduced and clarified, then extended and applied to this case to analyze robustness with respect to state estimation uncertainty. An approach is presented that uses the original robustness analysis method formulation, suggested for regulation MPC in order to analyze robustness for the investigated case of set point tracking MPC.

1.7 Chapters description

The objectives and research focus formulated lead to literature review, research activities and associated results that are presented in the following chapters.

Chapter 2 introduces more detailed background on some generally known methods and techniques used in this dissertation.

Chapter 3 updates with the current state of heating and cooling systems in buildings and provides an overview of the related literature concerning control and robustness. Based on the gaps in the achievements of the scientific community and the advances in recent research the objectives of this dissertation are translated into research questions.

Chapter 4 first describes the investigated HyGCHP system and the way it is modeled for the purposes of this research. Then a detailed derivation of the system simulation, optimization and control setup is presented. This setup is later used in Chapter 5. The setups in Chapter 6 and Chapter 7 incorporate some differences compared to the main setup, which are described locally in these two chapters.

Chapter 5 studies the integrated short-and-long-term optimal operation of the considered HyGCHP system for the case of a single BHE.

Chapter 6 investigates to what extent the conclusions in Chapter 5 change if the HyGCHP system comprises a borefield of thermally interacting BHEs.

Chapter 7 is dedicated to robustness analysis of the considered HyGCHP system with MPC with respect to state estimation uncertainty.

Chapter 8 summarizes the conclusions of this dissertation and marks some points for future research.

Chapter 2

Concepts

In this chapter theoretical background is provided on some common concepts used to develop the methodology for optimizing the HyGCHP system operation. First, the general idea of mathematical optimization is outlined. Further, MPC is explained in more mathematical details. Then System identification is explained, which is a framework for obtaining models of dynamical systems. The ideas about Regulation MPC and Setpoint tracking MPC are summarized, as well as a technique for using the regulation solution for the purpose of setpoint tracking by means of coordinate transformation of the system states and inputs. Finally, state measurement uncertainty and state estimation uncertainty are elaborated.

2.1 Mathematical optimization

"Optimization" has become a very popular term in daily life especially in the engineering world and when using it people mostly refer to "improving" something. More rarely they refer to one of the most disseminated definitions: "making something as fully perfect, functional and effective as possible." In mathematics optimization is defined as "selecting the best element, according to a certain criterion, out of some set of available alternatives." By following this definition "the optimum"—the result of optimization as a mathematical problem—is restricted to be only one and to be optimal. "More optimal," "most optimal," etc. are considered false terms.

A mathematical optimization problem is the problem of seeking extrema of

functions, subject to constraints. A formulation called Non-Linear Programming (NLP) (2.1) generalizes the cases of different types of objective functions, which can be linear or non-linear. The value of the objective function $f(z)$ is minimized by finding the right decision variables $z \in \mathbb{R}^d$, such that the equality constraints $g(z)$ and the inequality constraints $h(z)$ are satisfied.

$$\begin{aligned} \min_{z \in \mathbb{R}^d} \quad & f(z) \\ \text{s.t.} \quad & g(z) = 0 \\ & h(z) \geq 0 \end{aligned} \tag{2.1}$$

If the objective function and the constraints are affine functions the optimization problem is linear (2.2), also called Linear Programming (LP)

$$\begin{aligned} \min_{z \in \mathbb{R}^d} \quad & v^T z \\ \text{s.t.} \quad & Kz - p = 0 \\ & Lz - q \geq 0 \end{aligned} \tag{2.2}$$

If the objective function is linear-quadratic and the constraints are affine functions the optimization problem is quadratic (2.3), also called Quadratic Programming (QP)

$$\begin{aligned} \min_{z \in \mathbb{R}^d} \quad & v^T z + \frac{1}{2} z^T G z \\ \text{s.t.} \quad & Kz - p = 0 \\ & Lz - q \geq 0 \end{aligned} \tag{2.3}$$

Solutions to mathematical optimization problems are computed by using numerical solvers (e.g. Cplex by IBM, 2012).

2.2 Model predictive control

MPC is a control method based on a dynamic model of the plant to be controlled and iteratively solving a mathematical optimization problem to compute the optimal control inputs. Linear and quadratic optimization problems (Section 2.1)

within MPC formulations are nicely suited with discrete linear state space plant models.

A discrete linear state space model (2.4, 2.5) can be derived from differential equations describing the processes in the plant or by means of system identification (Section 2.3). Such model is characterized by a states vector $x \in \mathbb{R}^n$, an inputs vector $u \in \mathbb{R}^m$ and an outputs vector $y \in \mathbb{R}^l$

$$\begin{bmatrix} x_1(k+1) \\ x_2(k+1) \\ \vdots \\ x_n(k+1) \end{bmatrix} = A \begin{bmatrix} x_1(k) \\ x_2(k) \\ \vdots \\ x_n(k) \end{bmatrix} + B \begin{bmatrix} u_1(k) \\ u_2(k) \\ \vdots \\ u_m(k) \end{bmatrix} \tag{2.4}$$

$$\begin{bmatrix} y_1(k) \\ y_2(k) \\ \vdots \\ y_l(k) \end{bmatrix} = C \begin{bmatrix} x_1(k) \\ x_2(k) \\ \vdots \\ x_n(k) \end{bmatrix} + D \begin{bmatrix} u_1(k) \\ u_2(k) \\ \vdots \\ u_m(k) \end{bmatrix} \tag{2.5}$$

In each MPC time step the optimization problem represents optimization of the simulation performance of the dynamic processes based on the model along a prediction time horizon with length N. Criteria for optimality or performance indicators could be system operation cost, represented by the magnitude of the inputs u, and system performance, represented by the magnitude of the states x or outputs y. These criteria can be incorporated in the objective function of the optimization problem, whereas the discrete state space model simulation along the prediction horizon is incorporated in the equality constraints, (2.6). Decision variables are all states and inputs along the discrete time horizon. Initial conditions on the states vector are added to the constraints part.

$$\begin{aligned} \min_{x(k)\in\mathbb{R}^n, u(k)\in\mathbb{R}^m} \quad & \sum_{k=0}^{N-1} \Big(x(k+1)^T Q x(k+1) + u(k)^T R u(k) \Big) \\ \text{s.t.} \quad & \\ & x(k+1) = Ax(k) + Bu(k), \quad k = 0 \cdots N-1 \\ & x(0) = x \end{aligned} \tag{2.6}$$

After solving the optimization problem (2.6) in the current MPC iteration, the input vector values of the first time step in the prediction horizon are applied to the plant to be controlled. In the next time step the actual states of the plant (measured or estimated) are used to reinitialize the states vector in the optimization problem and the process repeats.

The MPC example presented above is one of the simplest MPC formulations, used to describe the control method. MPC is a whole scientific topic on its own and has been developed to a number of variants, additions, techniques, etc. For details the reader is redirected to (Rawlings and Mayne, 2009).

The major benefit of applying MPC is the presence of the constraints part, which is flexible for a variety of system designs. Also different and multiple criteria for control system performance and efficiency can be implemented in the objective function or also by means of additional equality and/or inequality constraints.

2.3 System identification

System identification represents the overall framework for obtaining a dynamic system model, including:

- generation of data set;
- selection of model type;
- selection of model structure;
- initialization of model parameter values;
- estimation of model parameters;
- validation of obtained model;
- repetition of steps above;
- selection of final model.

The system identification data set could be either composed of real plant measurement data or generated by detailed plant emulator simulations, where advanced software tools are used.

Three main types of models are distinguished: white-box, gray-box, and black-box. White-box models are based on physical first principles describing the processes in the plant and such models require only validation (after assigning values to the physical parameters). Black-box models are based on unified dynamic mathematical representations linking model outputs to model inputs via intermediate dependencies of states, which do not have a physical meaning. The mathematical formulations of such models are parameterized and the model parameters are subject of estimation. Gray-box models represent a

hybrid concept between the first two—inspired by first principles the physical parameters are subject to further estimation. This way model structure and parameter ranges are defined and the resulting model states do have a physical meaning, although they can not always be measured since they usually lump multiple processes.

Selection of model structure is relevant to gray-box and black-box models at which stage it is decided on the complexity of the model or on which plant processes will be represented by the model and which ignored.

Parameter estimation is a major part of the System identification process. At this stage optimization problems are solved (Section 2.1) in order to find optimal parameter values which determine the best fit of model simulated data to system identification data. Usually, modeling of real systems results in mathematical formulations comprising multiplication of model parameters. These, as well as other sources of nonlinearities, lead to non-convex formulations for the parameter estimation underlying optimization problem. High time resolution of the data and large data sets lead to optimization problems with large number of decision variables (parameters to estimate). Reasonable combination of data time sampling, time scale, model complexity and model structure should be selected in order to perform successful parameter estimation.

Due to the non-convexities in parameter estimation optimization problems the solutions are often local optima, instead of global optima. The results of a non-convex optimization problem can be very sensitive to the initial guess before starting the computation with the solver. Dedicated techniques and approaches are developed to make a good initial guess for parameter values before parameter estimation.

After obtaining candidate models with estimated parameters, at validation stage the model performance is compared to validation data sets from the plant or detailed emulator. A variety of indicators are defined to reflect different needs in the model validation stage to select good models.

System identification steps can form internal loops in the process of obtaining a good model. At that point flexibility of the concept exists to define different system identification strategies of passing through different steps upon finalizing the system identification with the best model according to the needs.

2.4 Regulation MPC

In the field of control systems “regulation” means applying a control law which brings all states of a dynamic system to zero. Another term with the same

usage in that context is “stabilization”. In the context of MPC, the mostly used optimization problem formulation for regulation penalizes the square of all states and all inputs, (2.7)

$$J = \min_{x,u} \left\{ x^T(N)Px(N) + \sum_{k=0}^{N-1} \left[x^T(k)Qx(k) + u^T(k)Ru(k) \right] \right\}$$
$$\text{s.t. } x(k+1) = Ax(k) + Bu(k) \tag{2.7}$$

Detailed literature can be found in (Rawlings and Mayne, 2009, Chapter 2).

2.5 Setpoint tracking MPC

“Setpoint tracking” means applying a control law which brings one or more system states to their predefined setpoints. In MPC a simple example is to penalize the square of the deviation from the setpoint, (2.8).

$$J = \min_{x,u} \left\{ \Big(x(N) - x^{sp}(N)\Big)^T P \Big(x(N) - x^{sp}(N)\Big) \right.$$
$$\left. + \sum_{k=0}^{N-1} \left[\Big(x(k) - x^{sp}(k)\Big)^T Q \Big(x(k) - x^{sp}(k)\Big) + u^T(k)Ru(k) \right] \right\}$$
$$\text{s.t. } x(k+1) = Ax(k) + Bu(k) \tag{2.8}$$

Detailed literature can be found in (Rawlings and Mayne, 2009, Section 2.9).

2.6 Coordinate transformation

A key characteristic of the robustness analysis method investigated in Chapter 7 is that it is based on regulation (penalizing the true states in the objective function), whereas the considered HyGCHP system with MPC is designed as setpoint tracking (penalizing the deviation of a state from its setpoint). The presence of the controlled state setpoint (x^{sp}) in the objective function is a problem for implementing the considered method. This problem is circumvented by relying on the applicability of a coordinate transformation for the investigated system.

The principle of coordinate transformation is shifting the variables (states and inputs) within a setpoint tracking problem in order to obtain a regulation

problem, then solving the regulation problem, and finally back-shifting the variables to reconstruct the solution as for the setpoint tracking problem. This technique is only applicable for linear models, so the original setpoint tracking problem is formulated as a linear optimization problem.

First a so called "target" is computed, which is a representative solution to the original setpoint tracking MPC based on (2.8). This target, the variables' profiles resulting from this solution, is denoted as

$$\begin{cases} x_t(i), & i = 0 \cdots N \\ u_t(j), & j = 0 \cdots N-1 \end{cases} \tag{2.9}$$

Rawlings and Mayne (2009, Subsection 1.5.1) described the coordinate transformation technique for the case of a steady state target, which would be the solution to (2.8) for dynamics of the kind

$$x_{ss} = Ax_{ss} + Bu_{ss}(k) \tag{2.10}$$

Even though the investigated HyGCHP system with MPC is designed as setpoint tracking, its behavior is influenced by fast changing disturbances (indoor heat gains from occupancy and appliances, solar radiation gains) which result in a specific profile of the controlled state. Consequently, the controlled state cannot be controlled steadily but it substantially deviates around the setpoint, though it is still possible to be kept within a desired range. The unsteady behavior of the controlled state is the reason why the target is a profile in both states and inputs (2.9), instead of being a steady state (2.10). For that reason (2.9) is chosen.

Second, the original variables are shifted by means of defining deviation variables:

$$\begin{aligned} \tilde{x}(k) &= x(k) - x_t(k) \\ \tilde{u}(k) &= u(k) - u_t(k) \end{aligned} \tag{2.11}$$

Third, the dynamics of the system with coordinate transformation is found:

$$\begin{aligned} \tilde{x}(k+1) &= x(k+1) - x_t(k+1) \\ &= Ax(k) + Bu(k) - \Big(Ax_t(k) + Bu_t(k)\Big) \\ &= A\Big(x(k) - x_t(k)\Big) + B\Big(u(k) - u_t(k)\Big) \end{aligned} \tag{2.12}$$

Having (2.11) and (2.12) the following is derived

$$\tilde{x}(k+1) = A\tilde{x}(k) + B\tilde{u}(k) \tag{2.13}$$

The dynamics (2.13) in fact represent the same system but with a setpoint being the zero level, which is implied by (2.11). Now, instead of solving the setpoint tracking problem (2.8) for given initial conditions $x(0)$, the aim is to solve the regulation problem (2.7) with corresponding initial conditions $\tilde{x}(0)$, found by (2.11). When a solution is found for regulation of the dynamics (2.13) then this solution can be back-shifted with (2.11) to reconstruct profiles to be used for setpoint tracking, instead of solving (2.8) directly.

In fact, neither regulation, nor coordinates transformation are needed to be implemented online in order to perform robustness analysis of the system investigated. The offline method investigated in Chapter 7 simply relies on the fact that these techniques are applicable for the investigated case of setpoint tracking and this is used as an argument to continue applying the method, which is based on regulation, and which is used for the dynamics (2.13) but for simplicity the tilde-accents over the variables are omitted.

2.7 State estimation uncertainty

In the context of system identification and feedback control, key sources of necessary information about the controlled real plant (here also called "system") are: state estimation, output estimation, state measurement and output measurement. Depending on the particular system model a system output can coincide with a system state or, for linear systems, it can be a linear combination of states or a linear combination of states and inputs. For simplicity, a case is assumed, in which the system output coincides with a state, so only that state is considered and denoted x. For the purpose of system identification or feedback control there should be information about the current system state. Depending on the case, this can either be obtained by state estimation or by state measurement. In any case, the estimated state or the measured state is denoted $\hat{x}$. In practice $\hat{x}$ differs from x and the difference between the two, depending on the case, is called state estimation uncertainty or state measurement uncertainty.

For the case of state estimation the state estimate $\hat{x}$ is obtained by means of incorporating a system model into a state observer, Kalman filter or a moving horizon estimation technique. These techniques result in state estimation uncertainty due to issues like inaccuracy of the used system model or computational limitations and errors.

For the case of state measurement $\hat{x}$ is either directly obtained by a sensor or possibly by measurement of one or several quantities and consequent computation. These techniques result in state measurement uncertainty due

to inaccuracy of the sensor, such as precision issues of the sensor, wrong measurement point or wrong mounting of the sensor, approximations in the computation, etc.

In all cases the provided estimate or measurement $\hat{x}$ will differ from the true system state x and this will have impact on the control system performance. For simplicity the term "state estimation uncertainty" is chosen in the remainder of the text but the results obtained are equally applicable for the case of state measurement uncertainty.

Chapter 3

State of the art

This chapter provides an overview of the state-of-the-art of heating and cooling systems in buildings in order to motivate the presented dissertation and formulate its objectives. The chapter starts with a brief summary of the current heating and cooling practice in the building sector and the potential for further development (Section 3.1). The evolution from conventional systems (e.g. gas boilers combined with radiators) to advanced systems (e.g. GCHP systems combined with TABS) is outlined, together with current trends in heating and cooling systems control leading to MPC (Section 3.2). The different actual control strategies are reviewed, drawing the path towards optimization based control. Finally a review on system operation robustness to uncertainties is presented, in the context of HyGCHP systems with MPC (Section 3.3). The chapter ends with a summary leading to the objectives of the presented doctoral research.

3.1 Heating and cooling systems in buildings

The most common heat production system for residential buildings, as for western Europe, eight years ago, was a fossil fuel fired boiler (Peeters et al., 2008). According to these authors 62% of the boilers in Flanders were fired by gas and the other 38%—by fuel oil. The most common heat emission system was a radiator (95% of the cases) and the rest had floor heating. The control of the heating system was achieved by central and/or local thermostats.

Bayer et al. (2012) report the possibilities of GCHP systems for cost- and greenhouse gas emission savings, based on 2008 data. The authors presented a country-specific review of the 2008 practice for heating systems, the shares of different heat sources and the actual savings on cost and greenhouse gas emissions. The data indicate that only in four countries there was some noticeable application of GCHP systems: Sweden (20%), Norway (10%), Finland (8%), Switzerland (5%). It is shown that the inclusion of GCHP systems can reach more than 30% cost savings if these systems are widely applied. Although having huge potential for such savings, Europe on average was in a very early stage of implementation, which leads to about 1.4% savings on cost and 0.7% savings on CO_2 emissions compared to conventional systems, which are almost entirely based on fossil fuels. Still, the study shows a significant growth of the GCHP units sold to the residential sector in the period 1998–2008.

Olesen and Kazanci (2015) presented the state of the art technologies for Heating, Ventilation and Air-Conditioning (HVAC) systems concluding that the differences in HVAC systems between North America, Europe and the rest of the world was in the heat emission/absorption system (indoor terminal units), whereas the energy sources and generators (production side) were similar. Low temperature heating and high temperature cooling were very important choices for increasing the HVAC systems' efficiency and the inclusion of renewable energy sources. The current technologies incorporating these concepts are radiant systems, all-air systems and passive/active beams. The publication provides a description of these state of the art technologies with their main characteristics, capabilities and limitations. A drawback of the study is that it doesn't provide statistical information about the current usage of these systems or a comparison to the usage of conventional systems.

One of the most efficient control strategies for GCHP systems is MPC (Hilliard et al., 2015). The authors made a classification of 19 case studies by several aspects of the MPC framework: system to be controlled (building, zone, single component), prediction horizon length, time step size, software tools, etc. The overview indicates that simplified control models (like reduced state space models) and linear or quadratic formulations will continue to dominate the optimization algorithms, because in real time it is still infeasible to compute with advanced emulators and nonlinear formulations. Self-learning modeling approaches gradually enter the field and they are now on the way of being fully explored in relevance to the buildings sector. The climate forecasts are still sampled at 1 hour in the applications, whereas a 15-minutes sampling appears more desired in the MPC algorithms. The desired prediction horizon remains concentrated around the 24-hours ahead approach, covering day and night occupancy schedules and electricity prices, as well as the majority of the building dynamics.

3.2 Control of HyGCHP systems

This section includes a review of the recently developed control strategies for HyGCHP systems. The different approaches found in the literature are structured in five subsections. First, some initial studies are mentioned addressing sizing, feasibility and performance potentials for HyGCHP systems (Subsection 3.2.1). Second, several studies on RBC are collected (Subsection 3.2.2). Third, some innovative recent applications follow, based on concepts like Artificial Neural Network (ANN)-based control and Extremum Seeking Control (ESC) (Subsection 3.2.3). Fourth, the studies on optimization based control strategies are reviewed (Subsection 3.2.4). Fifth, a review on BHE- and borefield modeling is placed (Subsection 3.2.5) since modeling is part of the optimization based control and the goals of this dissertation partially converge towards model development of this part of the system. The reviewed publications are preferably in the context of HyGCHP systems, since this is the focus of the current dissertation. For a broader look over control of GCHP systems in general the reader is redirected to the reviews by Atam and Helsen (2016) and Sarbu and Sebarchievici (2014).

3.2.1 Sizing, feasibility and performance evaluation

A method for sizing HyGCHP components like fluid coolers, cooling towers and BHEs for HyGCHP systems is presented by Kavanaugh (1998). The method is based on balancing the heating and cooling loads to the ground on the long term.

Chiasson and Yavuzturk (2003) published a system simulation approach to assess the feasibility of a solar assisted HyGCHP system. They considered school buildings which performance is simulated over 20 years. The study concludes for the minimum BHE depth of a conventional GCHP system which triggers the hybrid alternative to be more economically beneficial. An interesting observation is that the economical advantage of the hybridization increases exponentially with the increase of the ground thermal conductivity. Another simulation approach is presented by Man et al. (2008) for a small building with a cooling tower assisted HyGCHP system. Based on a very simple control strategy the authors provide a practical hourly simulation setup of the system. The results indicate a 40% total cost savings potential of the HyGCHP system compared to the conventional GCHP system for 10 years of operation.

An experimental study of HyGCHP system performance was published by Bi et al. (2004) for the case of a solar assisted building. The authors alternate the HyGCHP system between solar- and ground source in order to seek

maximum system efficiency. System efficiencies for the case of a vertical double spiral BHE resulted 20% higher compared to a horizontal single pipe heat exchanger. Another experimental investigation of HyGCHP system performance characteristics for a greenhouse was published by Ozgener and Hepbasli (2005).

Stojanović and Akander (2010) present a long-term performance test of a solar-assisted HyGCHP system for a real residential heating dominated building with some typical practical problems. Analysis of heat pump performance and total Seasonal Performance Factor (SPF) on the long term is carried out. The exact control strategy is not discussed.

3.2.2 Rule-based control

The studies included in this subsection are more focused on the development of the RBC strategy itself seeking the variant with most advantageous system performance.

Han et al. (2008) studied a solar assisted HyGCHP system with a latent heat energy storage tank to increase overall system efficiency. The control strategy switches between eight operation modes leading to RBC with many control parameters. The conclusions are based on a one year simulation and point out the positive impact of the solar collector on system efficiency and the possibility to reduce the buffer tank size by including latent heat storage.

A triple of related studies show successful RBC strategies for HyGCHP systems with cooling towers. Yavuzturk and Spitler (2000) used setpoint temperatures for the heat pump related to the ambient air temperature. The control strategy includes scheduled night cooling of the ground through the cooling tower to store cold for the next day and to prevent ground thermal build-up. The simulations indicate a substantial advantage of the hybrid system. The authors conclude that such systems are suitable for climates being at least moderately warm or warmer. Man et al. (2010) reported a reduction of investment cost by one third and reduction of operation cost by one half in ten years of operating the presented HyGCHPS. The work of Sagia and Rakopoulos (2012) is related to the other two studies by seeking minimal operation cost by testing three RBC control strategies.

Two studies are focused on simulation based design of HyGCHP systems and simulation based optimization of the used RBC strategies. Cullin and Spitler (2010) compared different design approaches and Hackel and Pertzborn (2011) based their investigation on three case studies. The optimization is performed either manually or with GenOpt (Wetter, 2001). The suggested control strategies may be conservative due to the lack of mathematical model-based optimization.

Due to computational limitations the number of optimized variables is also limited and there are difficulties to incorporate long-term effects with the presented methods.

Yang and Wang (2012)] investigated RBC of a solar-assisted ground to air heat pump system. Their method includes online heating demand computation. The computed heating demand is analytically translated to a sufficient condition for the solar collector outlet temperature. Such RBC strategy is tested in a 24 hour simulation. A drawback is that such a time frame is very short given the time constants of building (being in the order of magnitude from hours to days) and BHE (being in the order of magnitude from hours to multiple years). The authors also concluded that a longer simulation on the seasonal time scale is needed.

The last two studies on RBC investigated HyGCHP systems with cooling towers. The control is based on inlet- or outlet temperatures of the heat pump or the BHE or difference between such temperatures and the wet-bulb ambient temperature. Wang et al. (2015) performed multiple simulations of a cooling dominated hotel building on a 20-years time frame to design their best configuration based on two main control strategies with multiple operating points. Zhang et al. (2015) tested three other similar strategies on a 5-year basis. The conclusions are system-specific and describe the characteristics of the best found variant.

3.2.3 Non-dynamic model based control

Recently four studies were published suggesting alternative approaches to the widely applied RBC of HyGCHP systems. The first one is by Gong et al. (2012) who showed a theoretical control strategy for a solar assisted HyGCHP system. The strategy is based on multiple modes to control heating and cooling including domestic hot water. The different modes describe the efficiency and the utilization ratio for the heat pump and the solar collector in order to balance the loads to the BHE. The authors found that intermittent operation increases GCHP efficiency, but the true reason does not become clear from the study.

A triple of publications introduce ANN models in HyGCHP sytems control. Gang and Wang (2013) and Gang et al. (2014) present the usage of an ANN model of the BHE for controlling a HyGCHP system with a cooling tower. The authors observed that the developed ANN model is very accurate in many states of the system. However, this approach needs data to train the ANN, thus extrapolation to other system operation scenarios, not included in the training data sets is prone to large deviations. The control method is only compared to simple RBC methods as references. Optimization is not possible by the

suggested methodology. ANN modeling is also used by Mokhtar et al. (2013) for intelligent control of a HyGCHP system with a gas boiler. Simulations are performed over a couple of months. In fact these concepts represent a type of RBC but including an ANN model of the BHE (instead of for example a constant ground temperature).

ESC is the most recent alternative concept, which is published by Hu et al. (2016) investigating a HyGCHP system with a cooling tower. The method does not include dynamic models of system components but still an input-output relation is needed, so that it is often classified among the model-based optimization methods. The control uses feedback being the powers of the heat pump compressor, the cooling tower fan and the circulation pump. Control inputs are cooling tower fan speed and condensing water flow rate. The results show very low (3%) steady state errors and good potential for savings compared to a conventional control.

3.2.4 Optimization based control

Optimization based control strategies outperform the numerous RBC strategies and their pilot alternatives with the main characteristics that they are based on dynamic mathematical models of the real system components. This allows for optimization in the whole set of possible system operation profiles along a given time horizon while satisfying constraints on given process variables. While sub-optimality in RBC comes from the limitation to cover all possible operation profiles, the sub-optimality in optimization based control is mainly caused by model mismatch or non-convexity. Model mismatch could be compensated by different methods within the control framework. Non-convex optimization problems result from complexities in physical modeling, which may lead to a local optimum instead of a global optimum.

A convex approach is presented by Atam and Helsen (2015) giving an accurate solution for the short-term control of a HyGCHP system. The underlying mathematical model forms a non-convex optimization problem. This problem is convexified using the convex envelope approach in order to find a solution very close to the global optimum. The convexified result is compared to the result of a dynamic programming approach which is globally optimal and closed loop based. The comparison shows a very good similarity. The convexified formulation is very suitable for HyGCHP systems where a variable COP will otherwise cause problems with non-convexities. This research could broaden the results of this dissertation towards more accurate solutions with respect to the short-term effects. The focus though falls here on the long-term effects, such that the short term can remain approximated.

A comparison of three approaches for minimization of the total energy use of HyGCHP systems is presented by Atam et al. (2015). The comparison proves the success of using simple models in optimal control of HyGCHP systems. The compared approaches are (1) Prediction-based dynamic programming control, (2) Non-linear MPC (NMPC), and (3) Linear optimal control. A large-scale emulator of a single BHE is used to create simple models of the BHE to be used in the three approaches. System identification is carried out towards a non-linear autoregressive exogenous (NARX) model to use in dynamic programming. Proper orthogonal decomposition is applied to derive a lower order state space model to use in NMPC (with temperature dependent heat pump COP) and linear optimal control (with constant heat pump COP). The results for NMPC and linear optimal control were within a 10% error close to those for dynamic programming, which are globally optimal. The prediction horizon within optimization was 24 hours.

Preliminary summary 1: *Although part of the studies reviewed above include simulations on the long term (years, decades), they all suggest control strategies which are estimated to be satisfactory or proven to be optimal on the short term (days, weeks). On the long term these strategies are either not optimal, or their optimality is not explicitly guaranteed. This motivates part of the work in the current dissertation to investigate the optimal HyGCHP system operation on the long term. The core reason is that the dynamics of the ground storage volume have effect on the long term and only by finding the corresponding optimal solution it can be concluded whether the potential of the HyGCHP system in this direction is fully exploited. Such potential can be the concept of Seasonal Underground Thermal Energy Storage (SUTES), which means, for example, that cold is stored in the ground during winter in order to be used in the summer for increased system efficiency.*

The first relevant study on the long-term operation of a HyGCHP system was performed by Franke (1998) who investigated a solar assisted configuration. The author focused on the annual time scale. The optimization part was though oriented towards system design parameters and did not represent an optimization-based control approach. The borefield usage for underground thermal energy storage was not discussed. The borefield was rather considered as a heat source/heat sink without explicit intentional control strategy towards SUTES.

More recently Vanhoudt et al. (2010) investigated annually optimal control for the conventional case of a GCHP system. The authors used dynamic programming to optimize the borefield usage in order to avoid ground thermal build-up. Their publication, however, lacks a lot of important details. The control strategy and the controller models used have not been described.

Another study towards optimal operation of a GCHP system with focus on the optimal exploitation of the ground storage volume was published by De Ridder et al. (2011). Dynamic programming was again the used approach to optimize system operation over a time span of three years with a sampling time of one week. The authors performed computations based on the pre-estimated fixed heating/cooling weekly demand of an existing building. Usually the typical operation of GCHP systems is characterized by time constants in the order of magnitude of minutes or hours at the building side and the hydronic part of the BHE. Given these characteristics the presented sampling time of 1 week is a too coarse time grid to reflect the short-term effects of system operation. A simple BHE model of 1^{st}-order is used, which only partly presents the wide range of time constants in a ground storage volume, which is in the range from hours to years.

Preliminary summary 2: *The three studies reviewed above are relevant to the long-term optimal operation of GCHP systems. However, drawbacks and missing elements are observed, which motivate the work of the presented dissertation. One reasonable addition can be the inclusion of a short-term system model of the building, as well as of the borehole together with the long-term model of the ground storage volume. Another addition can be a model of the ground storage volume, which covers the corresponding time constants range more adequately. Third addition is of course the extension towards HyGCHP system where multiple units play role in the long-term optimal solution.*

Verhelst (2012) investigated the operation of a HyGCHP system on the short term (by means of MPC control on the daily time scale), as well as on the long term (by means of optimal control on the annual time scale). The MPC strategy optimizing on the daily time scale already incorporates short-term models of the building. She also developed low order ($n < 6$) state space models for BHEs, which cover the short-term hydronic dynamics of the BHE and the long-term dynamics of the ground storage volume along a reasonable range of time constants. The presented optimal control approach covers the long-term operation of the HyGCHP with an integrated building controller model in order to find the optimal system operation profiles for covering the pre-calculated fixed building heating and cooling demand. No constant thermal build-up has been observed in the ground storage volume. Only initial build-up was present (in a cooling dominated case) until reaching dynamic thermal equilibrium. Then the excessive heat injection to the ground is self regulated by the upper bound of the BHE outlet fluid temperature, imposed by the concept of passive cooling. Based on these observations the author concluded that the control should focus on the short term.

Preliminary summary 3: *The work of Verhelst (2012) fills the previously defined gaps about including a short-term model of the building in the long-*

term optimization, including a short-term model of the BHE and a detailed enough model of the ground storage model. The optimization on the long term, though, is performed in a way that fixed building heating and cooling demands are covered. The question arises how the short-term system operation profile will look like if the demand is not fixed but the short-term operation at building side is freely integrated in the long-term optimization which seeks the optimal long-term ground storage exploitation. More system insights will also be obtained if the core reason for the lack of ground thermal build-up is found, on top of the observation itself of this fact. Another useful contribution would be to answer how exactly the control should focus on the short term in order to reproduce the long-term optimal system operation. Last, in many systems borefield of thermally interacting BHEs are used, instead of one borehole. Whether and how the thermal interaction between adjacent BHEs influences the integrated short-and-long-term optimal operation is still an open question. These considerations motivate part of the work presented in the current dissertation to focus on two aspects: (1) Short And Long Term Optimization (SALTO) approach and investigation how a short-term approach only (MPC) can reproduce the long-term optimal system operation profile, and (2) inclusion of a borefield model as an extension of the approach with a BHE model.

3.2.5 Modeling of borehole heat exchangers and borefields

To fulfill the need for a borefield model in the SALTO approach first a literature review on borefield models follows. Initial inspiration is obtained from the BHE low-order model of Verhelst and Helsen (2011), which was also mentioned in the review above. The authors developed low order ($n \in [6, 11]$) state space models of a single BHE. Prior to that they provided a literature review on modeling of BHEs in the context of optimal control. BHE models created for different purposes were described—for simulation, design or control. Different modeling approaches were tried—using parameter estimation or model order reduction of high-order models (e.g. $n = 300$). It was concluded that low order state space models for BHEs can have a surprisingly good accuracy both on the short and long term. The authors developed such models, which were validated with a detailed BHE emulator (TRNSYS type 557b, see TESS, 2006; Pahud and Hellström, 1996).

A very relevant review paper describing the challenges in modeling of ground thermal heat transfer for vertical BHEs and comparing existing models has been published by Koohi-Fayegh and Rosen (2013).

Another extensive review on the topic precedes the work of Picard and Helsen (2014a,b) who developed their borefield emulator model to enable borefield

simulations with an improved computational speed by retaining high accuracy. The presented studies are especially focused on modeling of borefields of thermally interacting BHEs. Different modeling concepts were reviewed—analytical, numerical, and empirical. Recent achievements in modeling the dynamics of borefields in different time frames were reviewed—short-term, for solving the inner problem (interaction between the heat carrying fluid and the borehole wall) and long-term for solving the outer problem (heat dissipation in the surrounding ground and interaction with other BHEs in the borefield). The reviewed models and emulators have different complexities depending on their purpose, and as a consequence different computation times when they are used. The authors combined the reviewed methodologies and the obtained insights and developed a borefield emulator which reflects both the short- and the long-term dynamics of a borefield, it can be easily configured to represent different configurations of the BHEs (such as single and double U-tube, co-axial, etc.), and it is fast for computations.

The idea of SUTES mentioned above in *Preliminary summary 1* is also found in the work of Reuss et al. (1997). The authors did not include optimization based control of their system but they made use of SUTES of waste heat to store in the ground during summer and use for space heating in the winter. Their case has been characterized by storage temperatures above 40°C in clay with low thermal conductivities. High temperatures and low conductivities are counteracting characteristics with respect to underground storage. Nordell (1994) described the important relation between borefield density (distance between BHEs) and ground thermal conductivity. The optimal BHE distance is related to (along other factors) how far a heat pulse reaches in the course of six months and the temperature level in the ground storage volume in relation to undisturbed ground temperature. Prior to constructing the real GCHP system Reuss et al. (1997) performed simulations to facilitate the design, resulting in a full rectangular borefield of 140 BHEs, 30 m deep, located 2 m from each other. They developed a finite differences borefield model based on an analytical representation of the ground heat transfer including underground water flow. After simulations and real system operation the authors concluded that 64% of the stored heat is lost to the surrounding ground before it could be used. Due to these losses the total cost of reusing the waste heat after underground storage equaled the cost for running a gas-fired boiler to cover the heating demand of the building.

Preliminary summary 4: *A low-order state space model derived using simulation data from a detailed emulator appears a good way to model a BHE for the purpose of optimization based control of HyGCHP systems. However, when investigating a system with a borefield on both the short- and long-term time scale the thermal interaction between BHEs introduce complications, which*

make the detailed borefield emulator computationally heavy and case specific. The borefield emulator suggested by Picard and Helsen (2014a,b) copes with the modeling challenges by providing a flexible emulator in two aspects: (1) it can be easily configured for different borefield sizes and geometries, and (2) it is computationally fast and suitable for the creation of multiple long-term data sets. Therefore, another part of the work presented with the current dissertation will focus on the creation of a short-and-long-term low-order state space model of a borefield, which is identified and validated using the improved borefield emulator. The obtained low-order model can be used in a SALTO approach for the purposes formulated in Preliminary summary 3. Regarding the significant losses in SUTES indicated by Reuss et al. (1997) the efficiency of this strategy is an open question when the conventional RBC is replaced by SALTO or MPC. For example, Verhelst (2012) estimated that MPC has a potential for 20–40% cost savings and simultaneously better thermal comfort compared to conventional control of GCHP systems.

3.3 Robustness to uncertainties in HyGCHP systems control

In the context of the investigated HyGCHP system with MPC, the system performance is strongly dependent on both state estimation uncertainty and disturbance prediction uncertainty. The system investigated in this dissertation consists of an office building, heating and cooling devices and a BHE. The building is equipped with concrete core activation as heat and cold emission system. The concrete core temperature is a state in the state space model of the building. Sourbron et al. (2013a) concluded that the performance of such a system is highly sensitive to concrete core temperature estimation uncertainty as well as disturbance prediction uncertainty. For that reason system robustness to state estimation uncertainty is one of the focus points in the current dissertation and the corresponding state of the art is presented below.

Robustness to uncertainties is a key quality of MPC controlled systems and one of the methods to achieve this robustness is to determine the level of uncertainty which will be tolerated while retaining the desired control performance. In many cases robustness of control systems to uncertainties is naturally achieved to some extent by means of incorporating feedback. If this approach is insufficient additional actions should be taken at controller side in order to achieve robustness. Maciejowski (2002) formulated that the only purpose of applying feedback is to reduce the effect of uncertainties. When it comes to MPC, though, Doyle (1978) stated that the simple MPC strategy can never guarantee robustness. Contradictory to that, Heath and Wills (2005) observed

inherent robustness qualities of the MPC framework and defined the conditions which have to be satisfied in order to guarantee robustness. However, their approach is still not applicable to our HyGCHP system case due to reasons stated further in this section. More precise guarantee for robustness of MPC is needed and research on related topics has already been going on for a long time, as reviewed by Bemporad and Morari (1999); Mayne et al. (2000); Jalali and Nadimi (2006); Al-Gherwi et al. (2011).

Based on the performed literature review, in the context of MPC there exist two main directions to deal with robustness to uncertainties, both having advantages as well as difficulties to implement. The first direction is known as Robust Model Predictive Control (RMPC), in which, at system design stage, information about the uncertainties is explicitly incorporated within the optimization problem of the predictive controller. This way robustness is achieved by optimizing the control actions according to the expected uncertainties. This strategy, though, implies substantially more computations at each time step, which hampers the implementation. The other direction relies on robustness analysis of an existing system design. In this case the robustness to uncertainties is translated into particular conditions which are then checked only once based on the controller model and the optimization problem of the MPC formulation. The goal is either to give guarantee that the controlled system will be robust given particular parameters of the MPC formulation, or to compute the maximum allowed degree of uncertainty, for which robust performance is still guaranteed. The computation time does not drastically increase but the challenge is often related to deeper theoretical considerations. However, this approach is characterized by conservativeness in calculating the maximum allowed degree of uncertainty, for which system robustness is still guaranteed.

The conservativeness of the robustness analysis method needs to be the lowest possible. This way the full range of uncertainties will be determined for which the controlled system will have robust performance. The higher the conservativeness of the method, the lower the estimated maximum allowed degree of uncertainty. This means that if the method is conservative a margin will be created between the estimated allowed uncertainty and the real degree of uncertainty, which will trigger non-robust performance. The literature related to robustness analysis methods is shortly reviewed in the following paragraph.

Robustness analysis of MPC is a research topic which has mostly been developed in the '90s suggesting different theoretical methods to guarantee robustness to model mismatch and state estimation uncertainty. A few more publications appeared later but then the research in the field has been gradually redirected towards the explicit RMPC design which recently evolves towards nonlinear systems and distributed controllers. Zafiriou (1990) derived a sufficient condition for robustness to model mismatch based on contraction mapping. Due to

nonlinearities the condition is difficult to check; therefore he also derived easier to check necessary conditions. Megretski (1993) derived sufficient and necessary conditions in the frequency domain. He investigated robustness to feedback uncertainty with conic nonlinearities. Genceli and Nikolaou (1993) investigated robustness to model mismatch for the case of an impulse response model. They derived sufficient and necessary conditions for Single Input Single Output (SISO) plants, however, for the case of Multiple Input Multiple Output (MIMO) their formulations become difficult to use. Santos and Biegler (1999) used a sensitivity analysis approach to derive sufficient and necessary conditions for robustness to model mismatch for the SISO case. Heath and Wills (2005) reported the inherent robustness properties of MPC designs with model mismatch. Under the conditions of stable plant and model and feasibility of the optimization for zero input the authors related the robustness guarantee to sufficiently high inputs weighting factors. The majority of the most recent contributions to robustness analysis research are related to nonlinear discrete time systems and NMPC. Scokaert et al. (1997) investigated exponential and asymptotic stability for decaying perturbations. Scokaert et al. (1999) showed that for NMPC the feasibility is very important for stability and that a suboptimal solution is sufficient for stabilizing. Pannocchia et al. (2011) reported how suboptimal NMPC leads to robust exponential stability.

Particularly in the context of building heating and cooling systems with MPC two studies exist, both dealing with model mismatch by applying RMPC. Maasoumy et al. (2014) investigated a GCHP system for an office building. Each zone of the building is equipped with an independent GCHP unit so a single zone is considered. The authors compared two approaches to achieve robustness to model mismatch. The first one uses online state- and parameter estimation in order to implement adaptive modeling, which reduces the mismatch. The second approach is explicit RMPC. The system performance with the two approaches is compared to conventional MPC and to conventional RBC. The RMPC performs best for intermediate level of model uncertainty (30–67%). For lower level of uncertainty the conventional MPC performs best, and for higher level of uncertainty the RBC is the best option. In the second study Xu et al. (2010) investigated RMPC for model uncertainty in an air-conditioning system. On top of the linear state space model of the system the authors develop polytopic uncertainty modeling, which results in enhanced state space matrices. These matrices are included into Linear Matrix Inequality (LMI) based MPC.

Preliminary summary 5: *Despite the strong sides of the reviewed research on robustness analysis the cited studies have still characteristics, which do not fit the needs in the current dissertation. Mostly, model mismatch is considered as the source of uncertainty. The majority of the studies are also focused on the SISO case and the strength or the applicability of the approaches decreases when*

extended to the MIMO case. The research on nonlinear systems and NMPC reflects the development of the control systems, however in the frame of this dissertation still a linear representation is considered. The derived methods for estimation of the allowed uncertainties are difficult to compute or robustness to uncertainties is indirectly dealt with, by e.g. increasing the weighting factors within the MPC formulation.

Primbs and Nevistić (2000) presented a robustness analysis framework based on checking when the cost function of the MPC formulation is a Lyapunov function and will be decreasing in consecutive time steps, which is a sufficient condition for robust stability. The condition is checked by finding a feasible solution of the resulting LMI problem. After a successful LMI feasibility check the robust stability is guaranteed for a precise degree of uncertainty. The method can be used both for model mismatch and state estimation uncertainty. MIMO systems fit in the method and the original MPC formulation remains unaltered. A drawback of the publication is that it is written in a high-level theoretical style and some details are omitted. This is not supposed to be a problem for specialists, close to the field of control systems, but might represent a difficulty when being implemented by researchers with other background.

Preliminary summary 6: *For the case of HyGCHP system considered in the current dissertation, in order to retain the original MPC design, to guarantee its robust performance, and to obtain new insights into the system the focus is on the Robustness analysis approach and particularly on the framework of Primbs and Nevistić (2000). The high theoretical level of the related publication motivates for part of the work in this dissertation to be dedicated to clarifying the robustness analysis method. Afterwards the method can be extended for the case of a HyGCHP system and used for robustness analysis with respect to uncertainty in the concrete core temperature estimation.*

3.4 General chapter summary

This chapter provides an overview of the state of the art in heating and cooling systems in buildings with focus on two main aspects: system control and robustness to uncertainties. The general status of HyGCHP systems in practice is outlined. An extensive literature review of the recent research achievements is provided in the two focus fields. The discovered gaps related to important topics about SALTO of HyGCHP systems and Robustness analysis of HyGCHP systems with MPC motivate the research objectives listed below, which aim at further development of HyGCHP systems control and increased operation efficiency.

Research objectives with respect to Short and Long term optimal operation of the HyGCHP system

- Develop a SALTO method for evaluating the operation of the investigated HyGCHP system with freely integrated building short-term dynamics in the long-term optimization.
- Investigate how exactly a short-term only approach (e.g. MPC) can reproduce the long-term optimal system operation profile, obtained by SALTO.
- Evaluate the potential for seasonal underground thermal energy storage in the long-term optimal operation profile for a particular case of HyGCHP system.
- Create and validate a short-and-long-term low-order state space model of a borefield, include this model in a SALTO computation, and investigate the influence of thermally interacting BHEs.

Research objectives with respect to Robustness analysis of the HyGCHP system with MPC

- Clarify the method of Primbs and Nevistić (2000), eliminate mistakes, and provide the omitted details to enable smooth future implementations.
- Extend and apply the method to the HyGCHP system investigated.
- Implement the method and compute the precise range of allowed state estimation uncertainty with guaranteed system robustness.
- Validate the estimated uncertainty range with HyGCHP system simulations.

Chapter 4

Simulation setup

This chapter is partially based on the publication:
Antonov, S., Verhelst, C. and Helsen, L. (2014). Should the optimization horizon in optimal control of ground coupled heat pump systems cover the inter-seasonal time scale?. *ASHRAE Transactions*, 120(2):346–356.

This chapter describes the investigated case of HyGCHP system with MPC and the way it is represented in a simulation, optimization and control context. First, Section 4.1 starts with a brief description of the corresponding analog of a real system. The models of the system components are thoroughly presented. A specific way to integrate all component models into a global system model is shown. Different system designs are considered through sizing of the components, implemented by scaling factors. Second, the optimization problem used to investigate system operation is described in Section 4.2. The framework is described, which is used to investigate the performance of the integrated system operation by means of minimizing an objective function, which is subject to constraints. The described formulations are used as such in Chapter 5. With specific variations these formulations represent the base of the system setup in other chapters: instead of a single BHE, a borefield of thermally interacting BHEs is considered in Chapter 6. In Chapter 7 a quadratic objective function of both states and inputs is used, instead of a linear objective function of inputs only.

4.1 System description and modeling

The investigated system comprises an office building equipped with concrete core activation (CCA) which is fed by primary and back-up heating and cooling installations (Figure 4.1). The primary heating device is a ground coupled Heat Pump (HP); the primary cooling device is a ground-coupled heat exchanger for Passive Cooling (PC)—direct cooling of the CCA return water by means of passive heat rejection to the fluid circulated through the BHE. The back-up heating device is a Gas-fired Boiler (GB). The back-up cooling device is an active Chiller (CH). The ground-coupled devices are connected to a vertical BHE.

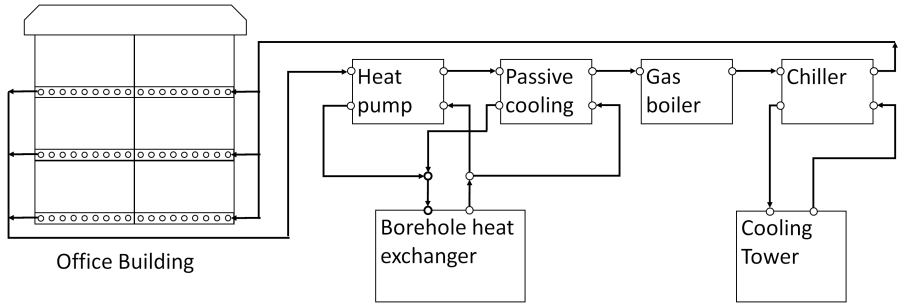

Figure 4.1: The investigated hybrid ground coupled heat pump system consists of an office building, ground coupled heating and cooling devices (heat pump, passive cooling) and back-up heating and cooling devices (gas boiler, chiller)

The chiller could be either air coupled or connected to a cooling tower, however the optimal choice of components and configurations is not the scope of the present study. According to the reference weather data and the thermal comfort requirements imposed, the heat and cold emission system at building side requires supply water temperatures near the wet bulb ambient temperature and even below it during the summer season. Since in the best case the cooling tower outlet water temperature can reach a few degrees above the wet bulb ambient temperature, a cooling tower alone would not cover the whole cooling demand. Therefore, an active chiller is needed as a back-up cooling device. In the way the heating and cooling devices are implemented by means of simulation setup, the chiller could also be seen as a reversible heat pump. For consistency in this research and for distinguishing the devices, active chiller is chosen.

The office building consists of identical office zones (Figure 4.2), which are represented by a linear state space model discretized with a time step $t_s = 1$ h,

(4.1). An office zone model of fourth-order is used, as developed by Sourbron et al. (2013b), for which the states are: concrete core temperature T_{CC}, office zone air temperature T_Z, internal walls temperature T_{WI}, and external walls temperature T_{WO}. The office model inputs are: supply water temperature T_{WS}, ventilation air temperature T_{VS}, ambient air temperature T_{AMB}, internal heat gains $\dot{Q}_{INT}$, and solar gains $\dot{Q}_{SOL}$.

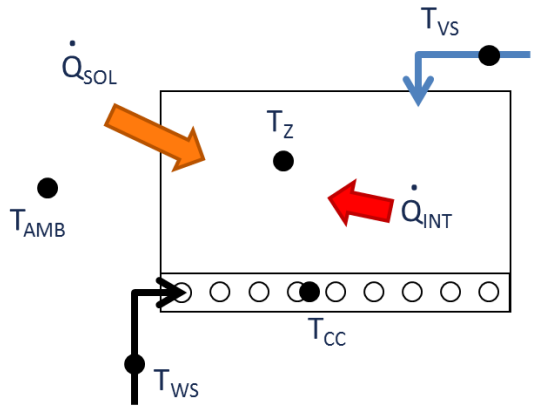

Figure 4.2: The office building is represented by a model of a single office zone comprising concrete core activation heat and cold emission system.

$$\begin{bmatrix} T_{CC}(k+1) \\ T_Z(k+1) \\ T_{WI}(k+1) \\ T_{WO}(k+1) \end{bmatrix} = A_{BD} \begin{bmatrix} T_{CC}(k) \\ T_Z(k) \\ T_{WI}(k) \\ T_{WO}(k) \end{bmatrix} + B_{BD} \begin{bmatrix} T_{WS}(k) \\ T_{VS}(k) \\ T_{AMB}(k) \\ \dot{Q}_{INT}(k) \\ \dot{Q}_{SOL}(k) \end{bmatrix} \tag{4.1}$$

The control input of the office zone model is T_{WS} only. The other four inputs of the model are assumed as perfectly predictable disturbances, for which reference weather data for one year and a fixed office occupancy schedule are used, described at the end of Section 4.2. Because of modeling characteristics (Sourbron et al., 2013b) the model represents the heating and cooling demand of two office zones with the same orientation. This way the overall office area modeled is 24 m^2 (12 m^2 per zone).

The building model, representing two identical office zones, cannot represent the diversity of the thermal demand profiles within the building. However, the current study investigates the entire building demand as a whole and more importantly how this entire demand can be delivered by the BHE and supplementary devices. Verhelst (2012, pages 101–109) observed that controlling

the thermal comfort of the investigated two zone building (north and south zone) based only on optimization of the north zone demand satisfies both zones thermal comfort criteria. This result has been experimentally obtained. It is explained with the particular relative difference between the heating demands (less than 10%) and the cooling demands (less than 30%) of the two zones, as well as the installed automated shading at the south zone. For that reason the particular heating and cooling demand of the worst case zone, i.e. the north-oriented zone (Verhelst, 2012, pages 101–104), is up-scaled to form a representation of the total conditioned area (building). Such configuration determines the entire building high-level control, investigated in this dissertation. In practice the-low level control of individual zones can be achieved for example by supplying water at common T_{WS} to all zones and locally controlling each zone's comfort by setting the CCA 2-way valves openings (Vána et al., 2014) and all that with taking into account the eventual automated shading control of the south zone.

The BHE is represented by an n^{th}-order linear state space model (4.2, 4.3), which calculates the BHE fluid mean temperature $T_{Fluid,Mean}$ and the temperature of the ground at n equal to 11 points, radially distanced from the BHE, as developed by Verhelst and Helsen (2011). The model does not include thermal effects of underground water flow. It is developed as a resistor-capacitor (RC) grid, which represents the thermal capacities and the thermal conductivities between n concentric cylinders of ground around the BHE. The states of charge of the capacitors represent the mean ground temperatures T_j, for $j = 1, 2, \ldots, n$ (Figure 4.3). The BHE model inputs are the heat flow rate of extraction $\dot{Q}_{BHE}$ and a fixed undisturbed ground temperature T_{GR} equal to 10°C located at the outer boundary of the storage volume. The BHE model output is $T_{Fluid,Mean}$.

$$\begin{bmatrix} T_1(k+1) \\ T_2(k+1) \\ \vdots \\ T_{11}(k+1) \end{bmatrix} = A_{BHE} \begin{bmatrix} T_1(k) \\ T_2(k) \\ \vdots \\ T_{11}(k) \end{bmatrix} + B_{BHE} \begin{bmatrix} \dot{Q}_{BHE}(k) \\ T_{GR} \end{bmatrix} \tag{4.2}$$

$$T_{Fluid,Mean}(k) = C_{BHE} \begin{bmatrix} T_1(k) \\ T_2(k) \\ \vdots \\ T_{11}(k) \end{bmatrix} + D_{BHE} \begin{bmatrix} \dot{Q}_{BHE}(k) \\ T_{GR} \end{bmatrix} \tag{4.3}$$

The RC-grid is composed applying the guidelines of Eskilson (1987) so that the 11 states of the model have the physical meaning of ground temperatures at the corresponding 11 nodes. The distance between each node and the center of the BHE ranges from 15 cm to 65 m according to Eskilson's guidelines for

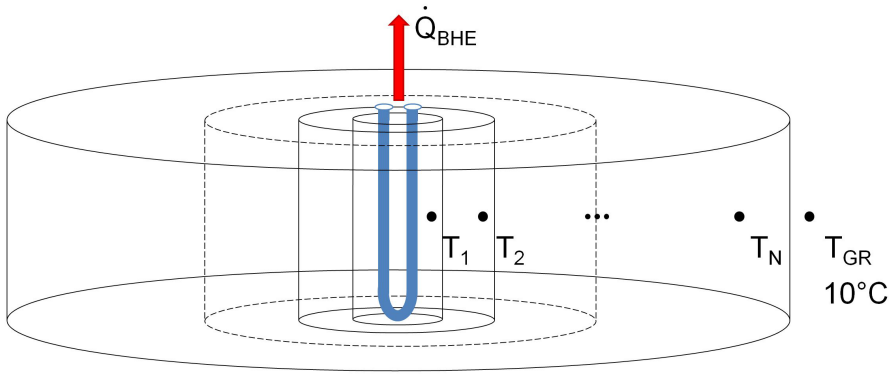

Figure 4.3: The borehole heat exchanger model incorporates concentric cylinders of ground and fixed undisturbed ground temperature as outside boundary.

composing the RC-grid and the fixed undisturbed ground temperature T_{GR} is applied to the outer boundary at 87 m from the BHE center. The model is validated by Verhelst and Helsen (2011) towards $T_{Fluid,Mean}$ using a detailed BHE emulator (TRNSYS type 557b, see TESS, 2006; Pahud and Hellström, 1996). For a step input with duration in the range [1 hour, 10 years] the model shows in the worst case a relative error of less than 4% (Verhelst and Helsen, 2011, Figure 4). For typical imbalanced annual BHE loads repeated for ten years the model shows an absolute error of less than 1 K (Verhelst and Helsen, 2011, Figure 10a) and a root mean square error of less than 0.2 K (Verhelst and Helsen, 2011, Figure 10c).

The BHE model represents an underground storage system with the following specifications: The borehole has a depth of 121 m, a header depth of 1 m, a borehole radius of 0.075 m, a tube radius of 0.02 m, and a specific borehole thermal resistance of 0.1 mK/W. The specific heat of the calorimetric fluid is 4 kJ/(kgK), the density is 1000 kg/m^3, and the mass flow rate is 750 kg/h. The ground has a thermal conductivity of 1.9 W/(mK) and a volumetric heat capacity of 2400 kJ/(m^{3}K).

The primary and the back-up heating and cooling devices are represented by their efficiencies and thermal powers (Figure 4.4). The heat pump is modeled by a constant approximation of its coefficient of performance $COP_{HP} = 6$, which links the thermal power at the condenser side $\dot{Q}_{HP}$ to the thermal power at the evaporator side $\dot{Q}'_{HP}$ as shown in (4.4), where k is the corresponding time step.

$$\dot{Q}_{HP}(k) = \frac{COP_{HP}}{COP_{HP} - 1} \dot{Q}'_{HP}(k) \tag{4.4}$$

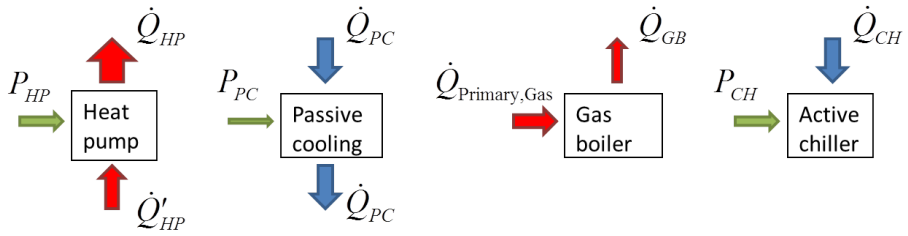

Figure 4.4: The heating and cooling devices are represented by static models accounting for their efficiencies and thermal powers.

The chiller for active cooling is modeled analogously but only the thermal power $\dot{Q}_{CH}$ at the evaporator side is incorporated. The chiller energy efficiency ratio $EER_{CH} = 4$ is defined as the ratio between $\dot{Q}_{CH}$ and the electrical power of the device. Ambient temperature dependency of the chiller efficiency is neglected. Passive cooling is characterized by the thermal power of extracting heat from the building $\dot{Q}_{PC}$. The passive cooling efficiency $\eta_{PC} = 12$ is defined as the ratio between $\dot{Q}_{PC}$ and the electrical power P_{PC} of the circulation pumps to feed the passive cooling heat exchanger. The addition of P_{PC} to the thermal power $\dot{Q}_{PC}$ is neglected, so $\dot{Q}_{PC}$ is assumed the same at both sides of the passive cooling heat exchanger. The gas-fired boiler is characterized by its thermal power $\dot{Q}_{GB}$. The gas boiler efficiency $\eta_{GB} = 0.9$ is defined as the ratio between $\dot{Q}_{GB}$ and the rate of primary energy use corresponding to the consumed gas.

The approximation of constant COP_{HP} and η_{PC} along the entire system operation time has been proven by Verhelst (2012, pages 205–212) to give the same results as the non-linear formulation, in which COP_{HP} and η_{PC} are functions of the BHE outlet fluid temperature $T_{Fluid,Out}$. That is done for a case similar to the case presented in this chapter (HyGCHP system with closed loop heat exchangers; same ground properties and same HyGCHP system characteristics); though with a much larger time step (loads aggregated in time intervals of about 1 week, instead of 1 h). Since in the current study the seasonal time scale of thermal energy storage is investigated the extrapolation of the work of Verhelst (2012, pages 205–212) towards smaller time steps will most probably hold (or not alter the fundamental conclusions of this chapter) but, nevertheless, this should still be proven. The numerical solvers that accept the formulation $COP_{HP} = f(T_{Fluid,Out})$ need to be non-linear. Currently, those non-linear solvers cannot solve the large-scale problem of this study (25 decision variables per time step; 8760 time steps; in total: 219,000 decision variables). Therefore, proving this assumption is future work. In fact, moderate inaccuracies in the values of $COP/EER/\eta$ will not alter the conclusions of the current study in the majority of the investigate cases. Although any constant

approximation will incorporate inaccuracy, the study shows that the chiller *EER* should be significantly smaller than its original value in order to start affecting the presented conclusions in cases of thermally non-interacting BHEs or in cases of small borefields, like the investigated 3×3 open rectangular configuration, and moderate or high ground conductivities. In these cases it is adequate to neglect the modest inaccuracies in the constant values for $COP/EER/\eta$. In cases of small borefields with low ground thermal conductivities the accuracy of devices efficiencies could influence the conclusions since these cases are on the border between the described thermal effects and optimal operation patterns. In the cases of larger borefields the conclusions would be again safe from that point of view, however such cases are not investigated.

All system component models are integrated into a global system model by (4.5) and (4.6):

$$\begin{aligned}\sum \dot{Q}_{Building}(k) &= \dot{Q}_{HP}(k) + \dot{Q}_{GB}(k) - \dot{Q}_{PC}(k) - \dot{Q}_{CH}(k) \\ &= F_l \frac{1}{R_{th}}(T_{WS}(k) - T_{CC}(k))\end{aligned} \tag{4.5}$$

$$\begin{aligned}\sum \dot{Q}_{Ground}(k) = &\quad \dot{Q}'_{HP}(k) - \dot{Q}_{PC}(k) \\ = &\frac{COP_{HP} - 1}{COP_{HP}} \dot{Q}_{HP}(k) - \dot{Q}_{PC}(k) = \dot{Q}_{BHE}\end{aligned} \tag{4.6}$$

In (4.5) $\sum \dot{Q}_{Building}(k)$ is the total thermal power of delivering heat to the CCA of the building in the corresponding time step k and in (4.6) $\sum \dot{Q}_{Ground}(k)$ is the total thermal power of heat extraction from the ground through the BHE by the ground coupled devices. The scaling factor F_l represents the exact sizing of the system components which is explained later below. The transition of $\sum \dot{Q}_{Building}(k)$ to $T_{WS}(k)$, in order to connect all devices to the building model, is carried out by the thermal resistance R_{th} characterizing the heat transfer between the supply water and the concrete core. The dynamics of the production devices and the dynamics of the heat and cold distribution system are neglected since their time constants are smaller than the sampling time $t_s = 1$ h. Hence, the heat flow from all devices to the supply water is assumed equal to the heat flow from the supply water to the concrete core as expressed in (4.5).

Sizing of the system components is based on dynamic calculation of the building heating and cooling loads for a reference year. It was described above that the building is represented by a model of two office zones with a total area of 24 m^2 and the BHE model which is used represents a 121 m deep BHE. Since

these two system components have these fixed models, in this work a scaling approach is adopted. The calculated heating and cooling loads of the building model are scaled up by a factor F_l to represent a demand large enough to suit the available BHE model. The GLHEPro tool (Spitler, 2000) is used to define the required depth of a BHE based on scaled annual heating and cooling loads of the building model. Sizing attempts with GLHEPro are performed with different scaling factors F_l until the required BHE depth matches the depth of the available BHE model. The resulting scaling factor F_l is then used in (4.5) for the further investigations. Following that concept, instead of different BHE sizes for a fixed building, different building sizes for a fixed BHE are considered. This is implemented by including different scaling factors F_l in (4.5).

In a first design scenario, the system is sized such that the BHE entirely covers both the heating and cooling loads of the building (respectively through HP operation and PC). The result from the sizing tool for this scenario corresponds to a building with 108 m^2 office area (scaling factor $F_l = 4.5$) coupled to the 121 m deep BHE. The design capacities of the primary heating and cooling devices equal the corresponding peak heating and cooling loads of the building (HP—1436 W_{th}, PC—3890 W_{th}).

A second design scenario represents the effect of reducing the BHE size, which, following the scaling concept above, is equivalent to increasing the amount of office zones and the heating and cooling devices capacities connected to the same BHE. This scenario corresponds to a building with 212 m^2 office area (scaling factor $F_l = 8.8$) coupled to the 121 m deep BHE. This sizing allows to investigate the operation of the back-up heating and cooling devices, respectively gas boiler and chiller, since the primary devices and the BHE will be insufficient to cover the building loads. The design capacities of the back-up devices are set to those of the primary devices and the intention is that they all equal the corresponding peak heating and cooling loads of the upscaled building (HP—2787 W_{th}, PC—7552 W_{th}, GB—2787 W_{th}, CH—7552 W_{th}). However, a PC device with a maximum power of 7552 W_{th} connected to a 121 m deep BHE results in a specific heat transfer rate to the BHE of 62 W/m. Compared to practice (Sanner, 2001), typical maximum specific heat transfer rates are 45–50 W/m for ground conductivity of 1.9 W/mK, like in the current case. For that reason the PC device is exceptionally sized with a maximum power of 6050 W_{th} in the second design scenario.

4.2 System simulation, optimization and control framework

The operation of the HyGCHP system is determined by solving an optimization problem, which minimizes the objective function (4.7) over a specified prediction horizon N and satisfies constraints.

$$J = \sum_{k=1}^{N} \Big(c_{el} \frac{\dot{Q}_{HP}(k)}{COP_{HP}} + c_{gas} \frac{\dot{Q}_{GB}(k)}{\eta_{GB}} + c_{el} \frac{\dot{Q}_{PC}(k)}{\eta_{PC}} + c_{el} \frac{\dot{Q}_{CH}(k)}{EER_{CH}} \Big) t_s \qquad (4.7)$$

In (4.7) $c_{el}(k) = 0.2$ €/kWh is the electricity price, $c_{gas} = 0.07$ €/kWh$_{\text{th}}$the gas price, N the prediction horizon length and $t_s = 1$ h the discretization time step. The decision variables are the thermal powers of the heating/cooling devices over the entire control horizon: $\dot{Q}_{HP}(k)$, $\dot{Q}_{GB}(k)$, $\dot{Q}_{PC}(k)$, $\dot{Q}_{CH}(k)$, for $k = 1 \cdots N$.

The main part of the optimization constraints is the dynamic integrated system model (Section 4.1). The discrete state space models of the building (4.1) and the BHE (4.2 and 4.3) are used to compute the model states and outputs along the optimization horizon N. For each time step along the optimization horizon the two state space models are algebraically incorporated by (4.5) and (4.6).

The desired thermal comfort is defined by (4.8) as upper and lower bounds on the office zone air temperature. These bounds depend on the ambient air temperature (Figure 4.5) as for an office room Category II according to CEN (2007).

$$T_{min}(k) - \varepsilon_1(k) \leq T_Z(k) \leq T_{max}(k) + \varepsilon_2(k) \qquad (4.8)$$

In (4.8) dummy decision variables $\varepsilon_1(k) \geq 0$ and $\varepsilon_2(k) \geq 0$ are introduced to represent deviations from the comfort range.

$$\varepsilon_1(k) \geq 0$$

$$\varepsilon_2(k) \geq 0 \qquad (4.9)$$

According to CEN (2007) a total deviation of 0.4 Kelvinhours is allowed during the daily occupation period. This constraint is implemented by (4.10), which is applied for all working days along the time horizon.

$$\sum \big[\varepsilon_1(r) + \varepsilon_2(r) \big] \leq 0.4, \quad r\text{—working hours during a working day} \qquad (4.10)$$

For periods during which passive cooling and chiller are needed to work simultaneously in serial hydronic connection the question arises what is the optimal order in which these two installations should operate in order to supply

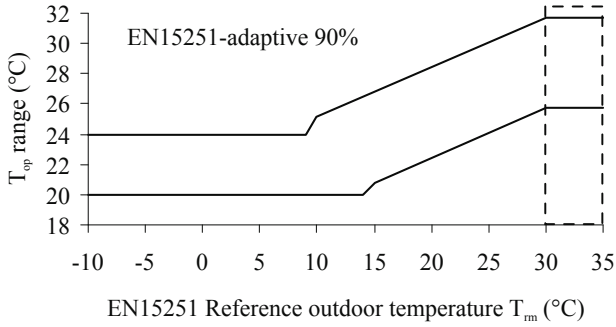

Figure 4.5: The thermal comfort bounds T_{min} and T_{max} of the zone air temperature T_Z depend on the ambient air temperature T_{AMB} according to the EN15251 standard (CEN, 2007). *Image source: (Sourbron, 2012)*

the required cooling to the CCA. In an initial stage the passive cooling feasibility is defined by (4.11), where the temperature difference $\Delta T_{PCHE} = 3°\text{C}$ between the supply water temperature T_{WS} and the BHE outlet fluid temperature $T_{Fluid,Out}$ is the minimal temperature difference across the passive cooling heat exchanger (Figure 4.6).

$$0 \leq T_{Fluid,Out}(k) \leq T_{WS}(k) - \Delta T_{PCHE} \tag{4.11}$$

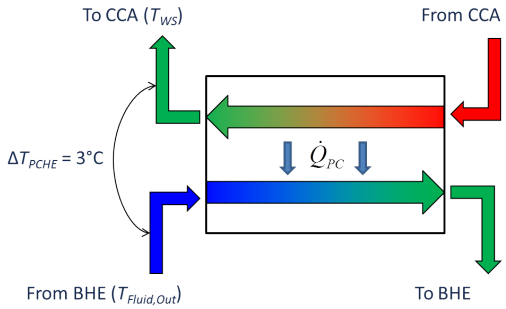

Figure 4.6: The counter-flow passive cooling heat exchanger is modeled by its thermal power and efficiency, as well as a minimal fluid temperature difference.

The BHE outlet fluid temperature $T_{Fluid,Out}$ is calculated based on the BHE fluid mass flow rate $\dot{m} = 750$ kg/h and specific heat $c_p = 4$ kJ/kg.K, (4.12).

$$T_{Fluid,Out}(k) = T_{Fluid,Mean}(k) + \frac{\dot{Q}_{BHE}(k)}{2\dot{m}c_p} \tag{4.12}$$

This means that passive cooling can be engaged either as first or second cooling device, however, in both cases it will transfer heat with the same efficiency. On the contrary, the active chiller is more efficient when engaged as first device (seen from the water that returns from the CCA component), due to the lower temperature difference, in that case, between the condenser- and evaporator side of the chiller. Thus, by applying (4.11) as optimization constraint the chiller is assumed the first installation in the serial connection and passive cooling the second one (Figure 4.7).

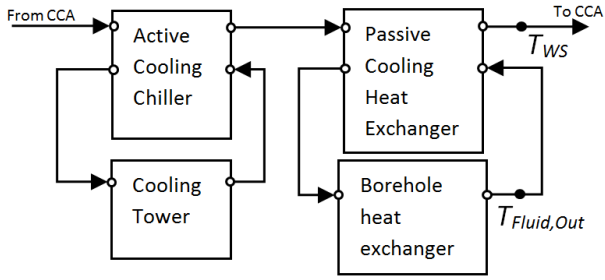

Figure 4.7: Hydronic configuration in which the chiller is the first cooling device in the serial connection

In practice it is possible to apply passive cooling as the first installation in the serial connection until the difference between T_{WS} and $T_{Fluid,Out}$ reaches 3°C and afterwards apply the active chiller to further decrease the supply water temperature even below the BHE outlet fluid temperature. This configuration obeys (4.13) as optimization constraint.

$$0 \leq T_{Fluid,Out}(k) \leq T_{WS,PC}(k) - \Delta T_{PCHE} \tag{4.13}$$

The intermediate variable $T_{WS,PC}$ in (4.13) represents the temperature of the water at the outlet of the passive cooling heat exchanger before applying chiller.

$$T_{WS,PC}(k) = T_{CC}(k) - \frac{\dot{Q}_{PC}(k)}{F_l} R_{th} \tag{4.14}$$

This way, by imposing (4.13) as optimization constraint it is guaranteed that the heat transfer carried out through the passive cooling heat exchanger will be indeed passive. The chiller can either further decrease $T_{WS,PC}$ towards T_{WS} or stay inactive. Thus, by applying (4.13) and (4.14) as optimization constraints passive cooling is assumed the first installation in the series and the active chiller—as the second one (Figure 4.8).

Additionally, T_{WS} is kept above 17°C to prevent moisture condensation on the CCA surfaces and below 40°C to reflect two aspects: low enough condenser

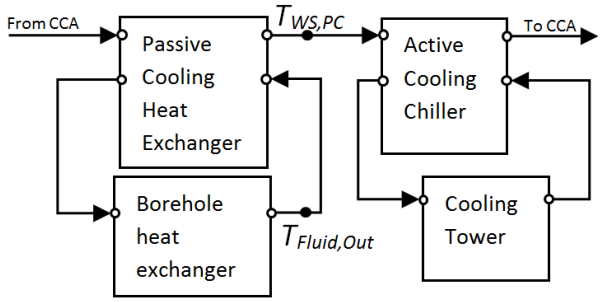

Figure 4.8: Hydronic configuration in which the passive cooling is the first cooling device in the serial connection

temperature for efficient operation of the heat pump, as well as thermal comfort as to low enough surface temperature of the CCA.

$$17 \leq T_{WS}(k) \leq 40 \tag{4.15}$$

The thermal powers of the heating and cooling devices are kept positive and below upper bounds representing the maximal capacity of those devices, as explained at the end of Section 4.1.

$$\begin{aligned}
\text{For } F_l = 4.5 \quad & 0 \leq \dot{Q}_{HP}(k) \leq 1436 \\
& 0 \leq \dot{Q}_{PC}(k) \leq 3890 \\
\text{For } F_l = 8.8 \quad & 0 \leq \dot{Q}_{HP}(k) \leq 2787 \\
& 0 \leq \dot{Q}_{PC}(k) \leq 6050 \\
& 0 \leq \dot{Q}_{GB}(k) \leq 2787 \\
& 0 \leq \dot{Q}_{CH}(k) \leq 7552
\end{aligned} \tag{4.16}$$

Fixed data for a reference year are used for the disturbances (T_{VS}, T_{AMB}, $\dot{Q}_{INT}$, $\dot{Q}_{SOL}$) of the building model. Meteorological data are used (TESS, 2006, Weather data file for Uccle, Belgium—`BE-Uccle-64470.tm2`) to obtain annual profiles for T_{AMB} and $\dot{Q}_{SOL}$. The source used provides fixed data from one particular year containing hourly measured realistic samples for T_{AMB} and data needed to compose the corresponding fixed profile for $\dot{Q}_{SOL}$. The disturbance profile for $\dot{Q}_{SOL}$ is obtained using the building model of Sourbron (2012) implemented with TRNSYS type 56 (TESS, 2006), in which the solar

radiation is calculated per vertical wall area with a specific orientation. Given the window area (4.32 m^2) of the modeled office zone the exact profile for $\dot{Q}_{SOL}$ is composed for solar radiation entering the office zone. Based on the annual profile for T_{AMB} and the definition of thermal comfort bounds (Figure 4.5) the annual profiles for the bounds T_{min} and T_{max} are computed to use in (4.8). The T_{min} and T_{max} annual profiles can be seen in Figure 5.1. To represent the internal gains $\dot{Q}_{INT}$ scheduled profiles are used for heat gains caused by office occupancy and appliances. Internal heat gain values are assumed (Table 4.1) similarly to information from several sources presented in details by Sourbron (2012, Appendix D). The data presented in Table 4.1 is scaled to suit the

human sensible heat gains	75	W per person
occupation density	1	person per 10 m^2
lighting heat gains	7.5	W/m^2
electrical appliances heat gains	7.8	W/m^2
residual night and weekend heat gains	2	W/m^2

Table 4.1: The internal heat gains of the considered office zone are based on typical heat gains caused by occupancy and electrical appliances.

considered office zone of 12 m^2 office area. The office is assumed occupied from 8:00 to 12:00 and from 14:00 to 18:00 o'clock, and the appliances are assumed turned on from 8:00 to 18:00 o'clock during the working days (Figure 4.9). In the weekend and during the non-working hours only the residual heat gains apply. The ventilation supply temperature T_{VS} coincides with the lower comfort bound T_{min} of the zone temperature. The undisturbed ground temperature $T_{GR} = 10°C$ is assumed yearly constant.

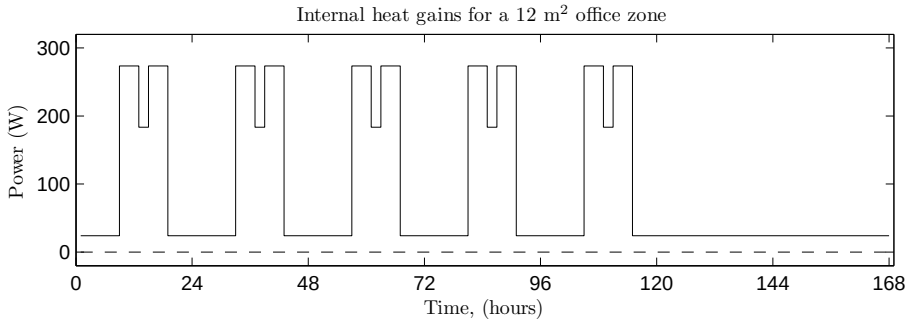

Figure 4.9: The fixed annual profile for office internal heat gains $\dot{Q}_{INT}$ is based on a weekly pattern representing the heat gains resulting from a scheduled office usage.

The optimization problem is composed as an LP-problem, (2.2), on the base of the objective function and constraints described above in this section:

$$
\begin{aligned}
\min_{z \in \mathbb{R}^d} \quad & (4.7) \\
\text{s.t.} \quad & (4.1),\ (4.2),\ (4.3), \\
& (4.5),\ (4.6), \\
& (4.8),\ (4.9),\ (4.10), \\
& (4.12),\ (4.13),\ (4.14),\ (4.15), \\
& (4.16), \\
& \textit{Fixed data for a reference year for disturbances}
\end{aligned}
\tag{4.17}
$$

In (4.17) the decision variables vector $z \in \mathbb{R}^d$, $d = 25 \times N$, consists of the 25 variables T_{CC}, T_Z, T_{WI}, T_{WO}, T_{WS}, T_j at all ground nodes j, $T_{Fluid,Mean}$, $T_{Fluid,Out}$, $\dot{Q}_{HP}$, $\dot{Q}_{GB}$, $\dot{Q}_{PC}$, $\dot{Q}_{CH}$, $\dot{Q}_{BHE}$, ε_1, ε_2 at each time step along the considered time horizon of length N.

The optimization problem (4.17) is implemented numerically in MATLAB (MathWorks, 2010) with the YALMIP interface (Löfberg, 2004) where the Cplex solver is called (IBM, 2012) to compute for all time steps along the optimization horizon the optimal solution for the decision variables. Per time step this amounts to 25 decision variables, 20 equality constraints, and 17 inequality constraints, described above in this chapter. In Chapter 5 it will be seen that the optimization problem is solved either on the short term (time horizon of $N = 24$ hours) or on the long term ($N = 8760$ hours, representing 1 year). The sizes of the resulting optimization problems and the corresponding computation times are given in Table 4.2.

Since this is an LP problem, if it is a feasible problem, the solver finds the global optimum meeting all constraints. Normally, in proper system designs, the problem is feasible. In case the LP is infeasible this might happen if for example the devices capacities are not large enough to meet the thermal comfort constraints given the fixed reference data for the disturbances, however infeasible cases were not reached.

In (4.17) a single objective is present, which is the devices minimal operation cost. The thermal comfort is implemented by including the hard constraints (4.8), (4.9), and (4.10). Such optimization problem is used in Chapter 5 as

	$N = 24$	$N = 8760$
decision variables	600	219000
equality constraints	480	175200
inequality constraints	408	148920
YALMIP parsing time	2.2 sec	4.4 min
Cplex solving time	0.5 sec	14.4 min

Table 4.2: The optimization problem representing the HyGCHP system operation is solved on the short term and on the long term on a 1.6 GHz quad-core intel CORE i7 machine with 4 MB RAM.

well as with some additions in Chapter 6. In Chapter 7, due to methodology limitations, the optimization problem is transformed to a QP, (2.3), and a double-objective function is introduced incorporating both devices operation cost and thermal comfort. In that case, instead of implementing thermal comfort by including hard constraints, it is implemented by penalizing the deviation of a decision variable from a reference value.

Chapter 5

HyGCHP system with thermally non-interacting borehole heat exchangers

This chapter is partially based on the publication:
Antonov, S., Verhelst, C. and Helsen, L. (2014). Should the optimization horizon in optimal control of ground coupled heat pump systems cover the inter-seasonal time scale?. *ASHRAE Transactions*, 120(2):346–356.

This chapter presents three studies on the optimal operation of the HyGCHP system described in Chapter 4 incorporating a single BHE, which is equivalent to a series of thermally non-interacting BHEs, in order to show the optimal operation methodology developed in this dissertation. One aim is to obtain and investigate the annually optimal operation profile of the system and to find how this profile can be reproduced by a realistic control strategy. Another aim is to investigate whether the HyGCHP system with a BHE uses the underground as a heat source/sink or as a thermal storage medium. The chapter begins with an introduction to these topics (Section 5.1). Further, an optimization framework is developed for obtaining the integrated short-and-long-term optimal system operation (Section 5.2). Then an MPC strategy is elaborated which reproduces the long-term optimal system operation profile (Section 5.3). The exact manner of optimal exploitation of the geothermal part is investigated through a modification of the developed methods (Section 5.4). The results of

the three studies are presented in the corresponding sections mentioned above. The chapter finalizes with overall conclusions for this case (Section 5.5).

5.1 Introduction

GCHP systems are ideally suited for buildings requiring both heating and cooling. The heat injected to the ground in summer recharges the ground for the heating season. And vice versa, heat extraction from the ground in winter cools down the ground such that one can make more use of passive cooling in summer. One of the important questions to be answered is how to operate the system when the building heating and cooling loads are imbalanced. Should we prevent ground thermal buildup in the case of a cooling dominated building? Should we restrict the use of passive cooling in order to balance the annual heat injection and extraction loads? Is it advantageous to extract more heat by the heat pump during the heating season, in order to have a colder ground at the start of the cooling season (actively "pre-cooling" the borefield)? Should we inject more heat than strictly necessary during the summer in order to have a higher ground temperature at the start of the heating season (actively "pre-heating" the borefield)?

Research on the optimal operation of GCHP systems is a relatively new area, which has gained interest with the rise of HyGCHP designs. The HyGCHP systems have a lower investment cost than conventional designs since their most expensive component, the BHE, which exchanges heat with the ground, is sized to cover only the heating or the cooling demand entirely, depending on which of the two is smaller. The downside is that the HyGCHP systems are more complex to operate since it should be additionally decided when and how to use the supplementary heating or cooling device.

In this study an optimization framework is adopted to address these questions. This approach radically differs from the approach adopted in most studies in two ways.

First, in most studies the controller is designed based on a set of heuristic rules with a number of tunable control parameters (like in RBC). Its influence on the system performance is assessed by multi-year system simulations in a dedicated simulation environment such as TRNSYS (TESS, 2006). The control is fine-tuned by varying the set of rules and/or by tuning the corresponding control parameters. This fine-tuning can be done through a trial-and-error-approach (Sourbron and Helsen, 2014), which can be relatively time-consuming, or through a derivative-free optimization tool such as GenOpt (Peeters, 2009). The drawback remains, however, that the tuning of the controller can only be

optimized for a limited subset of possible control actions, defined by the chosen set of heuristic rules. An optimization framework, by contrast, allows defining the control action at each point of time such that the control objectives are optimally met, under the constraints given.

Second, most studies on HyGCHP operation assume that the building heating and cooling demand profiles are given (De Ridder et al., 2011). The opportunities at building side for peak shaving (decreasing peak energy demand by anticipating the extreme needs and applying control actions in advance) and load shifting (making use of energy storage in order to apply control actions during low tariff periods) to minimize the energy cost, for instance, are thus not deployed. In this study, the control is optimized from an integrated building perspective, including the thermal dynamics at building side. This allows the controller to further reduce energy cost by shaping the heat and cold production profile based on the installed capacity of the different heating and cooling devices, the electricity price profile, and the available opportunities for (active or passive) thermal energy storage also at building level. A relevant integrated system approach for optimal operation of a HyGCHP system with solar thermal energy storage is presented e.g. by Franke (1998), however, the author investigates optimal system operation through system design optimization, whereas the current study focuses on system control optimization.

In this chapter the proposed optimization approach is applied to the HyGCHP system in a cooling dominated office building with concrete core activation (CCA), as described in Chapter 4. In the field of GCHP systems the ground is typically regarded as a storage medium: the heat extracted during winter for heating the building serves at the same time at "storing cold in the ground for summer" (and vice versa). These processes will be referred to as seasonal underground thermal energy storage (SUTES) further in this dissertation. Two types of SUTES are defined in this chapter, depending on the way they are performed: "basic SUTES" and "additional SUTES".

Basic SUTES refers to the normal utilization of the BHE to cover the instantaneous building heating and cooling demand. Such type of GCHP system operation results in a seasonal borefield temperature variation, which arises from the normal synergy of combining heating and cooling.

Additional SUTES refers to BHE utilization on top of the normal heating and cooling demand of the building. This might happen, for example in a cooling dominated case, by extracting more heat during winter than instantaneously needed, in order to increase the potential to inject heat during summer.

If the BHE is not sized to enable recovery from imbalanced heating and cooling loads, there are two options for the HyGCHP system control when the cooling

demand exceeds the BHE heat injection capability: to operate the supplementary chiller, or to apply additional SUTES in advance.

5.2 Annually optimal HyGCHP system operation: Short And Long Term Optimization (SALTO)

This section presents the method developed to obtain the HyGCHP system optimal operation profile on the long-term perspective (focused on annual thermal balance of the ground) when integrated with the short-term perspective (achieving the desired thermal comfort in the building while minimizing system operation cost). In fact, having described in Section 4.1 the system setup and in Section 4.2 the base of the optimization framework used throughout Chapters 5 and 6, the SALTO method is almost completely formulated. Few additions remain, which are given in Subsection 5.2.1 below. Then the results of applying the SALTO method for the different system design scenarios are presented in Subsection 5.2.2.

5.2.1 SALTO method

Next to minimizing system operation cost and fulfilling the desired thermal comfort level, the third main goal of the optimal system operation is to maintain long-term thermal balance of the BHE. This is desired in order to ensure that the BHE will be able to cover the imbalanced building heating and cooling demand after multi-annual system operation, without being overheated or thermally depleted. The optimal HyGCHP system operation, which achieves multi-annual thermal balance of the BHE is found by solving the optimization problem (4.17) over a horizon of one year and imposing annually cyclic boundary conditions on the ground temperatures by adding the equality constraints (5.1).

$$T_j(0) = T_j(8760), \quad \text{for } j = 1, 2, \ldots, 11 \tag{5.1}$$

By adding the constraints (5.1) to the optimization problem (4.17) the exact annually cyclic ground temperature values are not imposed. For that reason they could be called free annually cyclic boundary conditions. Those are free because their exact values are generated by the optimization solver and show what the optimal state of the ground is, which can be repeated year after year by keeping the BHE thermally balanced. The method is called “Short and Long Term Optimization” (SALTO) since it combines optimization at short term (system’s daily dynamics, using a sampling time of one hour) and long term (ground dynamics over one year, using 8760 time samples).

The approach with imposing free annually cyclic boundary conditions on the ground node temperatures is an abstraction and does not have a direct analogue in practice because there the meteorological weather conditions do not repeat annually and at the moment of installing a BHE the ground temperatures have either undisturbed values or they have been arbitrarily disturbed by other influencing factors. Below the motivation behind using such an abstraction is formulated.

One of the main goals of the current study is to investigate additional SUTES for the case of freely optimized hourly building loads. For that reason the intention is to isolate the system setup from influences of weather inter-annual trend or year-to-year intra-annual differences as well as to prevent the optimization from compensating imbalanced building heating and cooling demand by ground thermal build-up or depletion. The optimal solution obtained by using such simulation and optimization setup allows analysis solely related to basic and additional SUTES achieved by optimizing the hourly building loads. This way the expectation is to look for principles of operation and to discover and analyze optimal control patterns. Once revealed, such principles and patterns could be translated to practice. Then with the inter-annual weather variations it is logical to expect inter-annual ground temperature variations, which are, however, not related to ground thermal build-up or depletion as a consequence of compensating imbalanced building heating and cooling demand.

A real HyGCHP system, installed and started at the state of undisturbed ground, would also follow initial inter-annual ground thermal transient process. Afterwards the ground node temperatures are expected to approach their more stabilized annual profiles which are expected to be similar to the ones obtained by optimization with imposing free annually cyclic boundary conditions.

Imposing exact periodicity of the ground node temperatures might appear a too strict condition. One possible alternative is imposition of soft constraints by penalizing the deviation of $T_j(8760)$ from $T_j(0)$. Another possible alternative is imposing periodicity of averaged ground node temperatures over time periods of a suitable length. However, given the nature of the optimization problem (4.17), each degree of freedom can and will be used for compensating the imbalanced building heating and cooling demand because that will decrease the objective function value. This will result in non-cyclic ground node temperatures and the chance to analyze the effects solely dependent on basic and additional SUTES will be lost.

5.2.2 SALTO results

This section presents the results for the annually optimal HyGCHP system operation computed using the SALTO method for three design scenarios, previously described in Sections 4.1 and 4.2: (1) Initially sized system (GCHP system feeding a 108 m^2 office area coupled to a 121 m deep BHE); (2) Same BHE feeding a larger office building area (212 m^2 office area coupled to a 121 m deep BHE); (3) Alternative installation and operation of the primary and supplementary cooling devices.

In the first design scenario SALTO is performed for the initial system configuration, for which the building heating and cooling loads could be entirely covered by the BHE, by means of heat pump heating and passive cooling. This scenario corresponds to a hydronic serial connection of the heating and cooling devices, in which the chiller is the first cooling device if operating simultaneously with the passive cooling heat exchanger. (4.11), (Figure 4.7). Cyclic boundary conditions are imposed on the ground temperatures. The office zone air temperature T_Z is kept between the comfort boundaries (Figure 5.1). Exceptions are on the one hand the periods leading to the daily allowed 0.4 Kh of thermal discomfort during the occupation hours. This leads to a total annual discomfort of 80 Kh while the standard (CEN, 2007) allows 104 Kh for an office Category II. On the other hand there are deviations during periods without occupancy of the office when comfort evaluation is not a criterion.

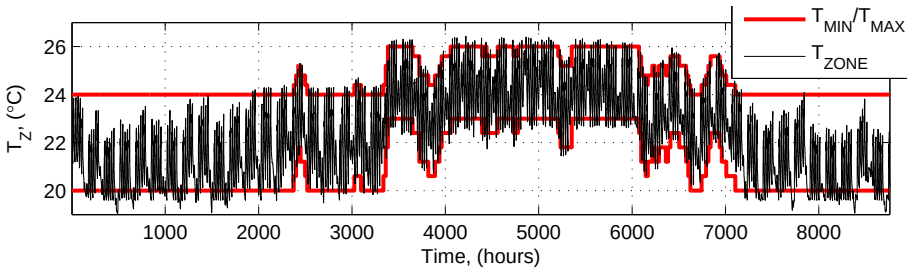

Figure 5.1: In the annually optimal HyGCHP system operation the office zone air temperature is kept between the comfort boundaries with a few deviations allowed by the thermal comfort standard.

The heat pump has an on/off control profile (Figure 5.2) due to the linear term of operation cost in the objective function. On the contrary, although having a linear operation cost term in the objective function too, the passive cooling operation not always hits its capacity upper bound. Instead, the PC is dictated

by constraint (4.11)—$T_{Fluid,Out}$ rises to a level, above which passive cooling is not feasible.

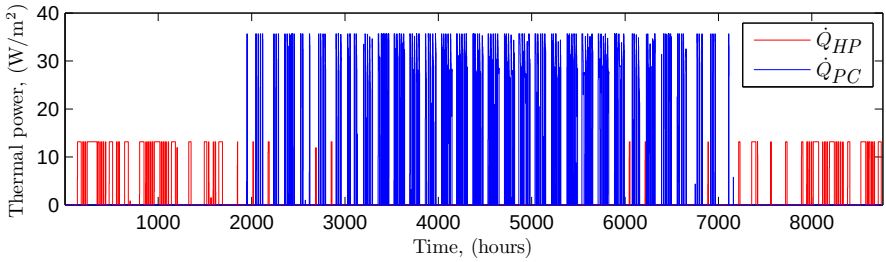

Figure 5.2: In the optimal operation of the HyGCHP system sized with a large enough BHE the building loads are entirely covered by heat pump operation and passive cooling, without operating the supplementary devices.

The temperatures of the ground storage volume (Figure 5.3) are annually cyclic. Their mean values are above the undisturbed ground temperature ($T_{GR} = 10°C$) due to the cooling dominated loads. The annual net heat injection to the BHE amounts to 0.81 kWh per m^2 office area, which dissipates in the ground adjacent to the storage volume.

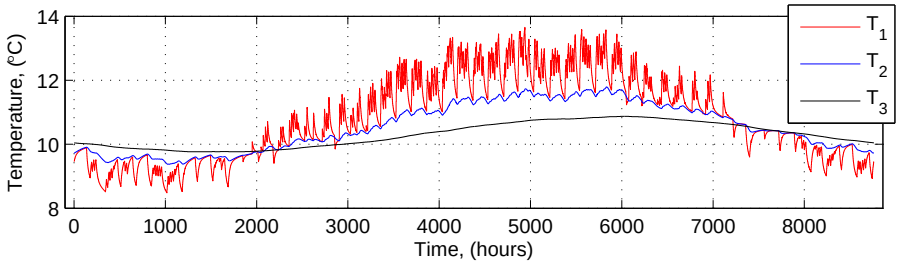

Figure 5.3: The annually optimal ground node temperatures have annually periodic profiles with a mean value above the undisturbed ground temperature $T_{GR} = 10°C$ in order to dissipate the heat of the dominating cooling loads of the building. (See Figure 4.3 for location of T_1, T_2, T_3.)

In the second scenario the same BHE feeds a larger office area (212 m^2 office area coupled to a 121 m deep BHE) requiring the supplementary devices to assist in supplying the required loads. Similarly to the heat pump operation the chiller has also an on/off control profile (Figure 5.4) due to the linear term of operation cost in the objective function. Gas boiler operation is not required

due to the cooling dominated office loads. The annual ground temperature profiles are similar to the ones from the previous scenario (Figure 5.3) but their magnitude is increased. The annual net heat injection to the BHE amounts to 1.26 kWh per m^2 office area.

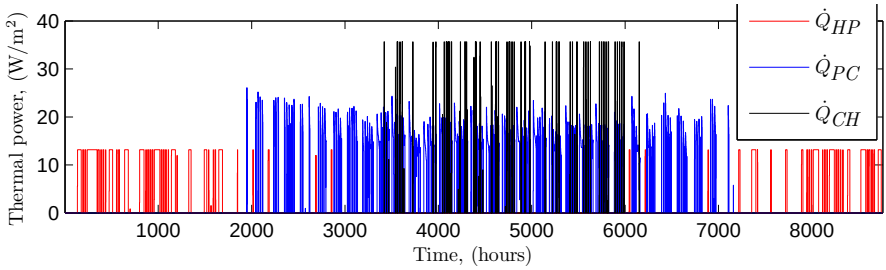

Figure 5.4: In the optimal operation of the HyGCHP system sized for larger office area for the same BHE the supplementary chiller compensates for the insufficient passive cooling capacity.

Due to the fact that the chiller acts before passive cooling in the serial hydronic connection, when simultaneous operation of the two installations is needed a particular profile is observed (Figures 5.5 and 5.6). In any case, the system should be able to cover the required cooling peaks while keeping the minimal difference between T_{WS} and $T_{Fluid,Out}$, (4.11), (Figure 4.7). In the period of simultaneous operation the passive cooling power decreases (Figure 5.5). The reason behind is that the water coming from the CCA (Figure 4.7) is already pre-cooled (by the chiller) when entering the passive cooling heat exchanger. Thus, the optimal solution is that the cooling peak is covered by increasing the share of the chiller, while the share of passive cooling is decreased to satisfy (4.11). In Figure 5.6 $T_{F,Out,max}$ represents the maximal $T_{Fluid,Out}$ according to the minimal difference relative to T_{WS}. This value ($T_{F,Out,max}$) is reached by $T_{Fluid,Out}$ in multiple periods.

In the third scenario the set up from the previous one is inherited, except for the passive cooling feasibility constraint. Passive cooling acts now as the first device and the chiller as the second one in the serial hydronic connection, (4.13), (Figure 4.8). It can be observed (Figure 5.7) that the passive cooling power does not decrease during the simultaneous operation and the chiller delivers less power compared to the alternative system configuration (Figure 5.5). The difference between the supply water temperature and the BHE outlet fluid temperature decreases below 3°C (Figure 5.8) but this is caused by chiller operation as second device after passive cooling as first device, therefore it is realistic. Although the chiller is less efficient when applied as second installation

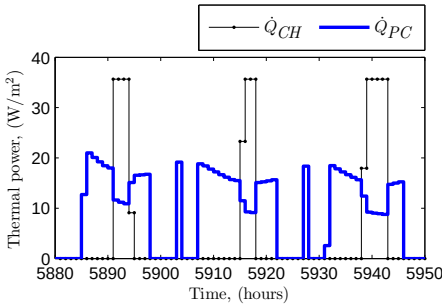

Figure 5.5: Operating chiller as the first cooling device in the serial hydronic connection leads to decreased passive cooling share.

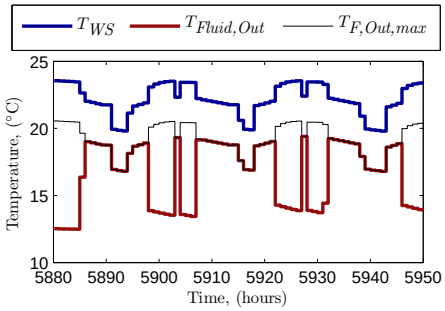

Figure 5.6: The decreased passive cooling share is caused by the too low supply water temperature as a result of chiller operation.

in the series, the annual load it covers is decreased by 11% in that case, while the share of Passive Cooling, which is much cheaper, is increased. As a result the annual primary energy use for the entire system operation is reduced by 1.3%.

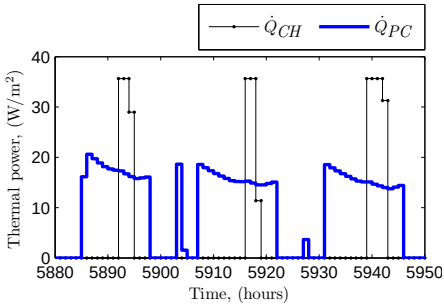

Figure 5.7: Operating passive cooling as the first device in the serial hydronic connection allows exploiting the full potential of passive heat transfer to the BHE.

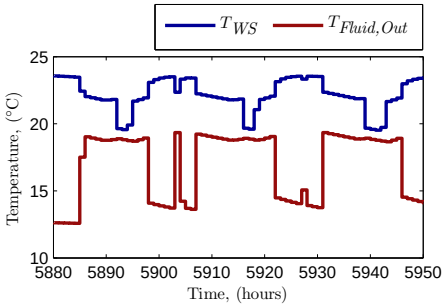

Figure 5.8: Chiller operation on top of passive cooling can further decrease the supply water temperature without affecting chiller operation.

5.3 Weekly optimal HyGCHP system operation: Short Term Model Predictive Control (STMPC)

This section presents a method to investigate how the annually optimal SALTO solution can be reproduced with a short-term control strategy. First, in Subsection 5.3.1 the details of the considered STMPC are presented followed by a description of several indicators used for the intended performance comparison. Then, in Subsection 5.3.2 the results for the HyGCHP system operated by STMPC are compared to the SALTO profiles obtained above.

5.3.1 STMPC method

The considered short-term control strategy is MPC with a prediction horizon of 1 week, which recedes with 1 day at each MPC iteration, having a sampling time of 1 hour. Therefore, after obtaining the optimal solution of the MPC optimization problem of each iteration, the first 24 samples of the control inputs are applied in an open loop control concept and the horizon of the next iteration is receded with 24 time samples, (Figure 5.9). The optimization problem solved

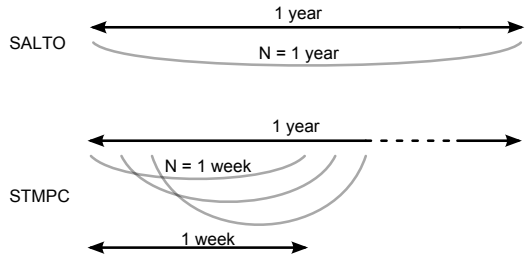

Figure 5.9: The integrated Short-And-Long-Term Optimization (SALTO) method finds the optimal system operation profiles by optimizing over the entire annual horizon at once. Unlike the SALTO, the annual system operation profiles resulting from applying a Short Term Model Predictive Control (STMPC) strategy are calculated by iteratively optimizing the system operation over a receding weekly horizon.

within each MPC iteration is also based on the formulation in Section 4.2 for a HyGCHP system with 212 m^2 of office area coupled to a 121 m deep BHE and passive cooling operating as first cooling device in the serial hydronic connection (Scenario 3). Hence, the optimization problem is almost identical to the one of SALTO (Section 5.2), with difference in the prediction horizon length and in the constraints. Annually cyclic boundary conditions are not imposed because

the approach is to compute the annual system operation profile by starting at initial conditions and iteratively receding the prediction horizon. The specific length of one week for the optimization horizon is chosen to be comparable to the time needed for the slowest thermal transient processes in the building to converge. A prediction horizon of three days (which is not presented) has been shown to be too short. The method is called Short Term MPC (STMPC) since it optimizes only the system's daily and weekly dynamics, using a sampling time of 1 hour.

In order to answer the question whether the SALTO solution, which is by definition cyclic over one year, can be reproduced with STMPC, for the first iteration of the STMPC all system states are initialized to the final states of the SALTO optimal solution. The solution obtained by SALTO will serve as a reference for the multi-annually optimal system performance. This way it can be investigated to which extent the system operation computed with STMPC deviates from the annually optimal system operation obtained by SALTO, or whether the two approaches lead to the same results.

By setting the prediction horizon for STMPC to one week, the optimization procedure does not have information about the annual profiles of the disturbances and therefore does not have any incentive to optimize system operation on the inter-seasonal time scale. The system performance achieved by applying STMPC will be governed only by short-term system operation cost and satisfying thermal comfort requirements. The STMPC solution will serve as a reference for system performance without additional SUTES.

The results for operation of the HyGCHP system controlled by STMPC are compared to the reference results obtained by SALTO by defining and comparing the following performance indicators:

- annual system operation cost, [€];
- annual thermal discomfort, [Kh] (Kelvinhours). The thermal discomfort for each time interval is the duration, [h], of the time interval multiplied by the deviation, [K], of the zone air temperature T_Z above the upper comfort bound T_{MAX} or below the lower comfort bound T_{MIN};
- ground thermal buildup, [°C], over a one-year period evaluated at all nodes of the ground model as the difference between the temperature of the node at the end of the year $T_j(8760)$ and the temperature of the node in the beginning of the year $T_j(1)$, therefore, an 11-values vector;
- annual heat/cold, [kWh_{th}], delivered to the building by each heating/cooling device;

- annual net heat transfer with the BHE, [kWh_{th}], calculated as the difference between the total annual heat extraction from the ground and the total annual heat injection to the ground.

5.3.2 STMPC results

In this subsection the system performance obtained with STMPC is compared to the system performance obtained with SALTO. For SALTO the ground thermal buildup is by definition zero, imposed by optimization constraints that the ground temperatures have annually cyclic values. For STMPC there might be ground thermal buildup, since the long-term performance criterion (cyclic boundary conditions on the ground temperatures) is not imposed in the optimization problem formulation. Due to the receding horizon of the STMPC, cyclic boundary conditions over one year cannot be imposed.

For the three performance indicators—energy cost, thermal discomfort, ground thermal buildup—the difference between STMPC and SALTO is negligible (Table 5.1). STMPC is marginally more expensive (0.04%) and provides slightly better thermal comfort than SALTO, but it also slightly raises the ground temperatures. For both cases the heat delivered by the heat pump is equal and the gas-fired boiler remains unused. STMPC however makes slightly more use of the passive cooling, and less use of the chiller. Generally, the annual performance indicators reveal no major differences between SALTO and STMPC.

It is also important to present the level of agreement along the investigated operation of one year, not only to evaluate annual performance indicators. More specifically, the aim is to check whether there is a potential for optimization of the system operation cost by varying the control profiles on the inter-seasonal time scale, which would result in additional SUTES. To this end, the profile for the BHE loads obtained with STMPC (one-week prediction horizon) is compared to the operation profile of the SALTO (one-year prediction horizon). The result of sample-wise subtraction of the SALTO profile for BHE loads from the STMPC profile represents a measure of the additional BHE loads which occur if switching from SALTO to STMPC. These load differences are lumped on a weekly basis in order to cancel the daily differences and to focus on differences on the inter-seasonal time scale. The results show that the differences between the two BHE load profiles do not represent a pattern related to the inter-seasonal time scale (Figure 5.10). Instead, the differences occur in particular weeks and cancel each other within neighboring weeks. This means that on the long term the STMPC tends to reproduce the system behavior given by the SALTO. The remaining differences (for instance in weeks 24, 27, 28, and

Indicator		SALTO	STMPC	Increase	Increase, [%]
Annual system operation cost, [€/m^2]		1.0267	1.0271	+0.0004	+0.04
Annual thermal discomfort, [Kh]		82.29	81.55	−0.74	−0.9
Ground thermal buildup, [K]	Node 1	0	0.0327	+0.0327	—
	Node 2	0	0.0312	+0.0312	—
	Node 3	0	0.0288	+0.0288	—
	Node 4	0	0.0244	+0.0244	—
	Node 5	0	0.0144	+0.0144	—
	Node 6	0	0.0048	+0.0048	—
	Node 7	0	0.0079	+0.0079	—
	Node 8	0	0.0060	+0.0060	—
	Node 9	0	0.0037	+0.0037	—
	Node 10	0	0.0006	+0.0006	—
	Node 11	0	0	+0	—
Heat pump operation, [kWh$_{th}$/m^2]		14.36	14.34	−0.01	−0.09
Gas boiler operation, [kWh$_{th}$/m^2]		0	0	+0	—
Passive cooling operation, [kWh$_{th}$/m^2]		36.22	36.59	+0.37	+1.02
Chiller operation, [kWh$_{th}$/m^2]		2.8	2.6	−0.2	−7.26
Annual net heat transfer with the BHE: extraction−injection, [kWh$_{th}$/m^2]		−24.26	−24.64	−0.38	−1.56

Table 5.1: Comparison of annual system performance indicators resulting from STMPC to the corresponding indicators resulting from SALTO. The two approaches lead to identical system performance.

29) show the slightly higher share (1.02%) of passive cooling when STMPC is applied, which leads to a minor increase of the ground temperatures.

Analysis of the SALTO solution allows to investigate whether the optimal HyGCHP operation on the inter-seasonal time scale makes use of additional

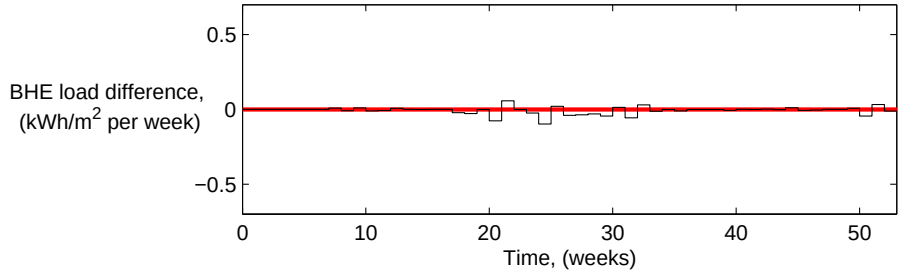

Figure 5.10: Difference between the borehole heat exchanger load profiles obtained with STMPC (receding prediction horizon of 1 week) and SALTO (one year prediction horizon). There are no differences on the inter-seasonal time scale.

SUTES by actively pre-cooling or pre-heating the ground. This pre-cooling or pre-heating could be achieved by increasing the use of the heat pump in winter and the use of the passive cooling in summer, hence pushing the building temperatures respectively towards their upper and lower boundaries.

The fact that the optimal solution from SALTO is reproduced by the STMPC while the STMPC by definition cannot optimize the BHE loads on the inter-seasonal time scale implies that there is no additional SUTES in the annually optimal SALTO solution. The degree of freedom in SALTO to apply additional extraction during winter by shifting the zone air temperature as close as possible to the upper thermal comfort bound is thus not used (Figure 5.11). The heat extraction from the BHE during the heating period, by means of heat pump heating, is not more than strictly needed to satisfy the thermal comfort requirements. T_Z is kept close to the lower comfort bound. No additional heat

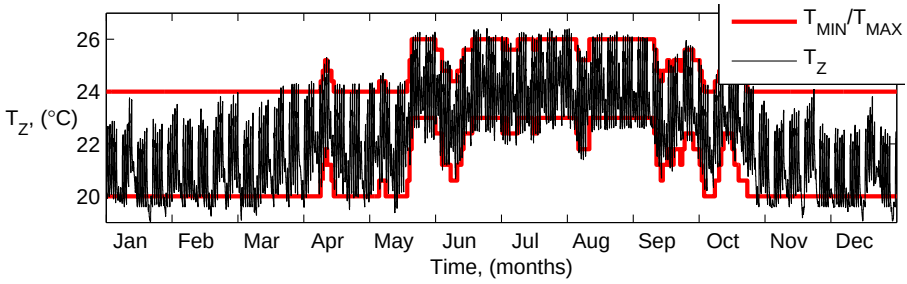

Figure 5.11: Office zone air temperature profile resulting from SALTO (similar for STMPC). The controllers do not make advantage of the entire thermal comfort bound to apply additional underground thermal energy storage.

extraction during winter is observed to store cold in the ground for use during summer by means of passive cooling in order to decrease the usage of the less efficient chiller. Since additional SUTES is possible but it does not occur, it is investigated in the next section which factors could make additional SUTES financially attractive.

The lack of ground thermal buildup in the STMPC annual profiles is a consequence of the ground node temperatures initial conditions for STMPC and the lack of incentive in the SALTO to inter-seasonally optimize the HyGCHP system operation. The STMPC simulation is started using initial values for the ground node temperatures T_j taken from the optimal SALTO solution, which is obtained incorporating free annually cyclic boundary conditions on T_j. Given the optimal SALTO solution for a particular case of HyGCHP system and particular meteorological weather data, these temperatures are the optimal temperatures which will be repeated year by year in case the meteorological weather conditions are repeated and the annual HyGCHP system control is performed optimally, as also explained in Subsection 5.2.1. Since there is no inter-seasonally related optimization pattern in the SALTO solution and the weekly long optimization in STMPC is long enough to include the required system dynamics, optimizing with a receding 1-week horizon results in the same BHE usage as if optimizing the entire 1-year operation at a time. For these reasons, starting from the optimal ground node temperatures taken from the SALTO solution, the STMPC results in annually cyclic ground temperatures as well. Would meteorological weather changes occur, thermal buildup or depletion is expected to be observed up to solely reflecting the weather changes, but not due to imbalanced annual heating and cooling loads.

5.4 Analysis of SUTES through a modified SALTO

This section aims at analyzing the HyGCHP operation performance for the case characterized by additional SUTES, as well as to find out the conditions causing additional SUTES to become financially attractive. The method, presented in Subsection 5.4.1, includes four steps. First, additional SUTES is forced by including an exaggerated underestimation of the chiller energy efficiency ratio. Then several indicators are introduced for analysis of the results obtained. Third, the exact $EER_{CH,critical}$ is searched, which triggers the system to incorporate additional SUTES. Last, the experiments of the third step are repeated for cases of different ground conductivity. The results of these steps are presented in Subsection 5.4.2.

5.4.1 Modified SALTO method

The first experiment is performed to evaluate the system performance in the case of enhanced deployment of the seasonal storage capacity of the ground. The aim is to analyze the impact of promoting higher shares passive cooling in summer through increased ground pre-cooling in the heating season. To this end, the use of the chiller is artificially decreased by replacing EER_{CH} in the cost function (4.7) by a modified value ($EER_{CH,m}$), which in this experiment is a large arbitrary modification:

$$EER_{CH,m} = \frac{EER_{CH}}{1000} \tag{5.2}$$

The solution of the SALTO with an $EER_{CH,m}$ which is 1000 times smaller than the original EER_{CH} is named "modified SALTO" and it is characterized by additional seasonal cold storage through additional heat extraction from the ground during winter and using the stored cold to cover the dominating cooling loads during summer. The corresponding annual system operation cost of the modified SALTO is post-computed with the original SALTO cost function (4.7).

The results for operation of the HyGCHP system controlled by the modified SALTO are compared to the reference results obtained by the original SALTO by defining and computing the following performance indicators:

- increase in annual heat/cold, [$\mathrm{kWh_{th}}$], delivered to the building by each heating/cooling device;
- increase in annual operation cost, [€] of each heating/cooling device;
- increase in annual load of the system including all devices, [$\mathrm{kWh_{th}}$];
- increase in annual operation cost of the system all devices, [€];
- increase in annual heat extraction from the BHE, [$\mathrm{kWh_{th}}$];
- increase in annual heat injection to the BHE, [$\mathrm{kWh_{th}}$].

As the results will indicate, operating the air-coupled active chiller is a cheaper alternative than additional SUTES to cover the imbalanced heating/cooling loads. For this reason, the second experiment is intended to show how far the chosen $EER_{CH,m}$ is from its critical value which would trigger the SALTO to incorporate additional SUTES. The $EER_{CH,critical}$ is estimated by computing several SALTOs starting from $EER_{CH,m} = EER_{CH}$ and each time decreasing the $EER_{CH,m}$.

A measure of the degree of additional SUTES to which the SALTO is forced by imposing a decreased $EER_{CH,m}$ will be the total annual heat extraction load from the BHE. Therefore, a reference value for the degree of storage which occurs with the original $EER_{CH} = 4$ in the cost function is the total annual heat extraction load from the original SALTO. The results will show how these loads increase with decreasing the $EER_{CH,m}$.

The experiments for determining $EER_{CH,critical}$, below which additional SUTES becomes economically beneficial, are repeated for lower ground thermal conductivities λ in order to see how much such conditions will add to the potential for additional SUTES. Since the BHE model (Section 4.1) is constructed based on Eskilson's guidelines, it is possible to locate the parameter λ in the elements of the BHE state space model matrices. By modifying these matrix elements accordingly, the corresponding new BHE models are derived. As described in Section 4.1 the original parameter is $\lambda = 1.9$ W/(mK). Two new BHE models are created, representing $\lambda = 0.95$ W/(mK) (twice lower ground conductivity) and $\lambda = 0.38$ W/(mK) (five times lower ground conductivity).

5.4.2 Modified SALTO results

In this subsection the use of the BHE for seasonal cold storage is evaluated. This evaluation will allow to clarify why it is possible to follow the optimal SALTO profiles with a STMPC strategy and why the additional SUTES is not economically beneficial for the investigated system.

The presence of additional SUTES in the case of the modified SALTO can be detected by the raised office zone air temperature T_Z during winter (Figure 5.12), compared to the case of the original SALTO (Figure 5.11). In contrast to the zone air temperature profile of the original SALTO (Figure 5.11) T_Z is kept as close as possible to the upper comfort bound during the heating period in the case of the modified SALTO (Figure 5.12). This is a consequence of the additional heat extraction from the ground in order to use the stored cold during the cooling period. This inter-seasonal behavior can be visualized by computing the interval-wise difference between the two BHE load profiles (for modified SALTO and original SALTO) and by lumping the result on a weekly basis in order to focus on the inter-seasonal time scale (Figure 5.13). Unlike the lack of difference when comparing STMPC to the original SALTO (Figure 5.10), the comparison of the modified SALTO to the original SALTO shows additional heat extraction (heat pump operation) in the winter for storing cold and additional heat injection (passive cooling operation) for decreasing chiller operation by using the stored cold (Figure 5.13).

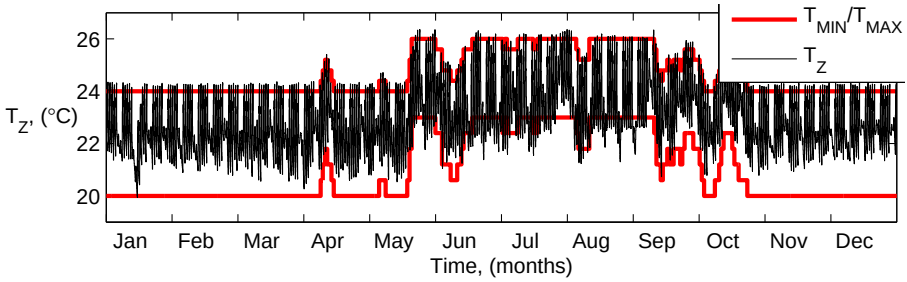

Figure 5.12: Office zone air temperature profile resulting from the modified SALTO. When the price for operating the supplementary chiller is artificially increased, the controller suggests additional underground cold storage to cover the excessive cooling loads.

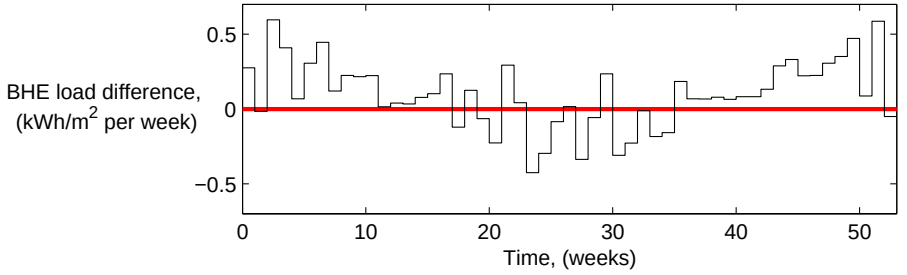

Figure 5.13: Difference between the BHE load profiles obtained with the modified SALTO (with a 1000 times underestimated chiller efficiency in the cost function (4.7)) and the original SALTO. The additional underground cold storage can be observed on the inter-seasonal time scale.

Quantification of the difference between the solutions for the original SALTO and the modified SALTO is performed by evaluating the annual system performance indicators (Table 5.2). The results show that the total heat delivered by heat pump operation has increased with 94% (almost doubled) in the modified SALTO solution. The corresponding heat extraction from the BHE provides the opportunity to increase the amount of passive cooling and thus decrease the use of chiller, which has a 1000 times lower efficiency than in practice.

With the modified SALTO the cooling demand is covered with almost only passive cooling, however, the total amount of cooling is increased with 13% compared to the optimal (original) SALTO. This effect has its explanation on the daily time scale. Since the maximal power of passive cooling is limited by the BHE properties and the prevailing temperatures (4.13), passive cooling is

	Annual Load Increase (from SALTO to Modified SALTO)		**Annual Operation Cost Increase** (from SALTO to Modified SALTO)	
	[kWh_{th}/m^2]	[%]	[€/m^2]	[%]
Heat Pump	+13.42	+94	+0.43	+123
Gas boiler	+0	—	+0	—
Passive cooling	+6.03	+17	+0.22	+43
Chiller	−0.88	−31	−0.04	−27
Total heating (HP + GB)	+13.42	+94	+0.43	+123
Total cooling (PC + CH)	+5.14	+13	+0.18	+27
Total operation (all devices)	+18.57	+35	+0.61	+59
Heat extraction from the BHE	+11.19	+94		
Heat injection to the BHE	+6.03	+17		

Table 5.2: Differences in some key factors when comparing the results from the modified SALTO (with additional seasonal underground thermal energy storage) to the results from the original SALTO. For the system specified the additional underground thermal energy storage is not economically beneficial.

started in advance to operate longer at less power, which slightly increases the total cooling load.

On the other hand, and more importantly, only half of the additionally extracted heat from the BHE, by increased heat pump operation during winter, is used for passive cooling during summer as additional heat injection to the BHE (Table 5.2). The other half of the stored cold is dissipated to the ground which surrounds the modeled storage volume. Hence, the efficiency of the underground cold storage, which could be defined as the ratio of the additional heat injection (6.03 kWh_{th}/m^2) to the additional heat extraction from the BHE (11.19 kWh_{th}/m^2), is only 54%. This result holds for the specific system investigated, more specifically for a single BHE, which is not thermally affected by other neighboring BHEs. However, Reuss et al. (1997) derived a similar

efficiency of 64% for underground heat storage with a full rectangular borefield, consisting of 140 BHEs, 30 m deep, located 2 m from each other. Such borefield can be seen as compact and expected to store thermal energy with a high efficiency. As reasons for the registered low efficiency in that case the high storage temperatures could be pointed (above 40°C) which would increase the heat losses to the surrounding ground. The characteristics of the thermally non-interacting BHEs investigated in this chapter differ substantially from the borefield characteristics in the case of Reuss et al. (1997). Nevertheless, the similar order of magnitude of the storage efficiencies is an indicator for the possible extrapolation potential of the results from the current chapter to other system designs.

The results show that when the BHE alone cannot completely cover the building cooling demand chiller usage is a cheaper strategy (original SALTO) than storing additional cold in the ground (modified SALTO, 59% more expensive system operation, Table 5.2). The strategy to use the chiller as stated in this chapter to be cheaper is relevant to those periods when after certain passive cooling usage the borehole outlet fluid temperature hits its upper bound (passive heat transfer to the ground is then no longer possible). Two alternatives exist to cover the remaining cooling demand: (1) to start the supplementary chiller; (2) in advance, to force additional SUTES in order to have a colder borehole for the cooling season. Then the BHE outlet fluid temperature will reach its upper bound after allowing more passive cooling. The results show that simply starting the chiller is cheaper than forcing additional SUTES. This observation confirms the presented results that there is no optimization potential at the inter-seasonal time scale, eliminating the need for a long-term prediction horizon within the optimal control problem for the specified system. This is the reason why an STMPC generates the same system operation profiles as the original SALTO.

By decreasing $EER_{CH,m}$ from the original value ($EER_{CH} = 4$, original SALTO) down to the unrealistic ten times lower value ($EER_{CH,critical} = 0.4$) there is still almost no change in the total annual extraction loads (Figure 5.14, $\lambda = 1.9$ W/(mK)). Only a further decrease of $EER_{CH,m}$ below the value of 0.4 leads to an increase in the total annual extraction loads, which is an indication for additional cold storage. All other parameters being equal, an $EER_{CH,m}$ value of 0.4 can thus be defined as the critical chiller energy efficiency ratio $EER_{CH,critical}$ below which additional SUTES can become important. Therefore, for realistic values of the performances of the ground coupled devices (HP and PC) and supplementary devices (CH and GB), it is energetically and economically better to combine the use of PC and CH for cooling dominated buildings, than to impose PC, without assistance of CH, by pre-cooling the ground in winter through additional HP operation.

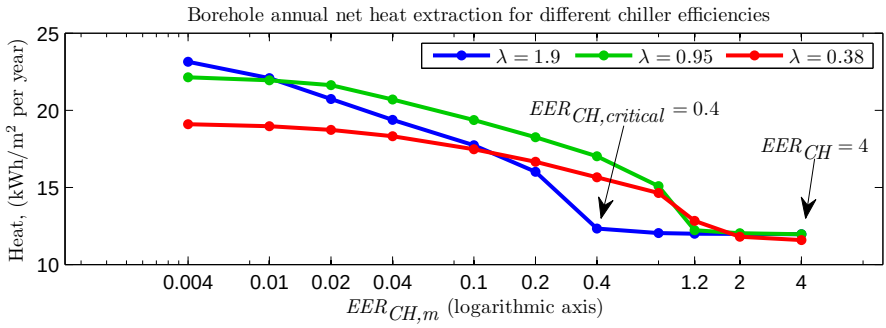

Figure 5.14: For reasonably high ground conductivities, additional seasonal underground thermal energy storage would be economically beneficial if the energy efficiency ratio of the chiller was at least ten times lower than in reality.

Decreasing the ground conductivity twice leads to $EER_{CH,critical} = 1.2$ (Figure 5.14, $\lambda = 0.95$ W/(mK)) and decreasing five times leads to $EER_{CH,critical} = 2$ (Figure 5.14, $\lambda = 0.38$ W/(mK)), which values are both still safely below the realistic $EER_{CH} = 4$, thus additional SUTES remains still not economically beneficial.

5.5 Conclusions

This chapter presents the HyGCHP system short-and-long-term optimal operation, its reproduction by a short-term control strategy and the fictive chiller efficiency which would trigger the system to incorporate additional seasonal underground thermal energy storage, for the case described in Chapter 4. The detailed conclusions of the three particular studies presented in this chapter follow below.

The wide range in time scales associated with GCHP systems asks for the combination of short- and long-term objectives when developing an optimal control strategy. This chapter presents an optimization of the heat and cold supply to office zones equipped with CCA based on weather and occupancy profiles for a reference year to achieve three main goals: (1) satisfying thermal comfort requirements in the office zones, (2) applying control signals that minimize the system operation cost, (3) retaining long-term thermal balance of the ground storage volume. Developing and solving a combined short- and long-term optimization (SALTO) allows analyses of the distribution of heating and cooling duties between the corresponding devices, guaranteeing a long-term

thermal balance of the ground storage volume, and thermal comfort inside the building at a minimal energy cost.

The long-term optimal solution, i.e. the control profile which satisfies the imposed thermal comfort level at the lowest annual energy cost and which can be repeated unaltered year after year (for the given weather and occupancy profile), is found by imposing cyclic boundary conditions on the ground storage temperatures. The results indicate that for a cooling dominated building the optimal operation is characterized by an annual net heat injection to the ground and mean ground storage temperatures which are higher than the undisturbed ground temperature. Passive cooling is constrained by the upper limit on the BHE outlet fluid temperature. Engaging passive cooling as first installation and active cooling as second installation in the serial hydronic connection is the cheaper of the two options when both installations are needed to run simultaneously.

There is no need to account for the inter-seasonal time scale when optimizing the control of the HyGCHP system investigated. It is sufficient to optimize the daily and weekly operation of the system only, which could be achieved by MPC with a receding horizon of one week.

There is no potential to further decrease the operation cost of the system by substituting supplementary chiller operation with additional seasonal underground thermal energy storage that allows more passive cooling. The amount of thermal energy storage resulting from optimally covering the weekly heating and cooling demand seems to be the optimal amount of thermal energy storage for the considered system of thermally non-interacting BHEs. The usage of the supplementary chiller to cover further cooling demand is a cheaper alternative than forcing additional cold storage, and could be started at any time and controlled with a weekly-optimal strategy. Forcing additional seasonal cold storage in the ground is less efficient because about half of the seasonally stored cold in the underground is lost in the far field ground before it could be reused. This could differ in cases with compact borefields where the BHEs are thermally interacting.

Chapter 6

HyGCHP system with a borefield

This chapter describes the investigation of the short-and-long-term optimal operation of the HyGCHP system in case the geothermal part consists of a borefield of thermally interacting BHEs, instead of a single BHE. The aim is to check whether for such system configuration additional seasonal underground thermal energy storage is an economically beneficial extension to the control strategy. The chapter starts with an introduction to this investigation (Section 6.1). For the purpose of this study a gray-box low-order short-and-long-term borefield model is obtained by variable time-scale system identification (Section 6.4). This method is based on an existing detailed borefield emulator (Section 6.2) and an existing system identification toolbox (Section 6.3). The HyGCHP system simulation/optimization setup is extended with an extra degree of freedom to store additional cold in the ground storage volume by rejecting heat to the ambient air (Section 6.5). At the end of this chapter the results of this case study are presented (Section 6.6), followed by conclusions (Section 6.7).

6.1 Introduction

For the annually optimal operation of the HyGCHP system with thermally non-interacting BHEs additional SUTES is not an economically beneficial control strategy (Chapter 5). The reason found was the high dissipation of the stored heat/cold for the case of thermally non-interacting BHEs. It remained an open

question whether SUTES can become economically beneficial if the geothermal part of the system is less dissipative, like for the case of borefield with a more compact configuration of the BHEs.

The developed SALTO method in Chapter 5 for evaluating the optimal performance of the HyGCHP system investigated was well suited with a low order state space model ($n \in [6, 11]$) of the geothermal part for the case of thermally non-interacting BHEs. Since in the current chapter the aim is to investigate the HyGCHP system's optimal performance for the case of a borefield, the ability of a low order state space model to accurately describe the BHE dynamics (Verhelst and Helsen, 2011) motivates to investigate a low order state space model of a borefield as well.

To investigate additional SUTES with the SALTO method described in Chapter 5 a borefield model is needed, which reflects the borefield dynamics on a time scale of at least 1 year sampled at a frequency of 1/h. In order to investigate the multi-annual system operation the SALTO method incorporates annually cyclic boundary conditions on the ground storage volume temperatures similarly to the method in Subsection 5.2.1. Therefore, the borefield model should also reflect the dynamics of the corresponding multi-annual time scale.

Unlike a BHE model, for which the dynamics allow system identification on the annual time scale and successful extrapolation to the multi-annual time scale (Verhelst and Helsen, 2011), a borefield model is expected to require system identification on a much longer time scale due to the thermal interaction between the individual BHEs. This difference in the dynamics has effect already in the first year of operation (Figure 6.1). The longer the operation time, the larger the divergence between the temperature profiles of a single BHE and a borefield.

Already for the case of a single BHE low-order state space model, the system identification with hourly sampled year-long data sets is computationally problematic (Verhelst and Helsen, 2011). Since the thermal interaction within a borefield has effect on the time scale from months to decades (Figure 6.1), for adequate modeling the system identification should cover this much longer time frame. Therefore, a specific system identification method is needed to cope with the large data sets of long borefield simulation times in combination with small sampling time. Such system identification method is developed in this chapter.

The specific system identification method is developed using existing software. For generating the system identification data sets a detailed borefield emulator model is used (Picard and Helsen, 2014a,b), which is characterized by high accuracy and low computation times for borefield dynamics simulated on a time scale of decades, sampled on a time scale of minutes. For estimating the

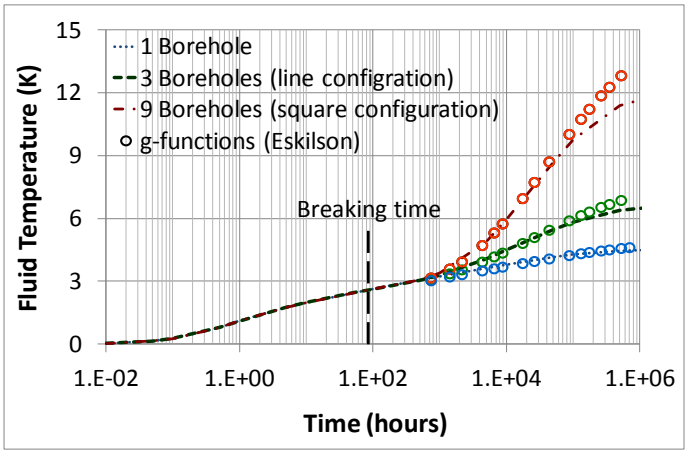

Figure 6.1: When injecting heat in a borefield the thermal interaction between the borehole heat exchangers leads to faster increasing fluid temperatures compared to a single borehole heat exchanger. *Image source: (Javed, 2012)*

borefield low-order state space model parameters a system identification toolbox is used (De Coninck et al., 2016), which is automated and flexible to estimate selected model parameters with conveniently re-sampled data sets.

In the current chapter the SALTO method is extended with an extra degree of freedom of the HyGCHP system to store cold in the ground by rejecting heat to the ambient air. The additional SUTES described in Chapter 5 was implemented by rejecting heat to the building as long as the office zone air temperature does not exceed the upper bound of the thermal comfort range. This possibility was exploited without using additional components in the HyGCHP system, thus it was straightforward and computationally effective, however providing limited additional SUTES capacity. In the current chapter the HyGCHP system is extended with a passive heat exchanger for heat rejection to the ambient air during winter in order to store more cold in the ground. This extension, together with the inclusion of a borefield, maximizes the chance for additional SUTES to become an economically beneficial control strategy.

6.2 Borefield emulator

The long-term training data sets for system identification of the borefield are generated using the detailed borefield emulator model of Picard and Helsen (2014a,b). This is a hybrid model which combines accurate representations of

both the short- and the long-term borefield dynamics including the thermal interaction between the BHEs. The model is implemented in Modelica (Elmqvist et al., 1998) and subsidiary external software tools. It allows for fast simulation (order of magnitude of minutes) of decades-long borefield operation with the flexibility to be easily configured for different borefield geometries and sizes. In this dissertation this detailed borefield model is called borefield emulator, since it is used to represent a real borefield. This representation allows for fast generation of decades long system identification data sets for a specific borefield configuration.

The short-term borefield dynamics are represented by a resistors-capacitors model, which reflects the heat transfer in the borehole components: heat carrier fluid, pipes, grout and immediately surrounding ground. The heat carrier fluid chosen (water or other) is represented by a corresponding fluid properties model from the Modelica Buildings library (Wetter et al., 2014). The thermal resistance between the fluid and the pipe is modeled using the correlation based method of Hellström (1991). The heat transfer between the internal pipe wall and the borehole wall is represented by the resistors-capacitors model of Bauer et al. (2011). The heat transfer between the borehole wall and the surrounding ground is modeled by discretizing the ground in one dimension (radially from the BHE) following the guidelines of Eskilson (1987) and applying a simplification of the heat conduction equation. This simplification assumes one-dimensional heat conduction and discretization in time, resulting in a resistors-capacitors model.

The long-term borefield dynamics are represented by the analytical solution of Javed (2012), which reflects the thermal interaction between the boreholes. The thermal interaction is implemented using spatial superposition of finite line sources. The model calculates the mean temperature of the borehole wall for the boreholes within the borefield.

The final hybrid borefield emulator of Picard and Helsen (2014a,b) is based on combining the borehole wall temperature step responses from the short-term and the long-term models. The long-term step response is lifted up to the short-term step response during a particular time period. This period starts when the transient process in the BHE is over and lasts until the thermal interactions between the boreholes start to appear in the long-term model step response.

Since the hybrid borefield emulator is meant to calculate the borefield temperatures during decades with a time step in the order of magnitude of minutes, the calculation is facilitated by the load aggregation method suggested by Javed (2012), described also by Picard and Helsen (2014a). The computational speed is increased by grouping heat loads into time intervals,

which duration is exponentially increasing.

The borefield emulator can be easily configured to represent different borefields. The type of BHEs within the borefield can be adjusted for co-axial pipes, single U-tube or double U-tube. The drilling pattern can be adjusted for different geometries, based on defining the coordinates and the depth of the BHEs.

The accuracy of the borefield emulator was validated by Picard and Helsen (2014a,b) both on the short term (50 hours of simulation) and on the long term (25 years of simulation). On the short term the emulator had good performance similarity compared to the dynamics of the sandbox experiment of Beier et al. (2011). The steady state deviation was expected due to the presence of an aluminum tube around the grouting in the sandbox experiment—9.5% deviation at the end of the simulation (2°C error at 21°C increase). Compared to the Modelica Buildings library model (Wetter et al., 2014) the deviation was 9.5% (2°C error at 21°C increase). Compared to the TRNSYS model (type 557b, see TESS, 2006) the deviation was 4.8% (1°C error at 21°C increase). On the long term the model was validated towards the g-functions of Eskilson (1987) and the infinite cylindrical heat source solution of (Bertagnolio et al., 2012). The borefield emulator had good accuracy for the case of a single borehole—5.4% error in borehole wall temperature after the 25 years of simulation (0.11°C error at 2.03°C increase) and a very good accuracy for the case of a line 8×1 configuration—0.9% error (0.08°C error at 9.1°C increase). Decreased accuracy was registered for the case of a full rectangular 8×8 configuration (64 BHEs)—13.7% error (6.5°C error at 47.5°C increase).

For the purpose in this dissertation and according to the accuracy described above, the borefield emulator is used for generating system identification data sets for up to 66 years of simulation for an open rectangular 3×3 configuration borefield (8 BHEs, no BHE in the center). The spacing between the BHEs is 5 m. Similarly to the BHE described in Section 4.1 the BHEs of the borefield in this section have a depth of 121 m, a header depth of 1 m, a borehole radius of 0.075 m, a tube radius of 0.02 m, a grout conductivity of 1.9 W/(mK), a grout volumetric heat capacity of 2400 kJ/(m^{3}K), and a grout density of 1785 kg/m^3. The specific heat of the calorimetric fluid is 4 kJ/(kgK), the density is 1000 kg/m^3, and the mass flow rate is 750 kg/h. The ground has a volumetric heat capacity of 2400 kJ/(m^{3}K), and a density of 1785 kg/m^3. System identification data sets are generated for three ground thermal conductivities: $\lambda = 3.5$, 1.9, and 1.6 W/(mK). These three values are used in order to represent a wider range of ground types, as found in (Di Sipio et al., 2013; Alishaev et al., 2012; Hamdhan and Clarke, 2010), as well as to compare the results to the case of thermally non-interacting BHEs (Chapter 5, $\lambda = 1.9$ W/(mK)).

6.3 System identification toolbox

The existing system identification toolbox used in this dissertation was originally developed by De Coninck et al. (2016) for the needs of simulation and control of buildings space heating and cooling. One purpose of the toolbox is to create gray-box building models for building heating and cooling loads forecasting, validated based on simulation performance. The other purpose of the toolbox is to create gray-box models for MPC of building space heating and cooling, validated based on k-step prediction performance. In this dissertation the toolbox is used to develop a borefield model instead, since the model structure is similar to the building model structure—resistors-capacitors grid.

The toolbox is composed of several modules:

- FastBuildings Modelica library (KU Leuven and 3E, 2014) with thermal zone models, HVAC components and building models;
- Different Optimica *.mop*-files (Åkesson, 2008) specifying the model components and the parameters to estimate;
- JModelica.org (Åkesson et al., 2010) for compiling the *.mop*-files and formulating and solving of the optimization problem;
- *Greybox.py* module, developed in Python (van Rossum, 1995), providing user interface and top-layer functionality.

The workflow of creating a model with the toolbox consists of several steps (Figure 6.2):

- Data handling: The available system identification- and validation data sets can be loaded, re-sampled and sliced. Slicing means creating different subsets of data, which can be used for multiple identification/validation steps in order to obtain a better model.
- Model selection: The system identification can be performed using different model structures or models with different sets of parameters to be estimated or fixed at provided values.
- Initial guess: Before estimation the parameters are initialized by randomizing several guesses within a specific statistical distribution around a given value for each parameter.
- Parameter estimation: Computation is performed with each set of randomized initial guesses. This increases the probability of converging

to good local minima in the NLP problem by still keeping a low number of trials.

- Validation: By using a specified slice of data the obtained models can be cross-validated.
- Model acceptance: The validation results for different models can be compared based on different accuracy criteria. The system identification can be repeated starting at different stages of the workflow until the best model is accepted.

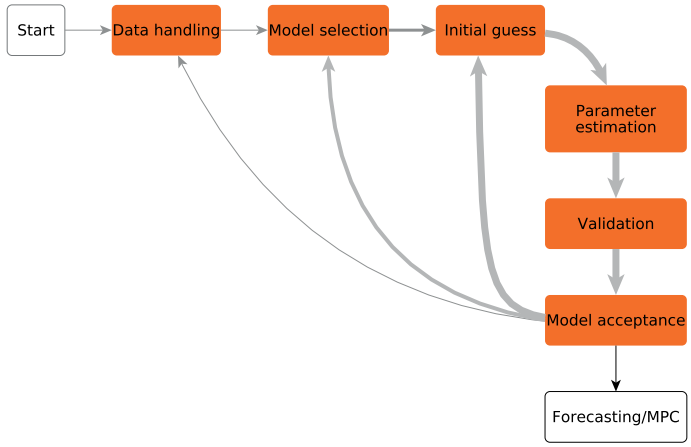

Figure 6.2: The flexible workflow of the toolbox allows for implementing custom system identification strategies. *Image source: (De Coninck et al., 2016)*

The parameter estimation within the toolbox is based on an optimization problem (dynamic programming) which minimizes the time-integrated quadratic deviation of the model output from measurement data. On low-level implementation the optimization uses the direct collocation method (Hargraves and Paris, 1987) to reduce the optimization problem to NLP. Algorithmic differentiation is performed using CasADi (Andersson et al., 2012) in order to obtain the first- and second-order derivatives of all expressions in the NLP. These derivatives are needed in third-party NLP solvers like IPOPT (Wächter and Biegler, 2006), which is called in a combination with a sparse linear solver like MA27 (HSL, 2013).

The characteristics of the system identification toolbox described above allow for designing a specific top-level system identification strategy. The toolbox is automated on the level of performing the different steps of the workflow. The user can customize the exact succession of steps and number of repetitions

with different settings, models and data subsets. Each single parameter estimation is represented as a unique *case* in the toolbox. For each *case* the entire corresponding information is saved (model structure, fixed parameters, parameter initial guesses, parameter final estimated values, etc.) and can be reused in future *cases*. This provides further flexibility of the toolbox and increases the chance of obtaining the best model.

6.4 System identification method

The developed system identification method represents an algorithm for a particular succession of system identification iterations. These iterations are needed in order to split in parts the too large nonlinear parameter estimation problem in case it is composed of a combination of decades long time frame and hourly sampling time. The iterative system identification method is implemented using the system identification toolbox described in Section 6.3 and a data set generated with the borefield emulator described in Section 6.2. The algorithm leads to obtaining a low-order borefield model having a resistors-capacitors structure. Each iteration is characterized by different sets of estimated model parameters and fixed model parameters, different time frame and sampling time of the data set. Several algorithms with different successions of system identification iterations were tested until the successful version presented in this section was found.

The low-order borefield model is based on a resistors-capacitors structure (Figure 6.3) represented as a linear state space model similarly to the BHE model (4.2, 4.3). The first borefield model input is the rate of heat injection $\dot{Q}_{BF}$, unlike the BHE model, for which the first input is the rate of heat extraction. This mismatch is caused for convenience of system identification—the detailed borefield emulator model also accepts heat injection rate as input. The second borehole model input is the undisturbed ground temperature T_{GR} at the outer boundary of the considered ground storage volume. Output of the model is the mean outlet fluid temperature of the borefield $T_{BF,Out}$. In the context of model structure (Figure 6.3) $\dot{Q}_{BF}$ is the thermal current through the thermal resistance R_0, T_{GR} is the thermal potential at the outer node of thermal resistance R_6 and $T_{BF,Out}$ is the thermal potential at the outer node of thermal resistance R_0. The model states (the thermal charge of the capacitors) represent the heat content of the borefield components and the ground volume, however, they do not have an exact physical meaning.

The development of a case-specific system identification procedure is caused

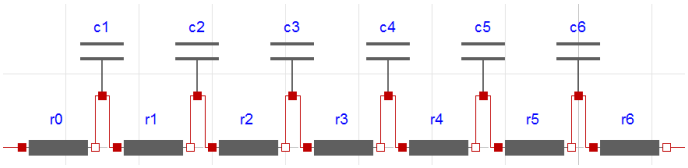

Figure 6.3: The low-order borefield model obtained is based on a resistors-capacitors circuit.

by the large time frame needed to represent the relevant borefield dynamics on the long term in combination with the fine sampling needed to represent the relevant short-term borefield dynamics, as motivated in Section 6.1. For a reasonable time frame representing the long-term borefield dynamics according to Figure 6.1, initially 70 years was chosen. In the case of hourly sampling, suitable for the short-term dynamics considered in the investigated HyGCHP system, such choice would result in a data set of 611,520 time samples and 13 parameters to estimate (7 thermal resistances and 6 thermal capacities, Figure 6.3). Given the fact that Verhelst and Helsen (2011) already experienced parameter estimation difficulties when having a data set of 4368 time samples for a similar model, the approach was adopted to develop an iterative, case specific system identification procedure based on data sets covering different time frames with different sampling time.

The length of the longest data set is limited by numerical characteristics of the system identification toolbox. Since the toolbox handles time data measured in seconds and because of the particular data type used in the low-level implementation of the toolbox, the maximum data set length which can be supported is 66 years.

Three data sets are used in the system identification algorithm in order to obtain a model which represents the borefield dynamics well from the hourly time scale to the multi-decades time scale. The data sets generated by the borefield emulator (Section 6.2) represent respectively: 66 years of simulation, afterwards re-sampled in the system identification toolbox with a 10 weeks sampling time, resulting in 343 samples; 5 years, re-sampled weekly, resulting in 260 samples; and 30 days, re-sampled hourly, resulting in 720 samples. All three sets represent borefield simulations started with the same initial conditions, being an undisturbed ground temperature of 10°C, when a step heat injection is applied.

The system identification algorithm that leads to a successful estimation of the borefield model parameters consists of the following system identification iterations, schematically depicted in Figure 6.4:

1. Estimate all model parameters ($R_j, j = 0 \dots 6$; $C_j, j = 1 \dots 6$) by system identification with the 66-years data set;

2. Fix parameters $R_j, j = 5 \dots 6$; $C_j, j = 5 \dots 6$ to the previous solution; Estimate parameters $R_j, j = 0 \dots 4$; $C_j, j = 1 \dots 4$ by system identification with the 5-years data set;

3. Fix $R_j, j = 4 \dots 6$; $C_j, j = 4 \dots 6$ to the previous solution; Estimate parameters $R_j, j = 0 \dots 3$; $C_j, j = 1 \dots 3$ by system identification with the 30-days data set;

4. Fix parameters $R_j, j = 0 \dots 4$; $C_j, j = 1 \dots 4$ to the previous solution; Re-estimate parameters $R_j, j = 5 \dots 6$; $C_j, j = 5 \dots 6$ by system identification with the 66-years data set;

5. Validate the borefield model with all data sets.

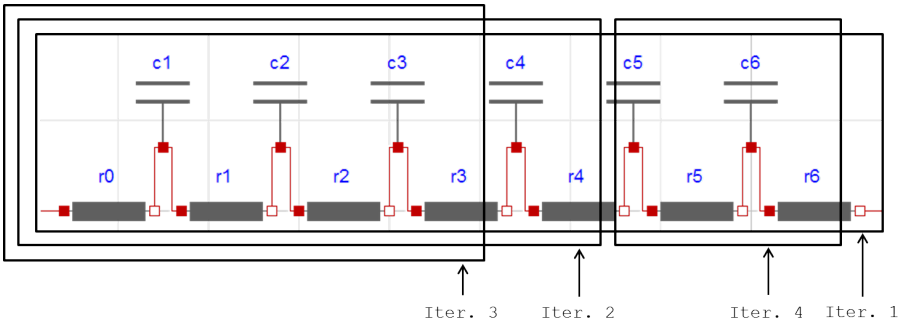

Figure 6.4: The borefield model parameters are estimated in groups in a succession of four system identification iterations, which are based on data sets of different time scales.

Multiple algorithms have been developed and tested, each consisting of a different combination of different system identification iterations. One approach was to estimate a limited set of parameters per iteration, which set corresponds to given borefield model nodes reflecting the time constants relevant to the currently used identification data set. In a next iteration the estimated parameters set and the identification data set were changed in the direction from the short term towards the long term (Figure 6.5). Another approach was the reversed of the first one—starting from the long term towards the short term. A third approach was in each next iteration to extend the estimated parameters set by adding parameters from adjacent model nodes and to change the identification data set accordingly (Figure 6.6). The results were either not satisfactory for some

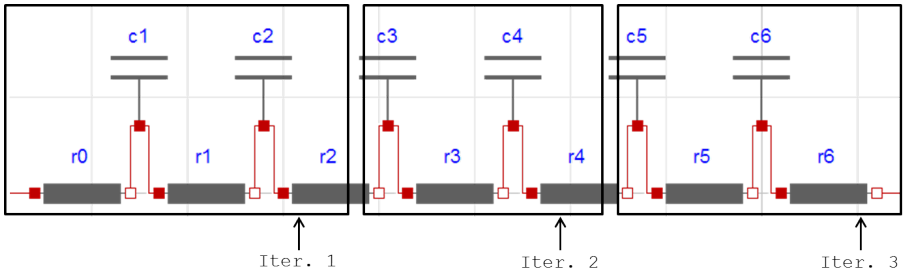

Figure 6.5: One of the unsuccessful system identification strategies was to estimate borefield model parameters in consecutive adjacent groups.

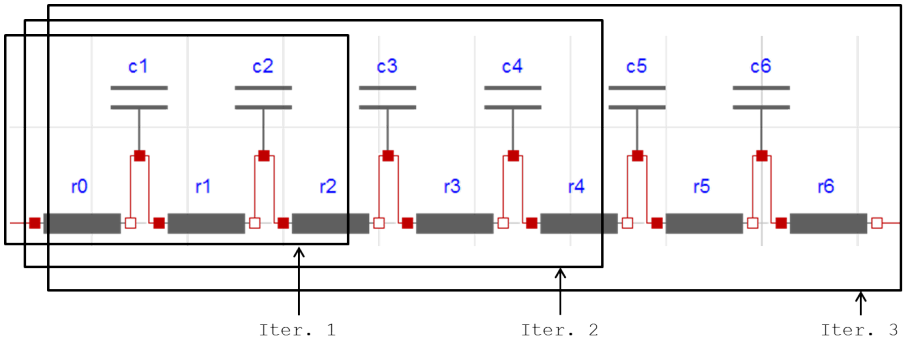

Figure 6.6: Another unsuccessful system identification strategy was to estimate borefield model parameters in consecutively extended groups.

iterations, or the results of a next iteration deteriorated the model performance on the time scale corresponding to the previous iteration. Then a correct step appeared to be to first estimate all parameters on the longest-term data set. Further it became clear that fixing parameters and removing them from the next iteration's estimated parameters set is the correct way to go. Finally it was found that the most successful model is obtained by starting with the full estimated parameters set and with the longest-term identification data set, then, with consecutive fixing of the farthest nodes parameters in the current parameters estimation set, the identification data set should be changed towards the short term.

6.5 Seasonal underground cold storage by heat rejection to the ambient air

The extension of the HyGCHP system towards more cold storage by heat rejection to the ambient air is accomplished by introducing a fifth device in the system, which representation in the optimization setup implies some additional steps in order to compute the solution. The included fifth device is a passive heat exchanger for rejecting borefield heat to the ambient air. The way this device is implemented in an extended SALTO method represents an extra degree of freedom, mathematically enabling more passive cooling of the building (by rejecting heat to the ground), which physically would not be feasible. For this reason the extended SALTO method is implemented by an algorithm of three steps, which lead to a realistic sub-optimal solution.

The passive heat exchanger transferring heat from the ground to the surrounding air, thereby increasing the cold storage in the ground, is called Cold Storing (CS) device to clearly differentiate from the passive cooling (PC) device, although this additional component is not a storage device itself. The CS device is represented by a static model describing its efficiency $\eta_{CS} = \frac{\dot{Q}_{CS}}{P_{CS}}$, where $\dot{Q}_{CS}$ denotes the device thermal power of extracting heat from the borefield and P_{CS}—the electrical power while running the CS device. Similarly to the case with PC efficiency $\eta_{PC} = 12$, it is chosen that $\eta_{CS} = 12$. The CS device is supposed to operate during winter when the ambient air temperature T_{AMB} is lower than the borefield outlet fluid temperature $T_{BF,Out}$. This process is similar to cooling the building during summer with the passive cooling device (PC) when $T_{BF,Out}$ is lower than the building supply water temperature T_{WS}.

In order to implement a SALTO including the CS device and the borefield considered, a few adaptations of the setup described in Chapter 4 are made. The inclusion of the CS device in the integrated system model is done by adapting (4.6) towards its new variant (6.1).

$$\begin{aligned}\sum \dot{Q}_{Ground}(k) = & \quad \dot{Q}'_{HP}(k) - \dot{Q}_{PC}(k) + \dot{Q}_{CS}(k) \\ = & \frac{COP_{HP} - 1}{COP_{HP}} \dot{Q}_{HP}(k) - \dot{Q}_{PC}(k) + \dot{Q}_{CS}(k) = -\frac{1}{F_b} \dot{Q}_{BF} \end{aligned} \quad (6.1)$$

In (6.1) $\dot{Q}_{BF}$ is negated compared to (4.6), since the borefield model accepts $\dot{Q}_{BF}$ being heat injection rate, instead of heat extraction rate, which was the case of BHE. The factor $F_b = 8$ represents the amount of BHEs in the considered borefield. In comparison to the system configuration in Chapter 5 the idea in the current chapter is to only include the thermal interaction between the BHEs in the borefield and to retain the system sizing. Therefore, since an open

rectangular 3×3 borefield of 8 BHEs is considered, the factor F_b enables to investigate the previously sized system by scaling the loads to the borefield.

The CS device operation cost is reflected in the objective function by adapting (4.7) towards (6.2).

$$J = \sum_{k=1}^{N} \Big(c_{el} \frac{\dot{Q}_{HP}(k)}{COP_{HP}} + c_{gas} \frac{\dot{Q}_{GB}(k)}{\eta_{GB}} + c_{el} \frac{\dot{Q}_{PC}(k)}{\eta_{PC}} + c_{el} \frac{\dot{Q}_{CH}(k)}{EER_{CH}} + c_{el} \frac{\dot{Q}_{CS}(k)}{\eta_{CS}} \Big) t_s \tag{6.2}$$

Similarly to the passive cooling feasibility constraint (4.11) the feasibility of the CS passive heat exchanger is represented by (6.3) with a temperature difference over the CS passive heat exchanger $\Delta T_{CS} = 3°\mathrm{C}$ analogously to the case of PC heat exchanger (Figure 4.6).

$$T_{AMB}(j) \leq T_{BF,Out}(j) - \Delta T_{CS} \tag{6.3}$$

Analogously to (4.16) the CS device thermal power is limited to reflect the maximum advised specific heat extraction rate from the borefield.

$$\text{For } F_l = 8.8 \qquad 0 \leq \dot{Q}_{CS}(k) \leq 6050 \tag{6.4}$$

Since in the SALTO method the mathematical representations of the devices are all integrated in the optimization formulation, without additional measures the following mathematical scenario will occur: during summer PC availability will be artificially increased by operating the CS device, since decreasing $T_{BF,Out}$ by CS is more efficient ($\eta_{CS} = 12$) than operating the supplementary cooling device—the air coupled chiller ($EER_{CH} = 4$). This situation is avoided by a step-wise approach of calculating the extended SALTO solution.

The algorithm for extended SALTO with cold storage by heat rejection to the ambient air consists of three steps, in which three consecutive SALTO solutions are calculated based on changes and additions in the constraints part:

1. Compute a conventional SALTO as in Section 5.2 to obtain initial device operation profiles;
   - Exclude the CS device from the SALTO formulation;
   - From the solution, note the periods with PC operation ($\dot{Q}_{PC}(i) > 0$);
2. Compute SALTO with enabled CS device operation during the heating periods;
   - Include the CS device in the SALTO formulation but exclude the constraints (6.3);

- Set constraints $\dot{Q}_{CS}(i) = 0$ during the periods with PC operation noted in step 1. This avoids simultaneous PC and CS operation;
- From the solution, note the periods with CS operation ($\dot{Q}_{CS}(j) > 0$) for which $T_{BF,Out}(j) < T_{AMB}(j) + \Delta T_{CS}$;

3. Compute SALTO including physical feasibility constraints during the heating periods with too low $T_{BF,Out}$—set constraints (6.3) during the periods noted in step 2.

Depending on the case it might be needed to repeat the algorithm from a particular step till the end if in the final solution new periods with PC operation appear or new periods appear with CS operation for which $T_{BF,Out}$ is too low.

6.6 Results

This section presents the findings about the potential advantage of additional seasonal underground thermal energy storage for the case of a 3×3 open rectangular configuration borefield with thermally interacting BHEs connected to the HyGCHP system with additional cold storing device. For comparison, the research in Section 5.4 has led to the conclusions that with no interaction between the BHEs in the borefield and with additional cold storing by rejecting underground heat only to the building, additional SUTES would be economically beneficial only if the chiller efficiency is below $EER_{CH,critical} = 0.4$, which is ten times smaller than realistic values. In this section, with added thermal interaction between the BHEs and maximized cold storing capacity, the critical chiller efficiency rises to $EER_{CH,critical} = 4.6$, which is higher than the realistic values, thus SUTES becomes an economically beneficial control strategy for particular parameters of the HyGCHP system.

The developed iterative system identification strategy (Section 6.4) provides a computationally efficient way (Table 6.1) to obtain low-order short-and-long-term borefield state space models for the three ground thermal conductivities, mentioned at the end of Section 6.2. For example, for ground thermal conductivity $\lambda = 3.5$ W/(mK), the model performance corresponding to model parameters obtained in each step of the algorithm is presented in Appendix A and described below for the final estimated parameters. The model output – borefield mean fluid temperature – deviates from the borefield emulator simulation data in the worst case with 1°C on a daily basis (Figures A.12), 0.25°C on the short term (1 month, Figure A.11), 2°C on the mid term (5 years, Figure A.10), and less than 0.25°C on the long term (66 years, Figure A.9). The models obtained for the other two ground thermal conductivities have similar performance.

	Number cases	Initialization time per case, (s)	Solution time per case, (s)	Total time, (min)
Iteration 1	5	7	25	3
Iteration 2	5	6	3	1
Iteration 3	5	15	15	3
Iteration 4	5	7	3	1

Table 6.1: Average computation times for the different cases and iterations of the system identification procedure, implemented on a 1.6 GHz quad-core intel CORE i7 machine with 4 MB RAM.

The three models are used in SALTO of the HyGCHP system with cyclic boundary conditions on the ground temperatures to represent the multi-annual sustainable operation profile. Below, results for $\lambda = 3.5$ W/(mK) are described. First, reference results for the original SALTO are obtained with the realistic chiller efficiency $EER_{CH} = 4$ (Figure 6.7). Then, following the extended SALTO algorithm (Section 6.5) computations with a modified $EER_{CH,m}$ lower than EER_{CH} are computed, which intend to reach the point where additional SUTES, by introducing CS device operation, increased PC operation, and decreased CH operation, is present in the optimal solution. The results show that for ground thermal conductivity $\lambda = 3.5$ W/(mK) $EER_{CH,critical} = 3$ is the border value, below which the CS device operation starts being included in the optimal solution (Figure 6.8).

Further reducing the chiller efficiency leads, as expected, to further increased CS and PC operation and decreased CH operation (Figure 6.9). Similarly to the investigation in Section 5.4 (Figure 5.14), in the current study the quantitative

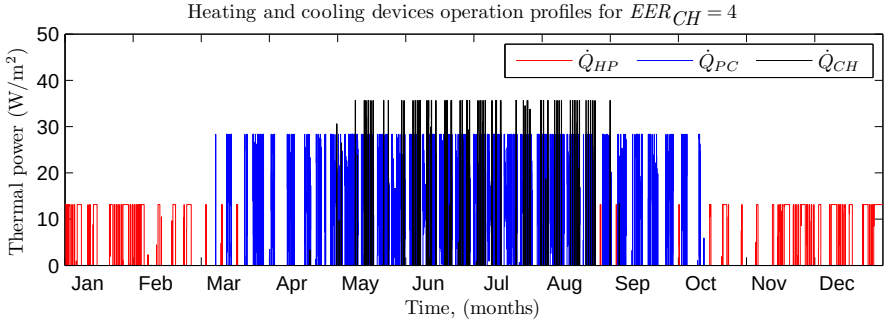

Figure 6.7: For the original chiller energy efficiency ratio $EER_{CH} = 4$ the reference heating and cooling device operation profiles are computed.

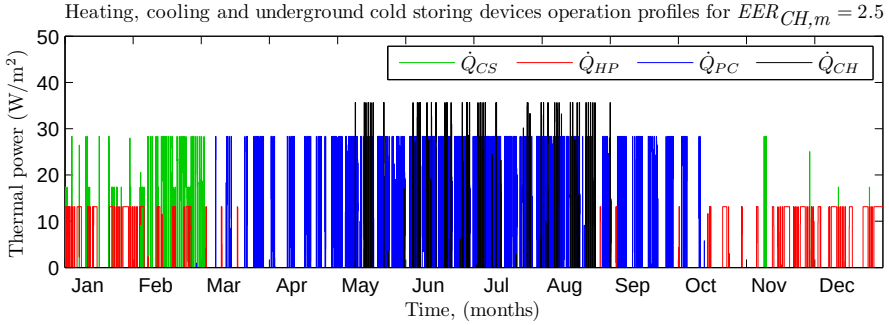

Figure 6.8: Additional seasonal underground cold storage becomes economically beneficial for chiller energy efficiency ratio below $EER_{CH,critical} = 3$, which is 1.33 times lower than in practice.

indicator for the amount of additional SUTES is chosen to be the increase in annual heat extraction from the ground (Figure 6.10). This indicator shows the trend of increasing additional SUTES for lower values of $EER_{CH,m}$. However, in a realistic case ($EER_{CH} = 4$), for $\lambda = 3.5$ W/(mK), the chiller is still safely the cheaper option to cover the dominating cooling load, although the system now comprises a borefield of thermally interacting BHEs and a more efficient cold storing installation than in Chapter 5.

Nevertheless, the results change for lower ground conductivities. Similarly to the computations described above, results for $\lambda = 1.9$ W/(mK) are obtained,

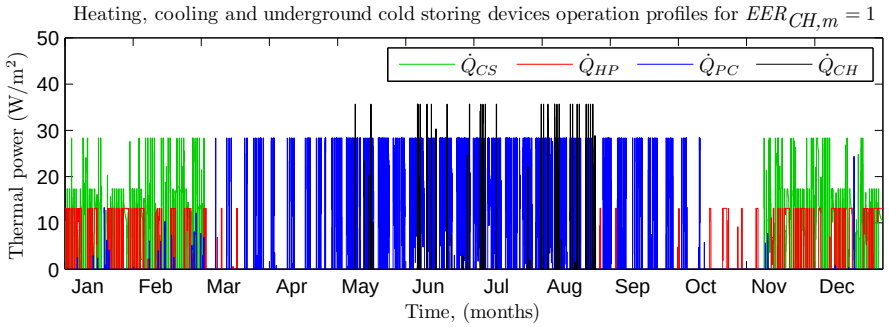

Figure 6.9: For chiller energy efficiency ratio, which is 4 times lower than in practice, the system operation is characterized by substantial seasonal underground cold storage and decreased chiller operation compared to the reference case (Figure 6.7).

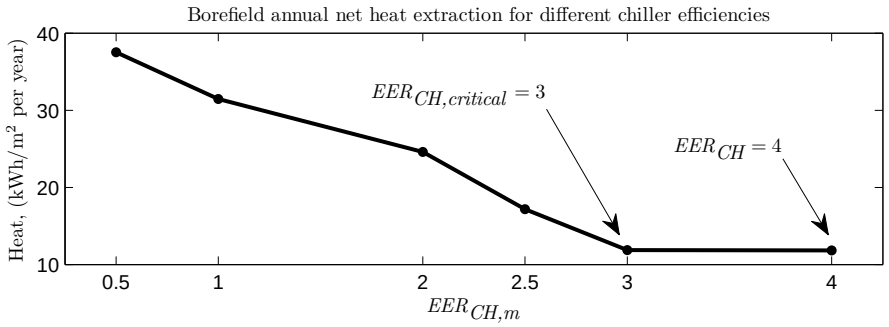

Figure 6.10: For the considered borefield and additional cold storing installation, additional seasonal underground thermal energy storage would become economically beneficial if the energy efficiency ratio of the chiller was 1.33 times lower than in practice.

which show that the critical chiller efficiency rises to $EER_{CH,critical} = 4$, thus the critical value coincided (accidently) with the assumed realistic value. Results obtained with $\lambda = 1.6$ W/(mK) indicate $EER_{CH,critical} = 4.6$, which is higher than the assumed realistic value. That means that for the investigated HyGCHP system with a 3×3 open rectangular configuration borefield and ground thermal conductivity $\lambda = 1.6$ W/(mK), additional SUTES is economically beneficial. For higher ground thermal conductivities additional SUTES is not economically beneficial, unless a more compact borefield configuration is used, which is not investigated. For clarity, all results for the potential of additional SUTES for both borefield types – with thermally non-interacting BHEs (Chapter 5, Figure 5.14) and with thermally interacting BHEs (from the current chapter) – are collected in Figure 6.11.

A point of attention is that the methodology presented in this section consists of the simultaneous inclusion of two main extensions compared to the methodology in Chapter 5: a borefield of thermally interacting BHEs, instead of a single BHE, and an additional device for increased cold storage in the ground by heat rejection to the ambient air. For that reason, in the case of $\lambda = 1.6$ W/(mK) for which additional SUTES is an economically beneficial control strategy given realistic chiller efficiencies, it is not distinguished which of the two extensions has the major contribution. The exact level of positive contribution of each extension separately towards making additional SUTES an economically beneficial strategy is therefore a mater for future research.

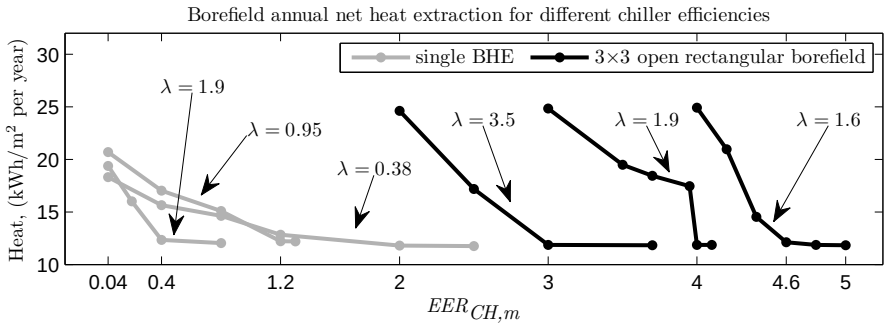

Figure 6.11: Lower ground thermal conductivities λ raise the critical chiller efficiency at which additional SUTES becomes economically beneficial and the borefield annual net heat extraction starts increasing. For $\lambda = 1.6$ W/(mK) and in the case of borefield, the HyGCHP system investigated can make economical advantage of additional SUTES because the assumed realistic chiller efficiency is $EER_{CH} = 4$ for all cases.

6.7 Conclusions

In this chapter the short-and-long-term optimal operation of a HyGCHP system is investigated for the case of thermally interacting BHEs in the borefield. The aim is to check whether additional SUTES is an economically beneficial control strategy for the case of a borefield. The borefield is represented by borefield low-order state space models developed for three values of ground thermal conductivity. The parameters of each model are estimated by the developed case-specific system identification algorithm based on an existing system identification toolbox and on system identification data sets generated by an existing detailed borefield emulator model. By including an additional cold storing installation the system potential is maximized to adopt additional SUTES as an economically beneficial control strategy.

The results indicate that for the investigated HyGCHP system with a 3×3 open rectangular configuration borefield and ground thermal conductivity $\lambda = 1.6$ W/(mK) additional SUTES is an economically beneficial control strategy. For $\lambda \geq 1.9$ W/(mK) and realistic chiller efficiencies additional SUTES is not economically beneficial. In contrast to the cases with thermally non-interacting BHEs (Chapter 5), for the investigated borefield of thermally interacting BHEs the critical chiller efficiencies $EER_{CH,critical}$ for lower ground conductivities are substantially moved towards the realistic value ($EER_{CH} = 4$). With this trend, for low enough but still realistic ground thermal conductivities the

system performance can be improved by incorporating additional SUTES. The presented case which includes additional SUTES could be considered as a case providing the minimum conditions for the investigated HyGCHP system to benefit from this inter-seasonally oriented control strategy.

Future research could focus on more compact borefields, which are logically expected to provide lower thermal dissipation to the surrounding ground, therefore, higher benefit from additional SUTES. Another direction for future research can be the exact implementation of an additional SUTES control strategy on the short term.

Chapter 7

Robustness analysis of the HyGCHP system with MPC

This chapter is based on the publication:
Antonov, S. and Helsen, L. (2016). Robustness analysis of a hybrid ground coupled heat pump system with model predictive control. *Under review with minor changes.*

This chapter presents the investigation of the level of state estimation uncertainty up to which the robust performance of the considered HyGCHP system with MPC can be guaranteed. The chapter begins with an introduction to the topic (Section 7.1). The study is based on an existing theoretical method used to compute the maximum allowed state estimation uncertainty for the HyGCHP system. This method is clarified and supplemented for improving its reproducibility (Section 7.2). Specific extensions are developed (Section 7.3) in order to implement the method to the considered HyGCHP system. A subsidiary method to validate the computed maximum level of uncertainty is designed (Section 7.4). The chapter continues with presenting the results obtained (Section 7.5) and finishes with a discussion, conclusions and suggestions for future research (Sections 7.6, 7.7 and 7.8).

7.1 Introduction

MPC of building heating and cooling systems usually results in robust operation with respect to uncertainties thanks to some key characteristics of the system

and the controller. Since a building is surrounded by the ambient air it represents a self-stable thermal system in the sense that the indoor zone air temperature would tend to converge to the ambient air temperature if there is no heating or cooling input, or disturbance. Moreover, the system disturbances, which act in practice (indoor appliances, solar radiation, occupancy) are bounded, and often they are either scheduled, or can be predicted up to a certain accuracy. The considered controller (MPC) incorporates feedback and this characteristic reduces the effect of uncertainties. However, MPC is model-based and the true limit until which the controlled system will actually be robust to state estimation uncertainty or disturbance prediction uncertainty is rarely known explicitly.

Robustness investigation for the considered HyGCHP system with MPC is important since this system is highly sensitive to uncertainty in concrete core temperature state estimation and disturbance prediction (Sourbron et al., 2013a). Two approaches exist for dealing with robustness of systems with MPC (Section 3.3). The more popular approach includes an explicit reformulation of the MPC optimization problem to assure robustness, which makes it computationally demanding. The alternative chosen in this dissertation is to perform robustness analysis of a system with conventional MPC. The analysis method includes complicated theoretical formulations and implicitness, however it retains the original MPC formulation.

The robustness analysis performed is based on an existing framework, which is re-described because of several reasons. First, the study in this dissertation will be more convenient if it is standalone, therefore a simple citation of the original source will not suffice. In any case, the existing method is not straight forward, but rather theoretical, abstract, difficult to understand completely by researchers of a broader field, whereas the authors describe it in a concise way for an audience of experts in control systems. Consequently, it is a challenge to implement the method. Moreover, the mathematical concept used (LMI) is in general likely to result in infeasible formulations for the smallest implementation mistake which can even be very hard to localize. All that motivates to add relevant detailed clarifications in the re-description of the method and to improve some points of incorrectness found in its original publication (Primbs and Nevistić, 2000). The alternative interpretation presented in this dissertation contributes to a better understanding of the method and hopefully a faster application in further studies.

The clarified robustness analysis method is extended and applied to the case of the investigated HyGCHP system with MPC to analyze robustness with respect to concrete core temperature estimation uncertainty. The original robustness analysis method is suggested for regulation MPC, whereas in this dissertation setpoint tracking MPC is considered. For that reason specific additional steps are

elaborated in order to implement the robustness analysis method. The aim is to find a precise range of allowed concrete core temperature estimation uncertainty, for which the robust performance of the HyGCHP system is guaranteed. The calculated range is validated by means of simulations of the HyGCHP system with MPC, based on which a quantitative robustness indicator is computed.

7.2 Clarification of Primbs' method for robustness analysis of systems with MPC and state estimation uncertainty

The Robustness Analysis method of Primbs and Nevistić (2000) represents an offline computation, which tries to prove robust performance of systems with MPC for a given range of uncertainty. The authors derived variants of the method for uncertainty in the system model parameters as well as in the state estimation during control. This chapter is focused on the variant of the method for dealing with state estimation uncertainty. The method is based on composing a sufficient condition for robustness in the form of LMI and checking for the feasibility of this LMI. To formulate the LMI one should provide the controller state space model, details of the optimization problem used in the MPC, and a representation of the uncertainty range. In this chapter first the top-level concept of the method is described (Subsection 7.2.1) and further a step-wise re-description of Primbs' method is presented. The sufficient condition in the method is based on a criterion for stability (Subsection 7.2.2), which should be robustly satisfied (Subsection 7.2.3). All formulations are structured in quadratic forms in order to derive the final LMI.

7.2.1 Concept of the robustness analysis method

The method of Primbs and Nevistić (2000) could be classified as a composition of two parts: the first part defining stability of a system with MPC, and the second part proving that this stability will hold for all possible errors considered (model parameter errors or state estimation/measurement errors).

The first part of Primbs' method is based on the principle of Lyapunov stability, which translates to the requirement the MPC objective function to decrease in time. In that sense a standard trick is at the current time step k to require objective function decrease in the next time step $k+1$. For that purpose an adequate solution for a feasible control action at $k+1$ is needed in order

to construct at k the objective function difference between time steps. This principle is explained in details in Subsection 7.2.2.

The second part of Primbs' method addresses robustness, which means stability for all possible errors of the considered variable, which is state estimation uncertainty in this dissertation. This is an ambitious goal in general. It depends on the creativity of the method developer to find a way to both represent the required robustness mathematically and to formulate it in a way feasible to solve and apply. Primbs and Nevistić (2000) solve this problem on the base of the S-procedure and an LMI: the feasibility of a quadratic function (objective function decrease) is guaranteed under quadratic constraints (defining the possible state estimation errors and binding the possible inputs in a set around their nominal trajectory). This implementation is described in details in Subsection 7.2.3.

7.2.2 Stability

In this subsection the stability of a system with MPC is elaborated as five steps of Primbs' robustness analysis method. The construction of the MPC optimization problem in quadratic forms is described. The convolution of the entire horizon states is described, resulting into a vector consisting of initial states and entire horizon inputs. The definition of the set containing the optimal inputs is presented. Finally, the stability criterion for objective function decrease in consecutive receding time horizons is elaborated, including the required solution for the extra time-step inputs.

Optimization problem formulation

The optimization problem within the MPC is represented in terms of quadratic forms in order to be used several times when composing the final LMI. The method adopts the following optimization problem:

$$J_i(x) = \min_{u(0),\ldots,u(i-1)} \left\{ x^T(i)P_0x(i) + \sum_{k=0}^{i-1} \left[x^T(k)Qx(k) + u^T(k)Ru(k) \right] \right\}$$

s.t. (7.1)

$$\begin{aligned} &x(k+1) = Ax(k) + Bu(k), k = 0, \ldots, i-1 \\ &x(0) = x \\ &c_u(u(k)) \leq 0, k = 0, \ldots, i-1 \end{aligned}$$

where the weighting factor matrices $Q \succ 0$, $R \succ 0$, $P_0 \succ 0$ are positive definite, thus there are no zero weights, and i is the horizon length. The authors of the method require the input inequality constraints to be feasible in a neighborhood containing $u = 0$. They accent that the method is designed without reflecting the state constraints in the formulations. For cases with state constraints, the authors comment that the results will hold for cases without model mismatch and suggest using soft state constraints when dealing with model mismatch.

The following notation is defined for convenience.

$u_{[j,r]} = [u(j), \ldots, u(r)]$
: is the sequence of inputs along the time steps from j to r.

$u^*(k; x, i), k = 0, \ldots, i-1$
: are the optimal inputs at time step k from the solution of the optimization problem for a horizon with length i starting with initial states x, i.e. from the solution corresponding to $J_i(x)$ (7.1).

$u^*_{[j,r]}(x, i) = [u^*(j; x, i), \ldots, u^*(r; x, i)]$
: is the optimal sequence of inputs along the time steps from j to r from the solution corresponding to $J_i(x)$.

$x^*(k; x, i), k = 0, \ldots, i$
: are the optimal states at time step k from the solution corresponding to $J_i(x)$.

In accordance to (7.1) the notation $J_i(x)$ stands for the cost function generated from the initial conditions x by applying the inputs $u^*_{[0,i-1]}(x, i)$. In this chapter the following notation is additionally defined:

$J_i(x_1; u^*_{[0,i-1]}(x_2, i))$
: as the cost generated from the initial conditions x_1 by applying the inputs $u^*_{[0,i-1]}(x_2, i)$. These inputs are not optimal in that case. They are optimal for another case, in which the initial conditions for J_i are x_2. Therefore, the following holds:

$$J_i(x_1; u^*_{[0,i-1]}(x_2, i)) \geq J_i(x_1)$$

which, in full notation, is

$$J_i(x_1; u^*_{[0,i-1]}(x_2, i)) \geq J_i(x_1; u^*_{[0,i-1]}(x_1, i))$$

Primbs and Nevistić (2000) represented the optimization (7.1) in terms of quadratic forms as

$$J_i(x) = \min_{\substack{u_{[0,i-1]} \\ c_u(u(k)) \leq 0, \\ k=0 \cdots i-1}} \begin{bmatrix} x \\ u_{[0,i-1]} \end{bmatrix}^T H_i \begin{bmatrix} x \\ u_{[0,i-1]} \end{bmatrix}$$

$$= \begin{bmatrix} x \\ u^*_{[0,i-1]}(x,i) \end{bmatrix}^T H_i \begin{bmatrix} x \\ u^*_{[0,i-1]}(x,i) \end{bmatrix} \tag{7.2}$$

The matrices H_i are not given by the authors of the method but they can be:

$$H_i = T_i^T Q_i T_i + R_i \tag{7.3}$$

with

$$T_i = \begin{bmatrix} A & B & & & \\ A^2 & AB & B & & \\ \vdots & & & \ddots & \\ A^i & A^{i-1}B & A^{i-2}B & \cdots & B \end{bmatrix}$$

$$Q_i = \begin{bmatrix} Q & & & \\ & \ddots & & \\ & & Q & \\ & & & P_0 \end{bmatrix}, \text{ square, of size } i \cdot n$$

$$R_i = \begin{bmatrix} Q & & & \\ & R & & \\ & & \ddots & \\ & & & R \end{bmatrix}, \text{ square, of size } n + i \cdot m$$

where n is the dimension of the state vector x and m the dimension of the input vector u. This formulation is known to represent the discrete convolution of the system states $x(k), k = 0, \ldots, i$, along the horizon by means of the so called Toeplitz matrices and only the initial system state together with the inputs along the horizon. The first column of T_i represents the autonomous system response and the rest of T_i represents a Toeplitz matrix, which columns form the system impulse responses starting at consecutive time steps along the horizon. Since the optimization cost function is formed by penalizing the states and the inputs along the horizon, the weighting factor matrices Q and R are incorporated accordingly.

This way, the cost of the optimization problem with horizon length i is represented by a quadratic form being the matrix H_i multiplied from both sides by a states-inputs vector.

At this point the authors of the method fixed the MPC horizon length to $i = N$. Further it is needed to deal with sub-horizons but that is only for the purpose of offline robustness analysis (not for online MPC) and then the subscript i has a different usage.

States-inputs vector

Within the framework of Primbs and Nevistić (2000) each quadratic form used in deriving the final LMI consists of a states-inputs vector multiplying from both sides an inner matrix, like in (7.2). The states-inputs vector consists of initial states and an inputs sequence along the horizon, all stacked in one long vector. In the end, the idea is to represent the condition for robustness as a system of inequalities of quadratic forms based on the same states-inputs vector. Further in the text the exact way of doing this is described, but for the moment a clarification of the notation is needed.

The cost corresponding to sub-horizons plays an important role in the method and therefore should be represented in a convenient way based on the full states-inputs vector. This is done by subsidiary matrices which simulate the system in order to calculate new initial states shifted in time. A sub-horizon begins at a certain time step later than the start of the main horizon and ends at the same time step, at which the main horizon ends. Therefore the subsidiary matrix should select the remaining part of the main states-inputs vector from the shifted new initial states till the end of the horizon. The authors of the method defined

$$\Phi_j = \begin{bmatrix} A & B & \\ & & I_{jm} \end{bmatrix}$$

where I_{jm} is the identity matrix of size $j \cdot m \times j \cdot m$.

This way, the states-inputs vector for a sub-horizon shifted with one time step can be represented by

$$\begin{bmatrix} x(1) \\ u_{[1,j]} \end{bmatrix} = \begin{bmatrix} Ax(0) + Bu(0) \\ u_{[1,j]} \end{bmatrix} = \begin{bmatrix} A & B & \\ & & I_{jm} \end{bmatrix} \begin{bmatrix} x(0) \\ u(0) \\ u_{[1,j]} \end{bmatrix} = \Phi_j \begin{bmatrix} x(0) \\ u_{[0,j]} \end{bmatrix}$$

Then the complete subsidiary matrix is defined as

$$\Phi_{[i,j]} = \prod_{k=j-i+1}^{j} \Phi_k \tag{7.4}$$

so that

$$\begin{bmatrix} x(i) \\ u_{[i,j]} \end{bmatrix} = \Phi_{[i,j]} \begin{bmatrix} x(0) \\ u_{[0,j]} \end{bmatrix}$$

where $\prod_k^j(\cdot) = 1$ when $j < k$.
(Primbs and Nevistić (2000) stated the last as "$j > k$", which is incorrect.)

Objective function upper bounds

The requirement all inputs to be close to the nominal trajectory is incorporated into the LMI by means of applying upper bounds of the cost function along sub-horizons of the main horizon. Primbs and Nevistić (2000) made an assumption which allows constructing quadratic upper bounds of the MPC cost along the sub-horizons. The bounds depend on the sub-horizons' initial states and on the matrices U_i, and they are defined as

$$\begin{aligned} J_{N-i}(x^*(i;x,N)) \quad &\leq \quad {x^*}^T(i;x,N)U_{N-i}x^*(i;x,N), \\ &\qquad\qquad \text{for } i = 0 \cdots N-1 \\ \text{and} \\ J_1(x^*(N;x,N)) \quad &\leq \quad {x^*}^T(N;x,N)\tilde{U}_1 x^*(N;x,N), \end{aligned} \tag{7.5}$$

While the first set of bounds might appear logical, the last one, determined by $\tilde{U}_1$, will be explained a bit further in the text.

The idea behind the upper bounds is that for $i = N-1$ the sub-horizon consists of a single step which is the last step of the current horizon. The corresponding cost function upper bound directly influences the inputs of that single step. Consecutively, for $i = N-2, N-3, \ldots$ and so on down to 0, each time an extra step is added to the beginning of the sub-horizon and the corresponding bound has effect. This way the entire state trajectory is kept close to the optimal one. In this dissertation the sub-horizons are graphically depicted in Figure 7.1. The bounds should be tight in order to reduce the conservativeness of the method and preferably they should coincide with a stabilizing trajectory, according to

the authors. To find such bounds appears straightforward for self-stable systems, like the one investigated in this dissertation. More particularly, the cost of the open loop trajectory is a suitable solution to determine upper bounds for such cases. This gives:

$$U_i = {A^i}^T P_0 A^i + \sum_{k=0}^{i-1} {A^k}^T Q A^k$$

and $\tilde{U}_1 = U_1$.

The upper bounds are applied in terms of quadratic forms using the previously derived subsidiary matrices (7.3) and (7.4) in the following way. According to the authors, if the set of all inputs $u_{[0,N-1]}$ is defined as

$$\left\{ u_{[0,N-1]} : \quad \begin{bmatrix} x \\ u_{[0,N-1]} \end{bmatrix}^T \Phi_{[i,N-1]}^T H_{[N-i]} \Phi_{[i,N-1]} \begin{bmatrix} x \\ u_{[0,N-1]} \end{bmatrix} \right.$$
$$\left. \leq {x^*}^T(i;x,N) U_{[N-i]} x^*(i;x,N), \text{ for } i = 0 \cdots N-1 \right\} \qquad (7.6)$$

then $u^*_{[0,N-1]}(x,N)$ is a member of this set. The authors suggested the following notation where they also add an extra control move $u(N)$, in the states-inputs vector, which multiplies 0 and is described later.

$$\Pi_i = \Phi_{[N-i,N]}^T \left\{ \begin{bmatrix} U_i & \\ & 0_{(i+1)m} \end{bmatrix} - \begin{bmatrix} H_i & \\ & 0_m \end{bmatrix} \right\} \Phi_{[N-i,N]}$$

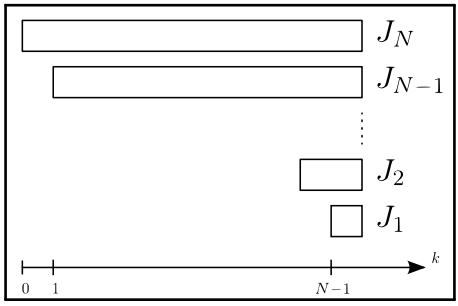

Figure 7.1: The system states are kept near to the optimal trajectory by applying upper bounds on the cost functions of all sub-horizons which end where the main horizon ends.

(In the last equation, the authors wrote $\Phi_{[i-1,N]}$, which is incorrect.) This way (7.6) becomes

$$\begin{bmatrix} x \\ u_{[0,N]} \end{bmatrix}^T \Pi_i \begin{bmatrix} x \\ u_{[0,N]} \end{bmatrix} \geq 0, \text{ for } i = 1 \cdots N. \tag{7.7}$$

If (7.7) holds, then the inputs are as close to the optimal trajectory as the used upper bounds are tight.

Stability criterion

Primbs and Nevistić (2000) based their method on the traditional concept of investigating whether the MPC cost function is a Lyapunov function for the system. To summarize the properties of a Lyapunov function for a dynamic system: such function is continuous, zero if its argument is zero, strictly increasing if its argument increases, unbounded from above, and its value in the next time step is smaller than its value in the current time step, (Rawlings and Mayne, 2009, Appendix B). Having the MPC cost function as described above it is only left to check for what parameters it decreases in the next time step.

Final feasible control action

The authors of the method compared the MPC cost at time step k for a horizon of length N to the cost at time step $k+1$ for a horizon of the same length, but receded with one time step, for which an extra control move in the end is needed. This is the additional control move, which has been incorporated in (7.7). This last control move has to be defined similarly to the inputs sequence $u^*_{[0,N-1]}$ by means of applying an upper bound of the corresponding cost function. The authors suggested different variants, of which the most realistic one is $u(N) = u^*(0; x^*(N; x, N), 1)$. This is the input which generates the cost $J_1(x^*(N; x, N))$ and in order to keep this input close to the nominal trajectory an upper bound is applied to that cost, as shown in (7.5). Similarly to the case of the inputs $u^*_{[0,N-1]}$ the bound associated to $u^*(N)$ is defined in quadratic form in the following way. If the set of all inputs $u(N)$ is

$$\left\{ u(N) : \begin{bmatrix} x \\ u^*_{[0,N-1]} \\ u(N) \end{bmatrix}^T \Phi^T_{[N,N]} H_1 \Phi_{[N,N]} \begin{bmatrix} x \\ u^*_{[0,N-1]} \\ u(N) \end{bmatrix} \right.$$
$$\left. \leq {x^*}^T(N; x, N) \tilde{U}_1 x^*(N; x, N) \right\}$$

then $u^*(0; x^*(N; x, N), 1)$ is an element of this set.

The authors also define

$$\Pi_0 = \Phi_{[N,N]}^T \left\{ \begin{bmatrix} \tilde{U}_1 & \\ & 0_m \end{bmatrix} - H_1 \right\} \Phi_{[N,N]}$$

(Note that although in the equation above the index of Π is 0, the indices of $\tilde{U}$ and H are 1 because the corresponding horizon consists of one time step. Π_0 corresponds to the final feasible control action, whereas Π_1—to the last sub-horizon included in (7.7).) Now all bounds can be combined by using quadratic forms with the full input sequence so if the set of all $u_{[0,N]}$ is

$$\left\{ u_{[0,N]} : \begin{bmatrix} x \\ u_{[0,N]} \end{bmatrix}^T \Pi_i \begin{bmatrix} x \\ u_{[0,N]} \end{bmatrix} \geq 0, \text{ for } i = 0 \cdots N \right\} \tag{7.8}$$

then the inputs sequence

$$[u^*_{[0,N-1]}(x, N), u^*(0; x^*(N; x, N), 1)]$$

is an element of this set $u_{[0,N]}$.
(In the last statement, the authors wrote

$$[u^*_{[0,N-1]}(x, N), u^*(N; x^*(N; x, N), 1)]$$

which is incorrect)

The idea of the authors is to prove robustness for the entire set $u_{[0,N]}$, which, by introducing conservativeness, will guarantee robustness also for $[u^*_{[0,N-1]}(x, N), u^*(0; x^*(N; x, N), 1)]$.

7.2.3 Robustness

In this subsection Primbs' implementation of the robustness sufficient condition is described. Four steps of Primbs' method serve for satisfying the stability criterion (Subsection 7.2.2) for all state estimation errors within the defined level of uncertainty. A way to include the state estimates $\hat{x}$ into the states-inputs vector is presented. A way to formulate the state estimation uncertainty is described. Special attention is put on the clarification of the robustness condition implementation—including the uncertain state estimates into the stability criterion. Finally the usage of the S-procedure for solving Primbs' robustness analysis method is outlined.

Estimated states $\hat{x}$ within the states-inputs vector

Primbs' method in the variant for state estimation uncertainty is based on an extended version of the states-inputs vector in order to include the states estimates. The extended states-inputs vector is

$$\begin{bmatrix} \hat{x} \\ x \\ u_{[0,N]} \end{bmatrix}$$

In order to apply the cost function bounds described above for trajectories starting with $\hat{x}$ as well as for trajectories starting with x the following notation is also introduced:

$$\hat{\Pi}_i = \begin{bmatrix} I_n & 0_n & \\ & & I_{(N+1)m} \end{bmatrix}^T \Pi_i \begin{bmatrix} I_n & 0_n & \\ & & I_{(N+1)m} \end{bmatrix}$$

$$\bar{\Pi}_i = \begin{bmatrix} 0_n & I_n & \\ & & I_{(N+1)m} \end{bmatrix}^T \Pi_i \begin{bmatrix} 0_n & I_n & \\ & & I_{(N+1)m} \end{bmatrix}$$

In such way, having (7.8), it can be formulated that if the set of all inputs $u_{[0,N]}$ is

$$\left\{ u_{[0,N]} : \begin{bmatrix} \hat{x} \\ x \\ u_{[0,N]} \end{bmatrix}^T \hat{\Pi}_i \begin{bmatrix} \hat{x} \\ x \\ u_{[0,N]} \end{bmatrix} \geq 0, \text{ for } i = 0 \cdots N \right\} \tag{7.9}$$

then the inputs sequence
$[u^*_{[0,N-1]}(\hat{x}, N), u^*(0; x^*(N; \hat{x}, N), 1)]$ is an element of this set $u_{[0,N]}$. Similarly, if the set of all inputs $u_{[0,N]}$ is

$$\left\{ u_{[0,N]} : \begin{bmatrix} \hat{x} \\ x \\ u_{[0,N]} \end{bmatrix}^T \bar{\Pi}_i \begin{bmatrix} \hat{x} \\ x \\ u_{[0,N]} \end{bmatrix} \geq 0, \text{ for } i = 0 \cdots N \right\} \tag{7.10}$$

then the inputs sequence
$[u^*_{[0,N-1]}(x, N), u^*(0; x^*(N; x, N), 1)]$ is an element of this set $u_{[0,N]}$. (Note the difference between $\hat{x}$ and x which initialize the optimal trajectories corresponding to the input sequences above.) With such concept two different sets are defined by using one common extended states-inputs vector.

State estimation uncertainty model

In order to prove robustness to a particular degree of state estimation uncertainty, information about this degree of uncertainty should be incorporated in the

final robustness condition. Primbs and Nevistić (2000) assumed that the state estimation uncertainty can be described by a quadratic form as

$$\begin{bmatrix} \hat{x} \\ x \\ u_{[0,N]} \end{bmatrix}^T \Psi_j \begin{bmatrix} \hat{x} \\ x \\ u_{[0,N]} \end{bmatrix} \geq 0, \text{ for } j = 1 \cdots r \tag{7.11}$$

and suggested state estimation uncertainty of the kind

$$\|\hat{x}(k) - x(k)\|_2 \leq a \|x(k)\|_2 \tag{7.12}$$

The exact way of composing the matrix Ψ_j and the meaning of the index j and its limit r are not explained by the authors so in the current dissertation this is elaborated below.

The squared of (7.12) gives

$$\|\hat{x}(k) - x(k)\|_2^2 \leq a^2 \|x(k)\|_2^2 \tag{7.13}$$

which can be represented as a quadratic form by

$$\begin{bmatrix} \hat{x} \\ x \end{bmatrix}^T \begin{bmatrix} I_n & -I_n \\ -I_n & I_n \end{bmatrix} \begin{bmatrix} \hat{x} \\ x \end{bmatrix} \leq \begin{bmatrix} \hat{x} \\ x \end{bmatrix}^T \begin{bmatrix} 0_n & 0_n \\ 0_n & a^2 I_n \end{bmatrix} \begin{bmatrix} \hat{x} \\ x \end{bmatrix}$$

which is equivalent to

$$\begin{bmatrix} \hat{x} \\ x \end{bmatrix}^T \begin{bmatrix} -I_n & I_n \\ I_n & (a^2 - 1) I_n \end{bmatrix} \begin{bmatrix} \hat{x} \\ x \end{bmatrix} \geq 0 \tag{7.14}$$

Should the system model be of 1st-order or should the system model be of nth-order with all states being checked for their total degree of estimation uncertainty described by a, (7.14) is easy to understand and a single matrix Ψ is required. However, a more probable need would be to check towards the estimation uncertainty of different states independently. In such a case matrices Ψ_j, for $j = 1 \cdots r$ will be required, where r is the number of independently checked states or combinations of states. Perhaps, it is more practical to consider the case where the estimation uncertainty of each state is checked independently. Then r will coincide with n. In order to compose such matrices Ψ_j, for $j = 1 \cdots n$ subsidiary state selection square matrices V_j of size n are introduced in this dissertation.

Let the following matrices of size $n \times n$ be

$$V_1 = \begin{bmatrix} 1 & & & \\ & 0 & & \\ & & \ddots & \\ & & & 0 \end{bmatrix}, V_2 = \begin{bmatrix} 0 & & & \\ & 1 & & \\ & & 0 & \\ & & & \ddots \\ & & & & 0 \end{bmatrix}, \cdots, V_n = \begin{bmatrix} 0 & & & \\ & \ddots & & \\ & & 0 & \\ & & & 1 \end{bmatrix}$$

meaning that the position of the unity element corresponds to the subscript of V and to the selected state. The quadratic form describing the state estimation uncertainty then is

$$\begin{bmatrix}\hat{x}\\ x\end{bmatrix}^T \begin{bmatrix}-V_j & V_j\\ V_j & (a_j^2-1)V_j\end{bmatrix} \begin{bmatrix}\hat{x}\\ x\end{bmatrix} \geq 0, \text{ for } j = 1 \cdots n$$

where each state estimation uncertainty is independently described by a_j. Finally the matrices Ψ_j from (7.11) are

$$\Psi_j = \begin{bmatrix}-V_j & V_j & \\ V_j & (a_j^2-1)V_j & \\ & & 0_{(N+1)m}\end{bmatrix} \tag{7.15}$$

Should a particular state be assumed accurately estimated and the robustness to its estimation uncertainty untested, the corresponding a_j can be set to zero. It is important to include corresponding information for all states, either by giving a particular a_j for each, or by setting a_j to zero, or by defining a combined estimation uncertainty for several states or for all states together like in (7.14). If a state is left without information about its estimation uncertainty (i.e. the corresponding Ψ_j is missing in the formulation), this will make the final robustness condition infeasible. The reason is that such a formulation means that the robustness is checked for unlimited estimation uncertainty of that state, which is infeasible.

Robustness criterion implementation; Decoupling $u^*(k;x,N)$ and $u^*(k;\hat{x},N)$

As mentioned in Subsection 7.2.2 the stability criterion is based on the idea that the objective function $J_N(x; u^*_{[0,N-1]}(x,N))$ is required to be a Lyapunov function and its decrease in time should only be proven. As the aim is to prove robustness to state estimation uncertainty, this state estimation uncertainty should also enter the stability criterion for decreasing objective function. This way the term "Robustness criterion" forms. Primbs and Nevistić (2000) provided a concise derivation of the robustness sufficient condition, based on this concept. Their exact derivation is difficult to understand and lacks clarifications to be smoothly implemented. Therefore a detailed explanation is provided below.

The initial formulation is:

$$J_N(x; u^*_{[0,N-1]}(x,N))$$
$$-J_N\Big(Ax + Bu^*(0;\hat{x},N); u^*_{[0,N-1]}\Big(Ax + Bu^*(0;\hat{x},N),N\Big)\Big)$$
$$-\epsilon \left\|x\right\|_2^2 \geq 0 \tag{7.16}$$

and it is explained in the following way. At each time step there exist two optimal states trajectories which should be distinguished: the true states trajectory of the controlled real plant (with cost $J_N(x; u^*_{[0,N-1]}(x,N))$) and the predicted states trajectory within the controller (with cost $J_N(\hat{x}; u^*_{[0,N-1]}(\hat{x},N))$). The predicted states trajectory within the controller is based on uncertainly estimated initial states $\hat{x}$. The focus is on the robustness of the controlled real plant. Therefore, the criterion is the objective function composed of true states trajectories to decrease from a given time step towards the next time step. The place where the uncertainly estimated initial states have effect is the computed control inputs $u^*(0;\hat{x},N)$ which form the true states $Ax + Bu^*(0;\hat{x},N)$ of this next time step. Or in other words, uncertainly estimated states $\hat{x}$ of the current time step are used in the controller to compute optimal inputs, which will be the actual inputs to be applied to the plant to form its true states of the next time step. The objective function $J_N(Ax + Bu^*(0;\hat{x},N); u^*_{[0,N-1]}(Ax + Bu^*(0;\hat{x},N),N))$ is initialized at these true states of the next time step and is checked for being lower than the objective function of the current time step, which starts from the initial true states. This is the condition set because the aim is to check robustness of the control performance (determined by the real plant and its true states) and not robustness of the prediction performance (determined by the simulated plant and uncertainly estimated states).

However, the first term of the criterion represents an objective function generated by the optimal inputs $u^*_{[0,N-1]}(x,N)$ but the second term represents an objective function generated by the optimal inputs $u^*_{[0,N-1]}(Ax + Bu^*(0;\hat{x},N),N)$, which are from a different input sequence. According to Primbs' method either the set (7.9) can be defined, which includes the inputs sequence $[u^*_{[0,N-1]}(\hat{x},N), u^*(0;x^*(N;\hat{x},N),1)]$ or the set (7.10), which includes the inputs sequence $[u^*_{[0,N-1]}(x,N), u^*(0;x^*(N;x,N),1)]$ So there are two disagreements in the above mentioned criterion: first, a simultaneous inclusion of two different input sequences in the same inequality, and second, the inputs $u^*_{[0,N-2]}(Ax + Bu^*(0;\hat{x},N),N)$ even differ from the inputs $u^*_{[1,N-1]}(\hat{x},N)$, and consecutively are not elements of the sets defined in Primbs' method. Therefore, on one side, the criterion above should be split in a system of inequalities, each of them consistent towards one particular input sequence, and

on the other side, the formulation should be modified to replace the inputs $u^*_{[0,N-2]}(Ax + Bu^*(0;\hat{x},N),N)$ by $u^*_{[1,N-1]}(\hat{x},N)$.

The system robustness criterion is split for consistency towards the inputs sequences and the resulting inequalities are modified to replace the inputs $u^*_{[0,N-1]}(Ax + Bu^*(0;\hat{x},N),N)$ by means of substituting part of the terms with their upper or lower bounds. This is done in three steps. First, the term $J_N(x;u^*_{[0,N-1]}(x,N))$ of the initial criterion is replaced by a lower bound of it, defined by the following inequality:

$$J_N(x;u^*_{[0,N-1]}(x,N)) \geq$$

$$J_N(\hat{x};u^*_{[0,N-1]}(\hat{x},N)) - \begin{bmatrix}\hat{x}\\ x\end{bmatrix}^T M \begin{bmatrix}\hat{x}\\ x\end{bmatrix}$$

where the matrix M is symmetric and it is needed for the final condition to be feasible. So it can be defined in the final LMI as a symmetric matrix to be found by the LMI solver. Using this lower bound only makes the robustness criterion stricter (safer, more conservative) but if the resulting system of inequalities holds it will still be a valid guarantee for robustness. So the criterion becomes

$$\begin{cases} & J_N(\hat{x};u^*_{[0,N-1]}(\hat{x},N)) - \begin{bmatrix}\hat{x}\\ x\end{bmatrix}^T M \begin{bmatrix}\hat{x}\\ x\end{bmatrix} \\ - & J_N\Big(Ax + Bu^*(0;\hat{x},N);u^*_{[0,N-1]}\Big(Ax + Bu^*(0;\hat{x},N),N\Big)\Big) \\ - & \epsilon\,\|x\|_2^2 \geq 0 \\ \\ & J_N(x;u^*_{[0,N-1]}(x,N)) \geq \\ & J_N(\hat{x};u^*_{[0,N-1]}(\hat{x},N)) - \begin{bmatrix}\hat{x}\\ x\end{bmatrix}^T M \begin{bmatrix}\hat{x}\\ x\end{bmatrix} \end{cases} \tag{7.17}$$

Second, the term

$$J_N\Big(Ax + Bu^*(0;\hat{x},N);u^*_{[0,N-1]}\Big(Ax + Bu^*(0;\hat{x},N),N\Big)\Big)$$

is replaced by an upper bound of it, namely

$$J_N\Big(Ax + Bu^*(0;\hat{x},N);u^*_{[0,N-1]}\Big(A\hat{x} + Bu^*(0;\hat{x},N),N\Big)\Big)$$

(Note the change towards $\hat{x}$ multiplying the matrix A for initializing the optimization of the inputs.) The substituting term is an upper bound of the

original one, because it represents a cost, which is generated with non-optimal inputs, thus, it is a higher cost than the one generated with optimal inputs. Similarly to the previous substitution, this one here again only introduces conservativeness, but if a solution is found, the original criterion will also be satisfied.

Third, only in the second inequality of (7.17), the term

$$J_N(\hat{x}; u^*_{[0,N-1]}(\hat{x}, N))$$

is replaced by an upper bound of it, namely

$$J_N(\hat{x}; u^*_{[0,N-1]}(x, N))$$

(Note the change towards x for initializing the optimization of the inputs). The substituting term is an upper bound for the reason that it is a cost generated with non-optimal inputs. Again, this change only introduces conservativeness, but if a solution is found, the original criterion will also be satisfied.

The resulting robustness criterion is:

$$\begin{cases} & J_N(\hat{x}; u^*_{[0,N-1]}(\hat{x}, N)) - \begin{bmatrix}\hat{x}\\ x\end{bmatrix}^T M \begin{bmatrix}\hat{x}\\ x\end{bmatrix} \\ - & J_N\Big(Ax + Bu^*(0; \hat{x}, N); u^*_{[0,N-1]}\Big(A\hat{x} + Bu^*(0; \hat{x}, N), N\Big)\Big) \\ - & \epsilon \left\|x\right\|_2^2 \geq 0 \\ \\ & J_N(x; u^*_{[0,N-1]}(x, N)) \geq \\ & J_N(\hat{x}; u^*_{[0,N-1]}(x, N)) - \begin{bmatrix}\hat{x}\\ x\end{bmatrix}^T M \begin{bmatrix}\hat{x}\\ x\end{bmatrix} \end{cases} \tag{7.18}$$

For clarity, the state- and the input sequences corresponding to the mentioned horizons and cost functions, as well as some inter-dependencies between their initial conditions are represented graphically (Figure 7.2).

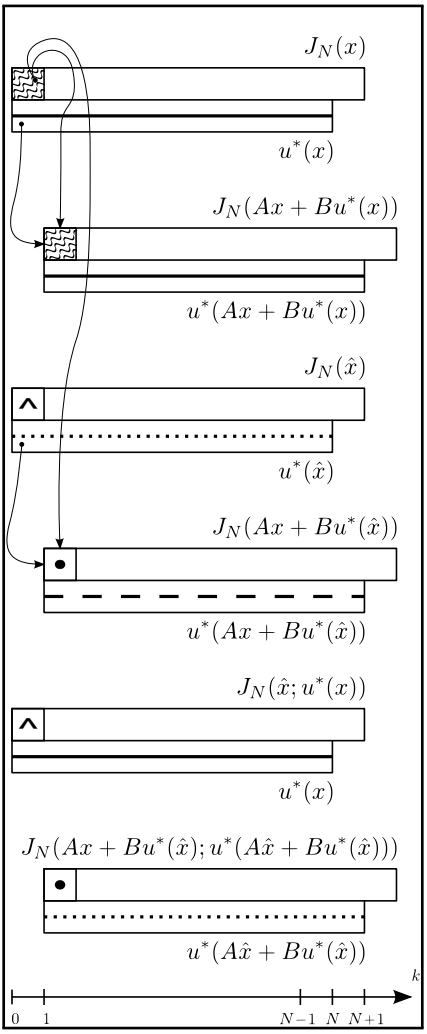

Figure 7.2: All different state-input trajectories considered in the formulation of the robustness condition are represented by relative dependencies with the trajectories formed by the states-inputs vector.

4-step algorithm of Primbs' method

Primbs and Nevistić (2000) presented an algorithm to build the sufficient condition for robustness in the form of LMI, in which the above derivations have been implemented. Below the re-description of Primbs' method is finalized with this algorithm, which consists of 4 steps.

1. Replace the robustness criterion by a sufficient condition in terms of quadratic forms.
The following notation is defined:

$$\hat{\Pi}_s =$$

$$\begin{bmatrix} I_n & 0_n & \\ & & I_{(N+1)m} \end{bmatrix}^T \begin{bmatrix} H_N & \\ & 0_m \end{bmatrix} \begin{bmatrix} I_n & 0_n & \\ & & I_{(N+1)m} \end{bmatrix} - \begin{bmatrix} M & \\ & 0_{(N+1)m} \end{bmatrix}$$

$$- \left\{ \begin{bmatrix} 0_n & I_n & \\ & & I_{(N+1)m} \end{bmatrix}^T \begin{bmatrix} A & B & \\ & & I_{Nm} \end{bmatrix}^T \begin{bmatrix} H_N & \\ & 0_m \end{bmatrix} \begin{bmatrix} A & B & \\ & & I_{Nm} \end{bmatrix} \right.$$

$$\left. \begin{bmatrix} 0_n & I_n & \\ & & I_{(N+1)m} \end{bmatrix} \right\} - \begin{bmatrix} 0_n & & \\ & \epsilon I_n & \\ & & 0_{(N+1)m} \end{bmatrix}$$

$$\begin{aligned} \hat{\Pi}^M = & \begin{bmatrix} 0_n & I_n & \\ & & I_{(N+1)m} \end{bmatrix}^T \begin{bmatrix} H_N & \\ & 0_m \end{bmatrix} \begin{bmatrix} 0_n & I_n & \\ & & I_{(N+1)m} \end{bmatrix} \\ & - \begin{bmatrix} I_n & 0_n & \\ & & I_{(N+1)m} \end{bmatrix}^T \begin{bmatrix} H_N & \\ & 0_m \end{bmatrix} \begin{bmatrix} I_n & 0_n & \\ & & I_{(N+1)m} \end{bmatrix} \\ & + \begin{bmatrix} M & \\ & 0_{(N+1)m} \end{bmatrix} \end{aligned}$$

With the use of these definitions, the first inequality in (7.18) is replaced by

$$\begin{bmatrix} \hat{x} \\ x \\ u^*_{[0,N-1]}(\hat{x}, N) \\ u^*(0; x^*(N; \hat{x}, N), 1) \end{bmatrix}^T \hat{\Pi}_s \begin{bmatrix} \hat{x} \\ x \\ u^*_{[0,N-1]}(\hat{x}, N) \\ u^*(0; x^*(N; \hat{x}, N), 1) \end{bmatrix} \geq 0 \qquad (7.19)$$

and the second inequality in (7.18) is replaced by

$$\begin{bmatrix} \hat{x} \\ x \\ u^*_{[0,N-1]}(x,N) \\ u^*(0;x^*(N;x,N),1) \end{bmatrix}^T \hat{\Pi}^M \begin{bmatrix} \hat{x} \\ x \\ u^*_{[0,N-1]}(x,N) \\ u^*(0;x^*(N;x,N),1) \end{bmatrix} \geq 0 \tag{7.20}$$

Note that the inputs in (7.19) result from optimization initialized at $\hat{x}$, whereas in (7.20) they are related to x.

2. Write (7.19) and (7.20) as implications.
(7.19) can be written as

$$\left.\begin{array}{l} u_{[0,N]} = [u^*_{[0,N-1]}(\hat{x},N), u^*(0;x^*(N;\hat{x},N),1)] \\ \begin{bmatrix} \hat{x} \\ x \\ u_{[0,N]} \end{bmatrix}^T \Psi_j \begin{bmatrix} \hat{x} \\ x \\ u_{[0,N]} \end{bmatrix} \geq 0, \text{ for } j = 1 \cdots r \end{array}\right\} \tag{7.21}$$

$$\Rightarrow \begin{bmatrix} \hat{x} \\ x \\ u_{[0,N]} \end{bmatrix}^T \hat{\Pi}_s \begin{bmatrix} \hat{x} \\ x \\ u_{[0,N]} \end{bmatrix} \geq 0$$

(7.20) can be written as

$$\left.\begin{array}{l} u_{[0,N]} = [u^*_{[0,N-1]}(x,N), u^*(0;x^*(N;x,N),1)] \\ \begin{bmatrix} \hat{x} \\ x \\ u_{[0,N]} \end{bmatrix}^T \Psi_j \begin{bmatrix} \hat{x} \\ x \\ u_{[0,N]} \end{bmatrix} \geq 0, \text{ for } j = 1 \cdots r \end{array}\right\} \tag{7.22}$$

$$\Rightarrow \begin{bmatrix} \hat{x} \\ x \\ u_{[0,N]} \end{bmatrix}^T \hat{\Pi}^M \begin{bmatrix} \hat{x} \\ x \\ u_{[0,N]} \end{bmatrix} \geq 0$$

3. Replace the input sequence conditions in (7.21) and (7.22) by the sets of quadratic forms (7.9) and (7.10).

$$\left.\begin{array}{l} \begin{bmatrix} \hat{x} \\ x \\ u_{[0,N]} \end{bmatrix}^T \hat{\Pi}_i \begin{bmatrix} \hat{x} \\ x \\ u_{[0,N]} \end{bmatrix} \geq 0, \text{ for } i = 0 \cdots N \\ \begin{bmatrix} \hat{x} \\ x \\ u_{[0,N]} \end{bmatrix}^T \Psi_j \begin{bmatrix} \hat{x} \\ x \\ u_{[0,N]} \end{bmatrix} \geq 0, \text{ for } j = 1 \cdots r \end{array}\right\} \tag{7.23}$$

$$\Rightarrow \begin{bmatrix} \hat{x} \\ x \\ u_{[0,N]} \end{bmatrix}^T \hat{\Pi}_s \begin{bmatrix} \hat{x} \\ x \\ u_{[0,N]} \end{bmatrix} \geq 0$$

$$\left.\begin{array}{l} \begin{bmatrix} \hat{x} \\ x \\ u_{[0,N]} \end{bmatrix}^T \bar{\Pi}_i \begin{bmatrix} \hat{x} \\ x \\ u_{[0,N]} \end{bmatrix} \geq 0, \text{ for } i = 0 \cdots N \\ \begin{bmatrix} \hat{x} \\ x \\ u_{[0,N]} \end{bmatrix}^T \Psi_j \begin{bmatrix} \hat{x} \\ x \\ u_{[0,N]} \end{bmatrix} \geq 0, \text{ for } j = 1 \cdots r \end{array}\right\} \tag{7.24}$$

$$\Rightarrow \begin{bmatrix} \hat{x} \\ x \\ u_{[0,N]} \end{bmatrix}^T \hat{\Pi}^M \begin{bmatrix} \hat{x} \\ x \\ u_{[0,N]} \end{bmatrix} \geq 0$$

4. Apply S-procedure.
The final step in deriving a sufficient condition for robustness from the implications above is to apply the so called S-procedure. More on the topic can be found by the author of the S-procedure, Yakubovich (1971), however his publication is difficult to reach. Alternatively the work of Derinkuyu and Pınar (2006) is referred, who reviewed the original S-procedure as well as many sources of further related research and gave enhanced formulations of the S-procedure. Primbs and Nevistić (2000) provided a good very brief explanation. For the purposes of this dissertation it is only important to know that a sufficient condition for the implications (7.23) and (7.24) to hold is that there exist scalars

τ_i, μ_i, α_i, β_i such that the following LMI is feasible.

$$\begin{cases} \sum_{i=0}^{N} \tau_i \hat{\Pi}_i + \sum_{j=0}^{r} \mu_j \Psi_j - \hat{\Pi}_s \preceq 0, & \tau_i \geq 0,\ \mu_j \geq 0 \\ \sum_{i=0}^{N} \alpha_i \bar{\Pi}_i + \sum_{j=0}^{r} \beta_j \Psi_j - \hat{\Pi}^M \preceq 0, & \alpha_i \geq 0,\ \beta_j \geq 0 \end{cases} \tag{7.25}$$

If (7.25) is feasible and a solution for τ_i, μ_i, α_i, β_i, and M is found, then the system is guaranteed to have robust performance to state estimation uncertainty specified by a_j in Ψ_j, (see (7.15)).

7.3 Implementation and application of Primbs' method to the HyGCHP system with MPC

Up to this stage a HyGCHP system with setpoint tracking MPC is investigated based on the optimization problem in Section 4.2 and Primbs' method for robustness analysis of regulation MPC with state estimation uncertainty is described in Section 7.2. Some preliminary steps are still necessary before applying Primbs' method to the HyGCHP system. First, an alternative formulation of (4.7) is derived in order to switch from a linear objective function to a quadratic one in accordance to Primbs' method. Second, the newly obtained MPC formulation with quadratic objective function is further reformulated in order to make the objective function include the building model control input T_{WS}. Third, a succession of implicit steps is described. These steps are needed to apply Primbs' method to the investigated HyGCHP system with MPC.

7.3.1 Reformulating the optimization problem to include a quadratic objective function

In this dissertation the available robustness analysis method implies to stick to conventional setpoint tracking formulations in quadratic form. Therefore, the aim changes towards keeping T_Z at its setpoint T_Z^{SP} at minimum quadratic cost for running the heating and cooling devices. The new MPC optimization

problem becomes

$$J = \min_{x,u} \Bigg\{ P\Big(T_Z(N) - T_Z^{SP}(N)\Big)^2 + \sum_{k=0}^{N-1} \Bigg[Q\Big(T_Z(k) - T_Z^{SP}(k)\Big)^2 + R\Big(c_{el}\frac{\dot{Q}_{HP}(k)}{COP_{HP}} + c_{gas}\frac{\dot{Q}_{GB}(k)}{\eta_{GB}} + c_{el}\frac{\dot{Q}_{PC}(k)}{\eta_{PC}} + c_{el}\frac{\dot{Q}_{CH}(k)}{EER_{CH}}\Big)^2 t_s^2 \Bigg] \Bigg\}$$

s.t.

$$(\dot{Q}_{HP} + \dot{Q}_{GB} - \dot{Q}_{PC} - \dot{Q}_{CH}) = F_l \frac{1}{R_{th}}(T_{WS} - T_{CC})$$

$$\dot{Q}_{HP} \geq 0; \quad \dot{Q}_{GB} \geq 0; \quad \dot{Q}_{PC} \geq 0; \quad \dot{Q}_{CH} \geq 0$$

Integrated system dynamics and constraints (7.26)

where P, Q and R are weighting factors. This is the optimization problem of the main MPC strategy for the investigated HyGCHP system and the robustness of this MPC formulation is analyzed.

7.3.2 Reformulating the optimization problem to include the building model control input T_{WS}

Besides penalizing heating/cooling devices quadratic operation cost, in (7.26) the term

$$\Big(c_{el}\frac{\dot{Q}_{HP}(k)}{COP_{HP}} + c_{gas}\frac{\dot{Q}_{GB}(k)}{\eta_{GB}} + c_{el}\frac{\dot{Q}_{PC}(k)}{\eta_{PC}} + c_{el}\frac{\dot{Q}_{CH}(k)}{EER_{CH}}\Big)^2 \tag{7.27}$$

also accounts for the exact distribution of the heating/cooling demand among the four devices. The constraint

$$(\dot{Q}_{HP} + \dot{Q}_{GB} - \dot{Q}_{PC} - \dot{Q}_{CH}) = F_l \frac{1}{R_{th}}(T_{WS} - T_{CC}) \tag{7.28}$$

is needed to integrate the building model, via T_{WS}, to the rest of the HyGCHP system (the four devices and the geothermal part) so that the distributed heating/cooling demand is delivered to the building. However, the exact distribution of this demand over the different units does not affect system

robustness. It is only important to have the term $F_l \frac{1}{R_{th}}(T_{WS} - T_{CC})$ in the objective function where T_{WS} will be the system's degree of freedom to remain robust to uncertainties. For that purpose the devices thermal powers and the BHE model are excluded from the reformulated optimization problem and for robustness analysis of the HyGCHP system based on (7.26) only the building model is kept.

To perform the reformulation of (7.26) the term (7.27) is substituted by a term including T_{WS} according to the constraint (7.28). First the term (7.27) is represented in the following way:

$$\Big(c_{el}\frac{\dot{Q}_{HP}(k)}{COP_{HP}} + c_{gas}\frac{\dot{Q}_{GB}(k)}{\eta_{GB}} + c_{el}\frac{\dot{Q}_{PC}(k)}{\eta_{PC}} + c_{el}\frac{\dot{Q}_{CH}(k)}{EER_{CH}}\Big)^2$$

$$= F_p^2 \cdot \Big(\dot{Q}_{HP}(k) + \dot{Q}_{GB}(k) + \dot{Q}_{PC}(k) + \dot{Q}_{CH}(k)\Big)^2 \qquad (7.29)$$

Such representation cannot be obtained with exact F_p. However, such representation can be assumed with respect to F_p being in the range $[min(Price), max(Price)]$, where $Price$ is the vector $\big[\frac{c_{el}}{COP_{HP}}, \frac{c_{gas}}{\eta_{GB}}, \frac{c_{el}}{\eta_{PC}}, \frac{c_{el}}{EER_{CH}}\big]$, and dealing further only with the two boundary values of this range.

For the range of F_p based on (7.28) and (7.29) and by leaving the devices- and the geothermal part out (since robustness is determined by the ability to supply the heat/cold demand, not by the exact distribution among the devices) in this dissertation the robustness of the HyGCHP system with MPC as in (7.26) is analyzed using the following MPC formulation:

$$J = \min_{x,u} \Bigg\{ P\Big(T_Z(N) - T_Z^{SP}(N)\Big)^2 + \sum_{k=0}^{N-1} \Big[Q\Big(T_Z(k) - T_Z^{SP}(k)\Big)^2 + R \cdot F_p^2 F_l^2 \frac{1}{R_{th}^2}(T_{WS} - T_{CC})^2 t_s^2 \Big] \Bigg\}$$

s.t.

$$x(k+1) = A_{BD}x(k) + B_{BD}u(k) \qquad (7.30)$$

and applying Primbs' method for the two boundary values of the range of F_p.

Theoretically the optimization problem (7.30) is different than (7.26) and possibly the optimal solutions of the two optimization problems will not coincide. At least, given the arguments above, the two optimal solutions are expected to be similar as it comes to the profiles of T_{WS} and T_{CC}. For that reason, the described substitution is adopted and its applicability and accuracy is a matter of validation in Section 7.4.

7.3.3 Implicit steps to motivate applicability of the method

After defining the alternative formulation (7.30) some implicit steps are still necessary before applying Primbs' method. The implicit steps, as mentioned at the end of Section 2.6, are only a theoretical motivation and do not need to be implemented explicitly. Once these steps can serve as motivation, Primbs' method can be applied as for regulation MPC derived from (7.30).

- Define deviation variables. Assuming that target profiles can be computed based on (7.26), the deviation variables can be defined according to (2.11).
- Compose regulation MPC with the deviation variables. The optimization problem of the regulation MPC can be derived from (7.30) according to (2.7).
- Eliminate the influence of disturbances. The disturbances from the building model should be eliminated because, since in practice they are non-controllable but predicted, in the regulation MPC they cannot be made available to contribute to system robustness. In the input vector of the building model only the first input (T_{WS}) is a control input and the other four ($[T_{VS}\ T_{AMB}\ \dot{Q}_{INT}\ \dot{Q}_{SOL}]^T$) are predicted disturbances. The target profiles computed with the setpoint tracking MPC must be followed by the control input T_{WS} only. The exclusion of the disturbances is done by taking only the first column of the building model B matrix and eliminating the rest in the regulation MPC, as well as correcting the A matrix elements, which are not consistent after the eliminated B matrix columns. (In the presented case this is possible thanks to the gray-box nature of the state space models, which provides information about the way the matrix elements have been composed.) The reduction of the state space model in this way is equivalent to using hard constraints to avoid all disturbances affecting the system operation. If a solution of the robustness sufficient condition is found for such formulation then robustness of the original controlled system can be achieved, with respect to the target profile, by the control input T_{WS} only, and independently of the disturbances, which is the goal.
- Omit input constraints. The remaining constraints are omitted except for the office building dynamics. Although the original optimization problem is rather detailed and the constraints part is substantial (Chapter 5), Primbs' method allows omitting those constraints (Subsection 7.2.2, Part *Optimization problem formulation*), because of the following reasons: all those constraints are input constraints, not state constrains; indirectly, these constraints are accounted for to a certain extent by means of applying

the objective function upper bound; target profiles have already been computed and they should be tracked, instead of reproducing the original way they were created, in which case these constraints are implicitly incorporated, (7.26).

- Penalize all states and all inputs. In the original optimization problem (7.26) only the states $T_Z(k)$ are penalized. However, as stated in Primbs' method above, the penalties on the states and inputs vectors should be positive definite matrices or, in other words, all states and inputs should be penalized in the cost function. With the reformulations in Subsections 7.3.1 and 7.3.2 the entire inputs vector is included in the cost function, so similarly to (2.7) and (7.2) the necessary optimization problem formulation for regulation MPC is completed.

After deriving the alternative MPC formulation (7.30) and explaining the implicit steps above as arguments to formulate a regulation problem, Primbs' method can be applied. For that purpose the following information is included in the LMI formulation: the office building model state space matrices A_{BD} and B_{BD}; the weighting factor matrices P, Q, and $R_p = R \cdot F_p^2 \cdot F_l^2 \frac{1}{R_{th}^2}$ for the two boundaries of the range of F_p (see explanation of (7.29)); T_{CC} is selected, which will be tested for robustness to estimation uncertainty, together with the corresponding degree of the tested uncertainty—in that case one single parameter a_j in (7.15) ($j = 1$ since T_{CC} is the first state in the states vector). Due to computational limitations, commented in Section 7.6, the presented implementation cannot solve towards the theoretical maximum a_1^{max} for which the LMI is still feasible. For the sake of presenting an example solution, within few attempts the LMI problem is solved by manually setting different a_1 values until a_1^* is found (close to a_1^{max}) for which the LMI is feasible. Once a_1^* is obtained the value is validated by means of MPC simulations.

The described methodology is implemented in MATLAB (MathWorks, 2010) using YALMIP (Löfberg, 2004) with the SeDuMi solver (CORALLab, 2003). On a 1.6 GHz quad-core intel CORE i7 machine with 4 MB RAM the computation times were about 1.2 s YALMIP parsing time and 1.25 s SeDuMi solving time.

7.4 Validation of Primbs' method by HyGCHP system simulation with included state estimation uncertainty

To validate the robustness analysis method for the HyGCHP system investigated system simulations are performed with MPC based on the optimization problem (7.26). Initially target profiles are computed by performing an MPC simulation without uncertainty. Then several simulations are performed by incorporating different degrees of uncertainty, defined by (7.12), in the re-initialization of the corresponding state at each MPC iteration. The introduced uncertainty is of the kind $\hat{T}_{CC} = T_{CC} \cdot (1 + a_1 * rand(-1, 1))$ where $rand(-1, 1)$ randomly takes values at each time step either -1 or 1 with uniform distribution. In fact, one such random sequence is generated beforehand with a length corresponding to the simulation time. Then, for the sake of comparison, this same sequence is used in all simulations with different degree of uncertainty, which is defined by the magnitude of a_1.

To quantify the validity of the obtained maximal degree of state estimation uncertainty and to compare the results, a quantitative robustness indicator is defined. Actually, this indicator represents the computation of the robustness condition (7.16) at each time step using the objective function from (7.26), which is in the setpoint tracking domain. However, this condition has to be computed in the regulation domain because in the setpoint tracking domain the state and input profiles are influenced by the system disturbances.

During each simulation, at each time step, before solving the current MPC iteration (initialized with uncertainty) and simulating one future step with the obtained input, a duplicate of the optimization problem is also solved by initializing with the true states, instead. This duplicate optimization solution, being in the setpoint tracking domain, corresponds to the term $J_N(x; u^*_{[0,N-1]}(x, N))$ in (7.16) in the regulation domain. The duplicate optimization solution corresponding to the term

$$J_N\Big(Ax + Bu^*(0; \hat{x}, N); u^*_{[0,N-1]}\big(Ax + Bu^*(0; \hat{x}, N), N\big)\Big)$$

in (7.16) is computed in the next simulation time step.

The obtained state- and input profiles from the duplicate optimizations are converted to the regulation domain. Therefore, for the entire simulation with a given degree of uncertainty, for each time step, the duplicate profiles of the target simulation (the one without uncertainty) are subtracted from the corresponding state- and input profiles of the duplicate optimization solutions. The resulting state- and input profiles are in the regulation domain.

With the resulting profiles of each time step the corresponding generated objective function values are computed according to (7.26). These objective function values correspond to the condition (7.16) and are related to the original MPC formulation (7.26), but converted to the regulation domain. It remains to compute the time step wise differences of these costs, which boils down to evaluation of (7.16) in time and serves as robustness indicator. Positive differences mean that the objective function value (converted to the regulation domain) of the real plant decreases in the next time step, which is necessary for robust convergence. In the setpoint tracking domain that means robust convergence to the target profiles. Negative differences mean increase of the cost in the next time step, due to uncertainty at the current moment. If such increase (negative values of the indicator) keeps evolving for consecutive time steps, the system with MPC is not robust to the uncertainty and cannot immediately start converging to the target.

This robustness indicator (the cost of the real plant generated with state- and input profiles converted to the regulation domain) is computed along the simulation time for all simulations with different degree of uncertainty. The existence of time intervals with consecutive negative values of the robustness indicator is a measure for non-robustness. As additional information the corresponding profile of the controlled variable T_Z is plotted to double-check whether it diverges when the incorporated uncertainty turns the system non-robust.

Model mismatch is not incorporated in the validation. The simulations are performed with the same controller model as the one used in the LMI problem of Primbs' method. This is further commented in the Discussion section.

For validation the code developed in Chapter 5 is used (with modified objective function as in (7.26)) which is implemented in MathWorks (2010) using YALMIP (Löfberg, 2004) with the Cplex solver (IBM, 2012) for the MPC iterations. On a 1.6 GHz quad-core intel CORE i7 machine with 4 MB RAM the computation times per MPC iteration were about 0.65 s YALMIP parsing time, 0.03 s Cplex solving time, and 0.62 s results post-processing total time. This all gives about 8 min total computation time for each 2-weeks simulation presented. The computation times could be substantially reduced if the YALMIP parsing time is avoided by using the YALMIP "`optimizer()`" command instead of its "`optimize()`" command.

7.5 Results

This section demonstrates for the investigated HyGCHP system with MPC to what extent the maximal allowed degree of state estimation uncertainty, found by means of the described robustness analysis approach, coincides with the state estimation uncertainty which turns this system non-robust in a validation experiment, based on simulations.

As being mostly important for the investigated HyGCHP system, the performed robustness analysis is focused towards uncertainty in the concrete core temperature estimation, T_{CC}. Following the methodology described in Section 7.3 maximum allowed degree of uncertainty $a_1^* \in [0.02, 0.05]$ is obtained, according to the factor F_p in range $[min(Price), max(Price)]$ described in Subsection 7.3.2. This means that T_{CC} state estimation uncertainty in the range $[2, 5]\%$ is expected to turn the system unstable.

Validation experiments are performed as described in subsection 7.4 for four values of imposed uncertainty: $a_1 = 0, 0.02, 0.04, 0.06$ corresponding to T_{CC} state estimation uncertainty of $0, 2, 4, 6\%$, respectively.

For the case of $a_1 = 0$ (no uncertainty in T_{CC} estimation) a system simulation with setpoint tracking MPC is performed in order to determine the states- and inputs target profiles. The setpoint T_Z is chosen in the middle of the thermal comfort range (CEN, 2007) and has a variable profile since the thermal comfort range depends on the ambient temperature T_{AMB}. The setpoint tracking MPC for a representative period of two weeks (starting on Monday) results in an office zone air temperature (T_Z) profile situated around the setpoint with deviations caused by the system disturbances (gray line in Figures 7.3, 7.6 and 7.9).

For the case of 2% uncertainty (the safer side of the determined interval for maximum uncertainty with guaranteed robustness) the profile of T_Z slightly changes but the system performance is still satisfactory (black line in Figure 7.3).

Computation of the robustness indicator described in subsection 7.4 shows that for 2% uncertainty the indicator has negative values for single time steps along the simulation time (Figure 7.4, zoom in Figure 7.5). Few exceptions exist with negative indicator values for two consecutive time steps. Once the system is diverged from the target (negative indicator value) due to uncertainty, the MPC leads to a profile converging back to the target (positive indicator values) although the uncertainty continues influencing the controller.

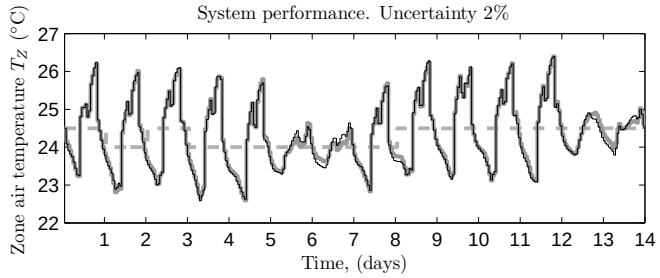

Figure 7.3: The reference case is not characterized by uncertainty and the temperature T_Z (thicker line) is kept around its setpoint (dashed line). For the case of 2% state estimation uncertainty of T_{CC} the controlled system is still robust and has an almost similar T_Z profile (black line).

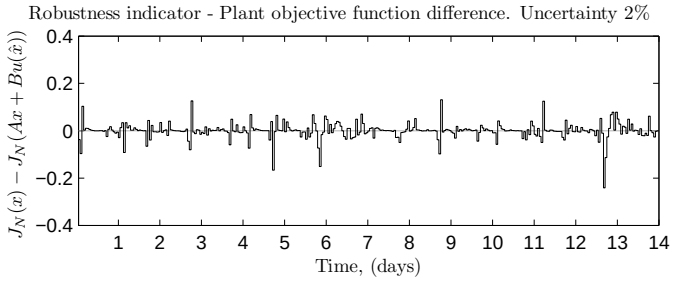

Figure 7.4: The almost complete absence of consecutive time steps with negative values of the robustness indicator means that once diverged from the target profiles due to uncertainty the system can converge robustly to the next time steps.

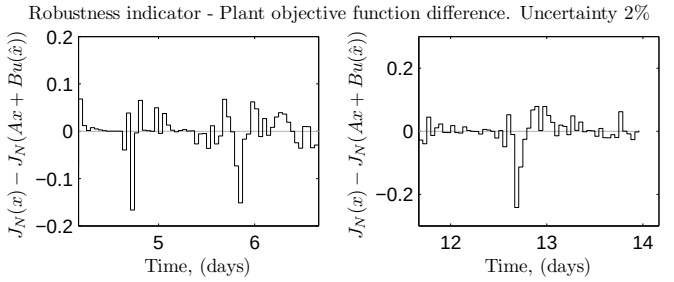

Figure 7.5: Close view over selected time intervals from Figure 7.4.

For the case of 4% uncertainty (inside the range where the uncertainty is expected to turn the system non-robust) a T_Z profile is observed which is more deviating from the setpoint (Figure 7.6).

The computed robustness indicator has several consecutive negative values in different time intervals, which means that once the system is diverged from the target profile the MPC cannot immediately control the profile back to the target profile (Figure 7.7, zoom in Figure 7.8).

For the case of 6% uncertainty (beyond the estimated range of maximum allowed uncertainty) there is a trend for the T_Z profile to often keep diverging from the target for longer time intervals (Figure 7.9). The system performance is not robust to the posed uncertainty.

The computed robustness indicator reflects the increased divergence from the targets (Figure 7.10, zoom in Figure 7.11). Periods of tendentious increase of the plant objective function are indicated by monotonously decreasing consecutive negative values of the robustness indicator.

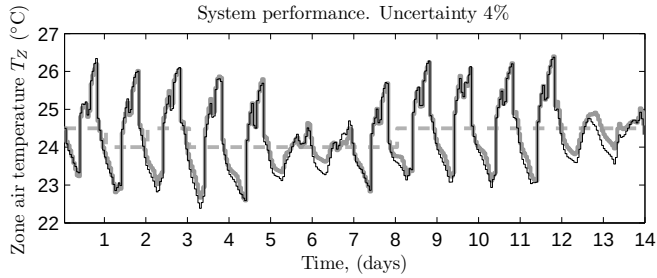

Figure 7.6: For 4% T_{CC} state estimation uncertainty (inside the predicted maximum allowed range of $[2, 5]\%$) some short time periods appear with a T_Z profile (black line) diverging from its target profile (thicker line). (Dashed line is setpoint T_Z.)

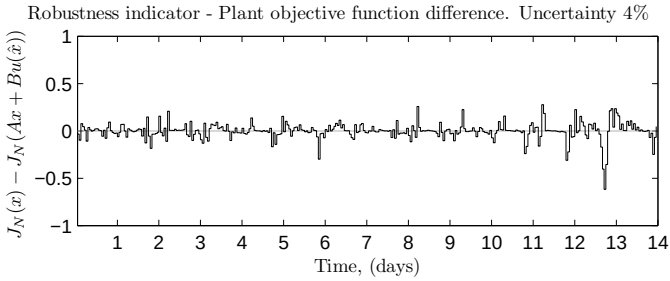

Figure 7.7: The short time periods of system non-robustness are visible from the consecutive time steps with negative robustness indicator values.

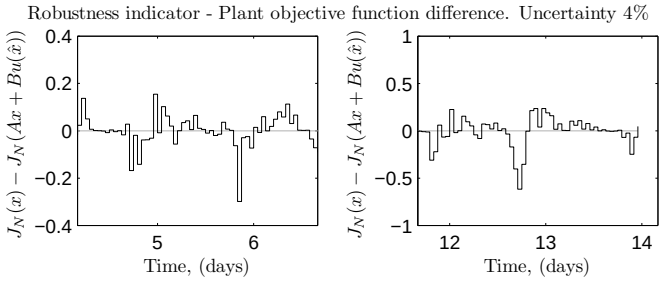

Figure 7.8: Close view over selected time intervals from Figure 7.7.

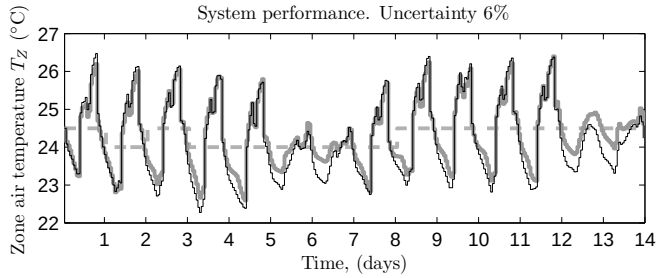

Figure 7.9: T_{CC} state estimation uncertainty of 6% affects the system performance with frequent tendencies of T_Z (black line) not converging to its target profile (thicker line). (Dashed line is setpoint T_Z.)

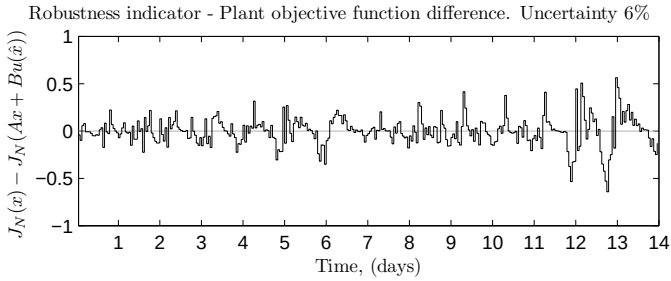

Figure 7.10: The frequent periods of system non-robustness in the case of 6% uncertainty are shown with the many periods of consecutive time steps with negative robustness indicator values meaning increase of the plant objective function in time.

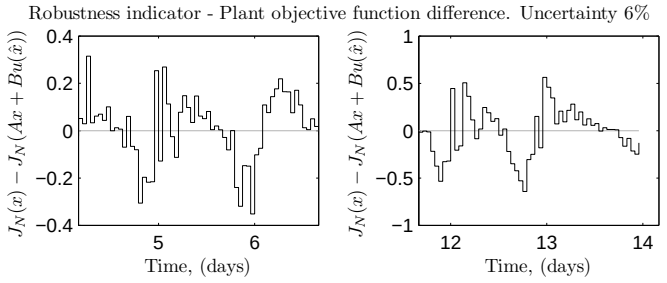

Figure 7.11: Close view over selected time intervals from Figure 7.10.

7.6 Discussion

Despite the successful understanding, clarification and application of Primbs' method to the investigated HyGCHP system with MPC, the transition from regulation to setpoint tracking in the context of robustness analysis incorporates some assumptions which still can be better supported by stronger motivation and proves. Also the LMI solvers used are lacking non-linearities treatment functionality in combination with the specific LMI problem composed in order to broaden the robustness analysis. These points are discussed in this section.

A convincing theoretical explanation should be found about the reliability of using a robustness analysis framework based on regulation MPC for performing robustness analysis of setpoint tracking MPC. The arguments (Subsection 7.3.3) about the validity of such approach lead to the successful results obtained, however they do not represent a strong theoretical proof. Suggestions for future research to elaborate further on this issue are provided in Section 7.8.

The presented Primbs' method for robustness analysis for the case of state estimation uncertainty assumes no model mismatch, which may have impact in applications to real systems. Generally, the authors of the method stated that for cases with no state constraints the results will hold for model mismatch. For cases with state constraints they suggested soft constraints. The HyGCHP system investigated does not include state constraints in the original setpoint tracking MPC (7.26), consequently there are no state constraints in the regulation MPC either (2.7). For these reasons further research in that direction is not considered. Should model mismatch have larger influences one can also apply the variant of the method for robustness to model mismatch, also found in (Primbs and Nevistić, 2000), which is shorter, simpler, easier to understand and implement.

In Subsection 7.3.3 it is explained that the robustness analysis is performed by attempting to solve the final LMI problem with manually chosen guesses for the level of state estimation uncertainty a_1, because the solver is incompatible to optimize directly towards the theoretical maximum a_1^{max}. This incompatibility comes from (7.25) where multiplying the matrix Ψ_j by the decision variables μ_j and β_j creates nonlinearity, since a_j reside in the elements of Ψ_j . The variant of Primbs' method for robustness analysis in the case of model mismatch does not lead to such nonlinearity and there the same solver can directly find the maximum allowed model parameter uncertainty. For the case of state estimation error a different solver is needed.

7.7 Conclusions

In this chapter a method for robustness analysis to state estimation uncertainty, found in the literature, is reminded to the scientific community, re-explained by adding relevant clarifications and corrections, reproduced and extended in order to be applied to a HyGCHP system with MPC.

By validation experiments it is shown that the robustness analysis method gives a reliable estimation of the maximum allowed state estimation uncertainty, for which the system investigated retains robust performance. The system has a satisfactory robust performance when the state estimation uncertainty imposed is lower than the range of maximum allowed values, calculated by the method. State estimation uncertainty, which is higher than the maximum allowed values computed using the method, results in a deteriorated system performance.

It becomes evident that for the system investigated there is no need for a robustness analysis approach directly treating the setpoint tracking formulation. Robustness analysis of the corresponding regulation problem with the same system model gives reliable estimation of the maximum allowed degree of state estimation uncertainty.

The theoretical sources of conservativeness in the method did not appear to have a high influence on the obtained estimations. Although the robustness analysis approach includes some sources of conservativeness (using non-tight objective function upper bounds; using substitutions of mathematical formulation terms in order to fit the adopted LMI concept), in the presented case this conservativeness does not seem to influence the results severely. The obtained results have been successfully validated.

7.8 Future research

A very relevant contribution to the presented research would be to elaborate a more explicit proof of the validity of the approach to use the robustness analysis framework based on regulation MPC for robustness analysis of setpoint tracking MPC. One direction for elaborating such proof is related to the weighting factors for inputs and states. In a setpoint tracking MPC often the deviation from the setpoint of only some states and inputs is penalized, whereas the regulation MPC requires penalization of all states and inputs. Another direction is related to the translation of the percentage of the allowed uncertainty from the regulation domain, where it has been computed, to the setpoint tracking domain, where

it is used. Nevertheless, the results of other successful implementations will strengthen the reliability of this approach.

Another possible improvement is to implement the methodology using software and solver that allow finding the maximum state estimation uncertainty directly by incorporating it in the cost function of the LMI problem. This will especially facilitate cases where the robustness analysis is performed towards uncertainties in several states, where multiple $a_j > 0$ will describe the simultaneously acting uncertainties.

A third useful contribution would be to extend the method of Primbs and Nevistić (2000) towards the case of disturbance prediction uncertainty. This, however, might turn out to be not trivial. Besides the terms in (7.24) which are quadratic forms of the states-inputs vector, a linear term and a free constant term might appear in the formulations, once considering disturbance predictions. A possible way to circumvent the problem might be to extend the inner matrix of the quadratic form and add a unity at the end of the states-inputs vector, as in the example below.

$$\begin{bmatrix} \hat{x} \\ x \\ u_{[0,N]} \\ 1 \end{bmatrix}^T \begin{bmatrix} G & Gv \\ v^T G & v^T G v \end{bmatrix} \begin{bmatrix} \hat{x} \\ x \\ u_{[0,N]} \\ 1 \end{bmatrix} \geq 0$$

Chapter 8

Conclusions

Developing a combined short- and long-term optimization framework allows to analyze the annually optimal Hybrid Ground Coupled Heat Pump (HyGCHP) system operation with integrated short-term optimal distribution of heating and cooling loads among the heating and cooling devices. On the long term cooling dominated loads result in annual net heat rejection to the ground. It is optimal to supply cold by using the passive cooling device working at base load as long as the upper bound on the Borehole Heat Exchanger (BHE) outlet fluid temperature is not reached. Remaining cooling loads are covered by an active chiller, which is optimally used at peak load in case passive cooling is insufficient.

The long-term optimal operation profile of the investigated HyGCHP system case is reproducible by a short-term Model Predictive Control (MPC) strategy with a one week prediction horizon. This time scale of the short-term strategy corresponds to the slowest system dynamics at building level. Therefore, the HyGCHP system can be considered long-term optimal when the entire time constant range at building level is covered by the short-term MPC strategy.

Modification of the developed short-and-long-term optimization framework allows analysis of the potential for Seasonal Underground Thermal Energy Storage (SUTES) for the investigated HyGCHP system. Basic SUTES, which results from short-term system performance optimization, represents a system performance characteristic naturally caused by combining heat extraction from the ground during winter and heat injection to the ground during summer. Additional SUTES, which could only result from long-term system performance optimization, is concluded far from economically beneficial for the case of a single BHE because of substantial thermal dissipation in the surrounding ground.

The developed iterative system identification method is used for the creation of low order models of borefields comprising thermally interacting BHEs. For a 3×3 open rectangular borefield configuration additional SUTES is evaluated closer to economically beneficial compared to the case of a single BHE. For low enough but still realistic ground thermal conductivities such borefield being part of the investigated HyGCHP system enables additional SUTES to be an economically beneficial control strategy. In cases of higher ground thermal conductivities, when cooling dominated loads covered by passive cooling would lead to hitting the upper bound on the BHE outlet fluid temperature it is cheaper to use the air coupled active chiller for the remaining loads, instead of using additional SUTES in the ground.

An existing method for robustness analysis is studied in depth in order to be used for the case of the considered HyGCHP systems with MPC. Method exploration revealed lack of explanation of key details. Using the clarifications and corrections provided in this dissertation leads to successful and smooth implementation of the method.

Application of the robustness analysis method to the investigated HyGCHP system with MPC shows that case specific characteristics require additional formulations and adaptations of the original method. For the purpose of the presented research the existing robustness analysis method is applicable by including extended theoretical formulations and an adapted form of the optimization problem for MPC of the HyGCHP system.

Implementation of the extended method shows that the Linear Matrix Inequality (LMI) based complex robustness analysis method is error prone. By consistent implementation supported by thorough understanding of the underlying concepts the extended method is useful for computing the maximum allowed state estimation uncertainty for guaranteed system robustness.

Performed HyGCHP system simulation for the case of MPC with state estimation uncertainty validates the robustness analysis results. The robustness analysis method gives a reliable guarantee for the system robustness up to the computed maximum allowed state estimation uncertainty.

Future research

The developed methodology is directly applicable to other cases of HyGCHP systems. Results can be easily generated for cases characterized by e.g. other borefield drilling patterns besides the investigated case of a 3×3 open rectangular borefield (Chapter 6) as long as a suitable borefield model is provided. In the presented research the limitation to the particular borefield configuration investigated is imposed by the characteristics of the borefield emulator used. The underlying method for short-term solution of the borehole wall temperature is validated for the case of borefields of non-dense patterns (like open rectangular). The transition from a single BHE towards an open rectangular 3×3 borefield moved the potential for SUTES closer to economically beneficial and for particular ground thermal conductivity even reached the conditions for economically beneficial additional SUTES. For that reason, it is expected that this trend will continue for denser borefields and there it is relevant to know what are the borefield configurations to enable the benefit from additional SUTES for all ground thermal conductivities met in practice. Also, since additional SUTES is an annually optimal control strategy, it is still an open question how such control strategy can be efficiently implemented in the time frames of short-term controllers.

Other relevant future contributions in three directions are motivated from the presented research on robustness analysis. The theoretical reasoning upon constructing the presented extensions to the existing robustness analysis method welcomes a more enhanced proof of validity. The implementation of the method for the case of state estimation uncertainty requires optimization solvers of higher functionality in order to exploit the full potential of the method. Robustness analysis for the case of disturbance prediction uncertainty represents a challenge for implementing within the adopted LMI framework. Details on these suggestions are formulated at the end of Chapter 7.

Appendix A

Borefield system identification results

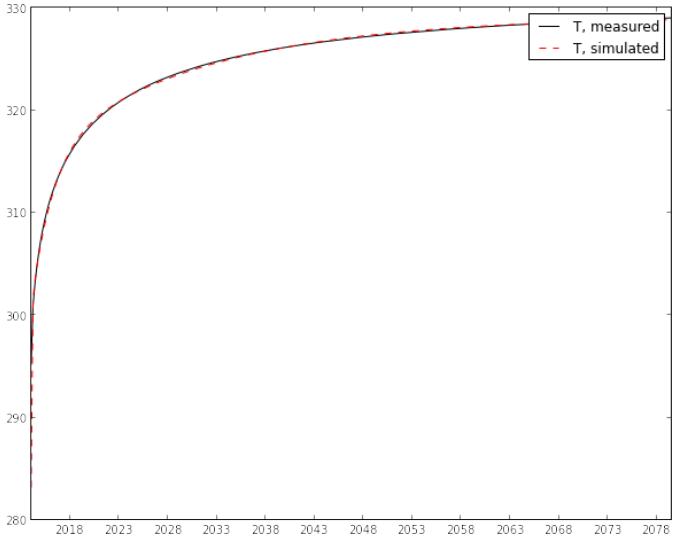

Figure A.1: Step 1 from algorithm in Section 6.4—System identification on the long-term

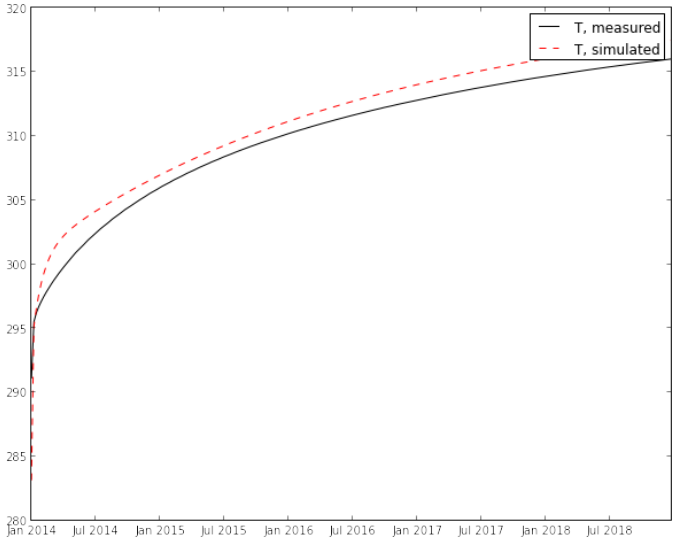

Figure A.2: Step 1 from algorithm in Section 6.4—Model validation on the mid-term

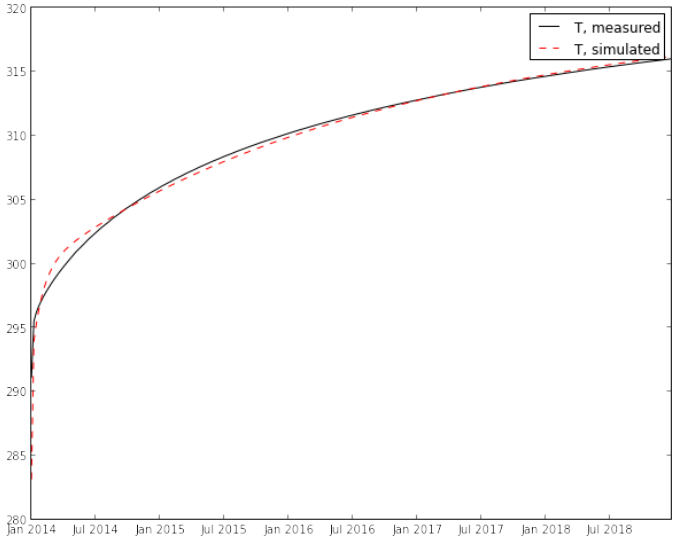

Figure A.3: Step 2 from algorithm in Section 6.4—System identification on the mid-term

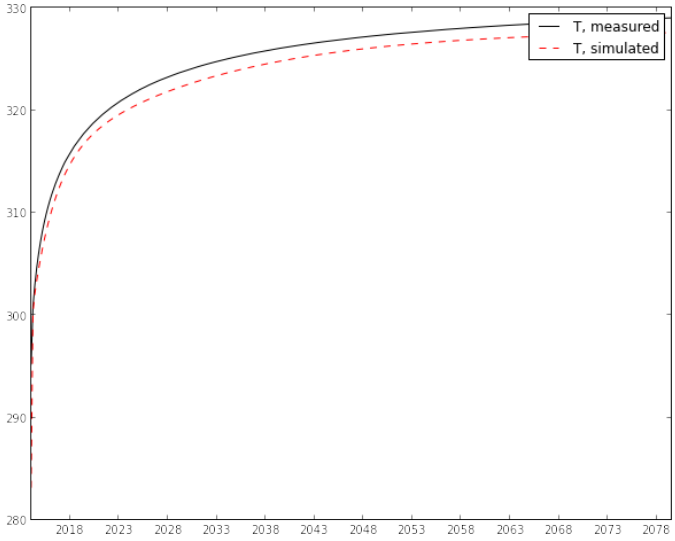

Figure A.4: Step 2 from algorithm in Section 6.4—Model validation on the long-term

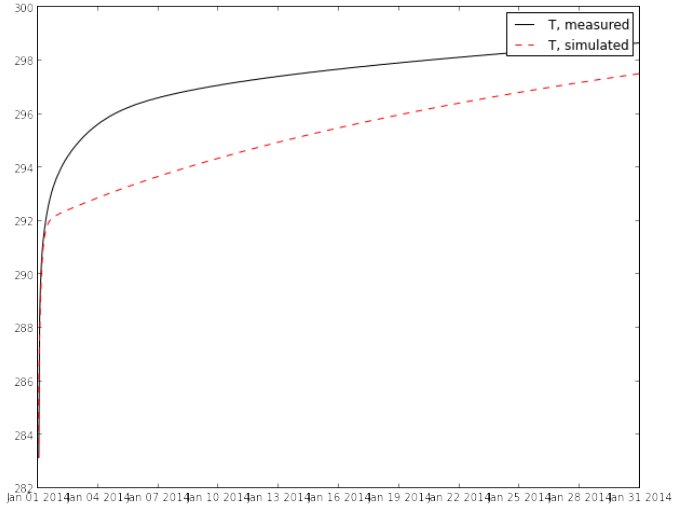

Figure A.5: Step 2 from algorithm in Section 6.4—Model validation on the short-term

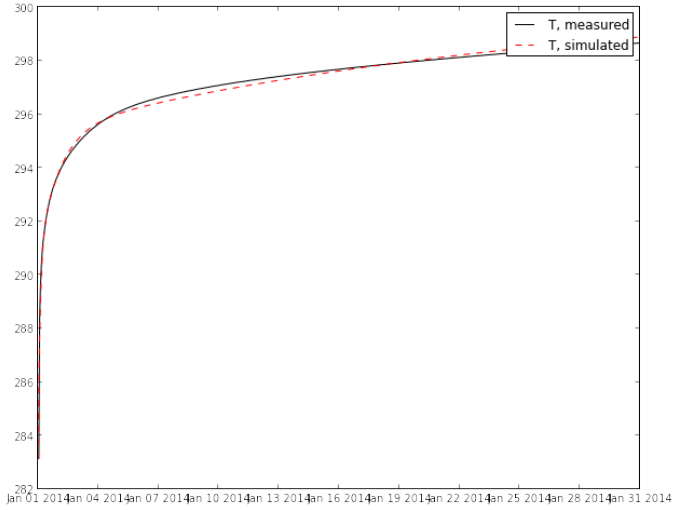

Figure A.6: Step 3 from algorithm in Section 6.4—System identification on the short-term

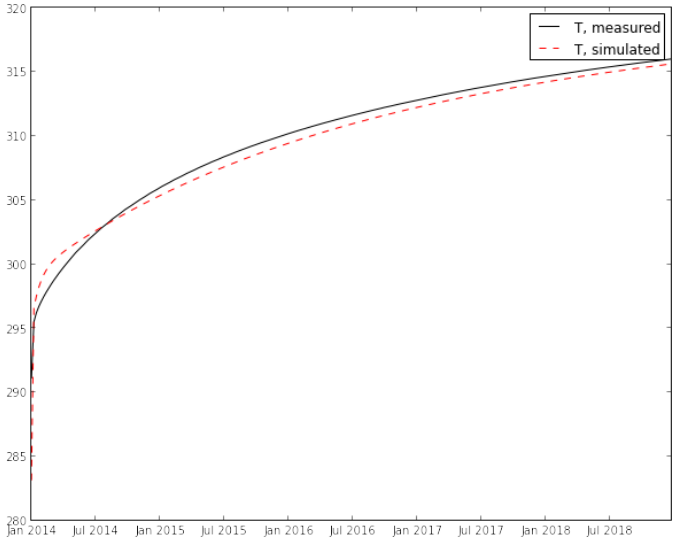

Figure A.7: Step 3 from algorithm in Section 6.4—Model validation on the mid-term

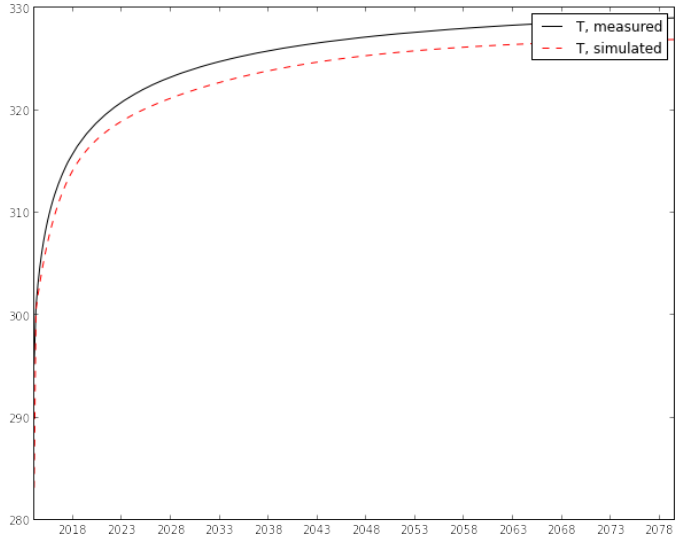

Figure A.8: Step 3 from algorithm in Section 6.4—Model validation on the long-term

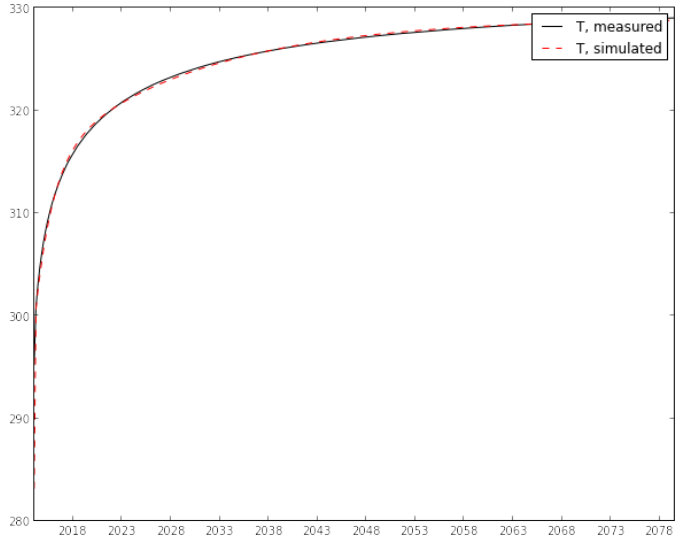

Figure A.9: Step 4 from algorithm in Section 6.4—Repeating system identification on the long-term

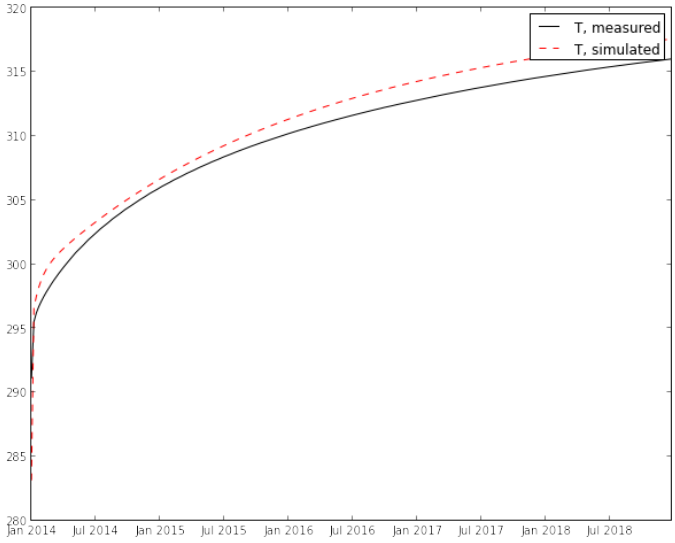

Figure A.10: Step 4 from algorithm in Section 6.4—Model validation on the mid-term

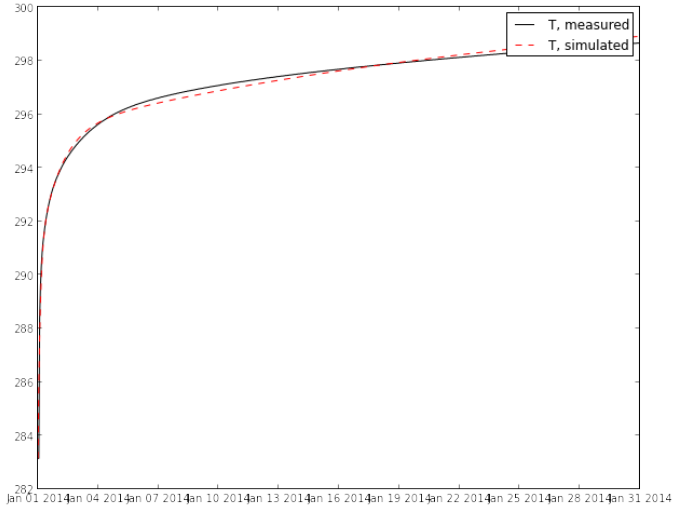

Figure A.11: Step 4 from algorithm in Section 6.4—Model validation on the short-term

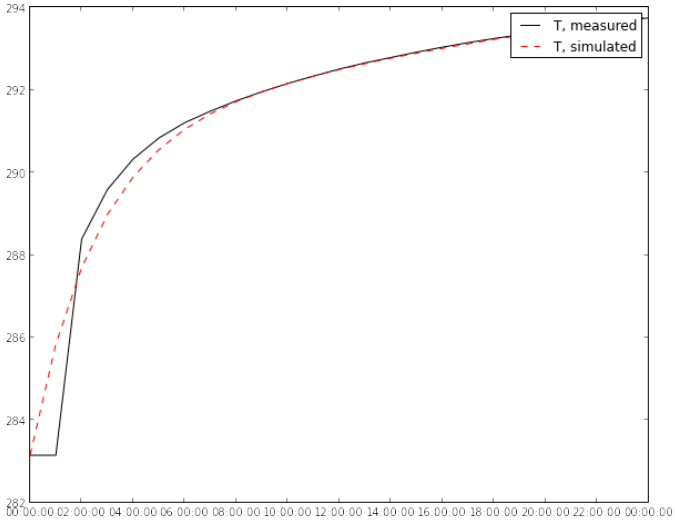

Figure A.12: Step 5 from algorithm in Section 6.4—Model validation on the hourly-term

Bibliography

Åkesson, J. (2008). Optimica—An extension of Modelica supporting dynamic optimization. In *Proceedings of the 6th International Modelica Conference*. Cited on page 80.

Åkesson, J., Årzén, K.-E., Gäfvert, M., Bergdahl, T., and Tummescheit, H. (2010). Modeling and optimization with Optimica and JModelica.org—Languages and tools for solving large-scale dynamic optimization problems. *Computers & Chemical Engineering*, 34(11):1737–1749. Cited on page 80.

Al-Gherwi, W., Budman, H., and Elkamel, A. (2011). Robust distributed model predictive control: A review and recent developments. *The Canadian Journal of Chemical Engineering*, 89(5):1176–1190. Cited on page 32.

Alishaev, M., Abdulagatov, I., and Abdulagatova, Z. (2012). Effective thermal conductivity of fluid-saturated rocks: Experiment and modeling. *Engineering Geology*, 135–136:24–39. Cited on page 79.

Andersson, J., Åkesson, J., and Diehl, M. (2012). CasADi: A symbolic package for automatic differentiation and optimal control. In Forth, S., Hovland, P., Phipps, E., Utke, J., and Walther, A., editors, *Recent Advances in Algorithmic Differentiation*, Lecture Notes in Computational Science and Engineering, pages 297–307. Springer, Berlin, Heidelberg. Cited on page 81.

Atam, E. and Helsen, L. (2015). A convex approach to a class of non-convex building HVAC control problems: Illustration by two case studies. *Energy and Buildings*, 93:269–281. Cited on page 26.

Atam, E. and Helsen, L. (2016). Ground-coupled heat pumps: Part 1 - literature review and research challenges in modeling and optimal control. *Renewable and Sustainable Energy Reviews*, 54:1653–1667. Cited on page 23.

Atam, E., Patteeuw, D., Antonov, S., and Helsen, L. (2015). Optimal control approaches for analysis of energy use minimization of hybrid ground-coupled

heat pump systems. *IEEE Transactions on Control Systems Technology*, pages – 16pp. *In press*. Cited on page 27.

Bauer, D., Heidemann, W., Müller-Steinhagen, H., and Diersch, H.-J. G. (2011). Thermal resistance and capacity models for borehole heat exchangers. *International Journal of Energy Research*, 35(4):312–320. Cited on page 78.

Bayer, P., Saner, D., Bolay, S., Rybach, L., and Blum, P. (2012). Greenhouse gas emission savings of ground source heat pump systems in europe: A review. *Renewable and Sustainable Energy Reviews*, 16(2):1256–1267. Cited on page 21.

Beier, R. A., Smith, M. D., and Spitler, J. D. (2011). Reference data sets for vertical borehole ground heat exchanger models and thermal response test analysis. *Geothermics*, 40(1):79–85. Cited on page 79.

Bemporad, A. and Morari, M. (1999). Robust model predictive control: A survey. In Garulli, A. and Tesi, A., editors, *Robustness in identification and control*, volume 245 of *Lecture Notes in Control and Information Sciences*, pages 207–226. Springer, London. Cited on page 32.

Bertagnolio, S., Bernier, M., and Kummert, M. (2012). Comparing vertical ground heat exchanger models. *Journal of Building Performance Simulation*, 5(6):369–383. Cited on page 79.

Bi, Y., Guo, T., Zhang, L., and Chen, L. (2004). Solar and ground source heat-pump system. *Applied Energy*, 78(2):231–245. Cited on page 23.

Bostrom, N. (2006). Welcome to a world of exponential change. In Miller, P. and Wilsdon, J., editors, *Better Humans?: The Politics of Human Enhancement and Life Extension*, pages 40–50. London: Demos. Cited on page 1.

CEN (2007). *EN15251:2007, Indoor environmental input parameters for design and assessment of energy performance of buildings addressing indoor air quality, thermal environment, lighting and acoustics*. Comité Européen de Normalisation, Brussels, Belgium. Cited on pages xxxi, 45, 46, 58, and 123.

Chiasson, A. D. and Yavuzturk, C. (2003). Assessment of the viability of hybrid geothermal heat pump systems with solar thermal collectors. *ASHRAE Transactions*, 109:487–500. Cited on page 23.

CORALLab (2003). *SeDuMi*. Department of Industrial and Systems Engineering at Lehigh University, Bethlehem, Pennsylvania. Cited on page 120.

Cullin, J. R. and Spitler, J. D. (2010). Comparison of simulation-based design procedures for hybrid ground source heat pump systems. In *Proceedings of*

the 8th International Conference on System Simulation in Buildings, pages – 15pp. Cited on page 24.

De Coninck, R., Magnusson, F., Åkesson, J., and Helsen, L. (2016). Toolbox for development and validation of grey-box building models for forecasting and control. *Journal of Building Performance Simulation*, 9(3):288–303. Cited on pages 77, 80, and 81.

De Ridder, F., Diehl, M., Mulder, G., Desmedt, J., and Bael, J. V. (2011). An optimal control algorithm for borehole thermal energy storage systems. *Energy and Buildings*, 43(10):2918–2925. Cited on pages 28 and 55.

Derinkuyu, K. and Pınar, M. Ç. (2006). On the S-procedure and some variants. *Mathematical Methods of Operations Research*, 64(1):55–77. Cited on page 115.

Di Sipio, E., Chiesa, S., Destro, E., Galgaro, A., Giaretta, A., Gola, G., and Manzella, A. (2013). Rock thermal conductivity as key parameter for geothermal numerical models. *Energy Procedia*, 40:87–94. Cited on page 79.

Doyle, J. C. (1978). Guaranteed margins for LQG regulators. *IEEE Transactions on Automatic Control*, AC-23(4):756–757. Cited on page 31.

Elmqvist, H., Mattsson, S. E., and Otter, M. (1998). Modelica: The new object-oriented modeling language. In *Proceedings of the 12th European Simulation Multiconference, Manchester, UK*. Cited on page 78.

Eskilson, P. (1987). *Thermal analysis of heat extraction boreholes*. PhD thesis, University of Lund, Grahns Boktryckeri AB, Lund, Sweden. Cited on pages 40, 78, and 79.

EU (2009). Directive 2009/28/EC of the European parliament and of the Council of 23 April 2009 on the promotion of the use of energy from renewable sources and amending and subsequently repealing Directives 2001/77/EC and 2003/30/EC. *Official Journal of the European Union*, L(140):16–62. Cited on page 2.

EU (2012). Directive 2012/27/EU of the European parliament and of the Council of 25 October 2012 on energy efficiency, amending Directives 2009/125/EC and 2010/30/EU and repealing Directives 2004/8/EC and 2006/32/EC. *Official Journal of the European Union*, L(315):1–56. Cited on page 2.

Franke, R. (1998). Modeling and optimal design of a central solar heating plant with heat storage in the ground using modelica. In *Proceedings of the Eurosim'98 Simulation Congress*, pages 199–204. Cited on pages 27 and 55.

Gang, W. and Wang, J. (2013). Predictive ANN models of ground heat exchanger for the control of hybrid ground source heat pump systems. *Applied Energy*, 112:1146–1153. Cited on page 25.

Gang, W., Wang, J., and Wang, S. (2014). Performance analysis of hybrid ground source heat pump systems based on ANN predictive control. *Applied Energy*, 136:1138–1144. Cited on page 25.

GBPN (2013). Investing in energy efficiency in Europe's buildings. A review from the construction and real estate sectors. *The Economist Intelligence Unit*, pages 1–17. Cited on page 2.

Genceli, H. and Nikolaou, M. (1993). Robust stability analysis of constrained l_1-norm model predictive control. *AIChE Journal*, 39(12):1954–1965. Cited on page 33.

Gong, X., Wei, L., and Feng, W. (2012). Theoretical investigation of operating control strategy of a new solar-water-assisted ground-source heat pump. In *Advances in Civil Engineering and Building Materials (2013) – Selected, peer reviewed papers from 2012 2^{nd} International Conference on Civil Engineering and Building Materials (CEBM 2012), 17–18 November, Hong Kong*, pages 383–389. CRC Press. Cited on page 25.

Hackel, S. and Pertzborn, A. (2011). Effective design and operation of hybrid ground-source heat pumps: Three case studies. *Energy and Buildings*, 43(12):3497–3504. Cited on page 24.

Hamdhan, I. N. and Clarke, B. G. (2010). Determination of thermal conductivity of coarse and fine sand soils. In *Proceedings of the World Geothermal Congress*, pages – 7pp. Cited on page 79.

Han, Z., Zheng, M., Kong, F., Wang, F., Li, Z., and Bai, T. (2008). Numerical simulation of solar assisted ground-source heat pump heating system with latent heat energy storage in severely cold area. *Applied Thermal Engineering*, 28(11–12):1427–1436. Cited on page 24.

Hargraves, C. R. and Paris, S. W. (1987). Direct trajectory optimization using nonlinear programming and collocation. *Journal of Guidance, Control, and Dynamics*, 10(4):338–342. Cited on page 81.

Heath, W. P. and Wills, A. G. (2005). The inherent robustness of constrained linear model predictive control. In *Proceedings of 16^{th} IFAC World Congress*, page 955. Cited on pages 31 and 33.

Hellström, G. (1991). *Ground heat storage: thermal analyses of duct storage systems*. PhD thesis, Lund University, Lund, Sweden. Cited on page 78.

Helsen, L. (2016). Geothermally activated building structures. In Rees, S., editor, *Advances in Ground-Source Heat Pump Systems*. Elsevier. Expected release 1 June, 2016. Cited on page 4.

Hilliard, T., Kavgic, M., and Swan, L. (2015). Model predictive control for commercial buildings: trends and opportunities. *Advances in Building Energy Research*, pages – 19pp. Published online. Cited on pages 2 and 22.

HSL (2013). *A collection of Fortran codes for large-scale scientific computation*. http://www.hsl.rl.ac.uk. Cited on page 81.

Hu, B., Li, Y., Mu, B., Wang, S., Seem, J. E., and Cao, F. (2016). Extremum seeking control for efficient operation of hybrid ground source heat pump system. *Renewable Energy*, 86:332–346. Cited on page 26.

IBM (2012). *IBM ILOG CPLEX Optimization Studio, Version 12.5*. IBM Corporation, Armonk, NY, USA. Cited on pages 12, 50, and 122.

IEA (2015). Key world energy statistics. *International Energy Agency*, pages 1–81. Cited on page 2.

Jalali, A. A. and Nadimi, V. (2006). A survey on robust model predictive control from 1999-2006. In *Proceedings of CIMCA-IAWTIC'06, International Conference on Computational Intelligence for Modelling, Control and Automation, International Conference on Intelligent Agents, Web Technologies and Internet Commerce*, page 207. IEEE Computer Society. Cited on page 32.

Javed, S. (2012). *Thermal modelling and evaluation of borehole heat transfer*. PhD thesis, Chalmers University of Technology (Technical report D – Department of Building Technology, Building Services Engineering, Chalmers University of Technology, no: D2012:01 Doktorsavhandlingar vid Chalmers tekniska högskola. Ny serie, no: 3304), Göteborg, Sweden. Cited on pages 77 and 78.

Kavanaugh, S. P. (1998). A design method for hybrid ground-source heat pumps. *ASHRAE Transactions*, 104:691–698. Cited on page 23.

Koohi-Fayegh, S. and Rosen, M. A. (2013). A review of the modelling of thermally interacting multiple boreholes. *Sustainability*, 5(6):2519–2536. Cited on page 29.

KU Leuven and 3E (2014). OpenIDEAS source code repository. *https://github.com/open-ideas*. Licensed under the Modelica License Version 2, https://www.modelica.org/licenses/ModelicaLicense2. Cited on page 80.

Kurzweil, R. (2004). The law of accelerating returns. In Teuscher, C., editor, *Alan Turing: Life and Legacy of a Great Thinker*, pages 381–416. Springer Berlin Heidelberg. Cited on page 1.

Löfberg, J. (2004). YALMIP: A toolbox for modeling and optimization in MATLAB. In *Proceedings of the 2004 IEEE International Symposium on Computer Aided Control Systems Design*, pages 284–289. Cited on pages 50, 120, and 122.

Maasoumy, M., Razmara, M., Shahbakhti, M., and Vincentelli, A. S. (2014). Handling model uncertainty in model predictive control for energy efficient buildings. *Energy and Buildings*, 77:377–392. Cited on page 33.

Maciejowski, J. (2002). *Predictive Control: With Constraints*. Pearson Education. Prentice Hall. Cited on page 31.

Man, Y., Yang, H., and Fang, Z. (2008). Study on hybrid ground-coupled heat pump systems. *Energy and Buildings*, 40(11):2028–2036. Cited on page 23.

Man, Y., Yang, H., and Wang, J. (2010). Study on hybrid ground-coupled heat pump system for air-conditioning in hot-weather areas like Hong Kong. *Applied Energy*, 87(9):2826–2833. Cited on page 24.

MathWorks (2010). *MATLAB, version 7.10.0 (R2010a)*. The MathWorks Inc., Natick, Massachusetts. Cited on pages 50, 120, and 122.

Mayne, D., Rawlings, J., Rao, C., and Scokaert, P. (2000). Constrained model predictive control: Stability and optimality. *Automatica*, 36(6):789–814. Cited on page 32.

Megretski, A. (1993). Necessary and sufficient conditions of stability: a multiloop generalization of the circle criterion. *IEEE Transactions on Automatic Control*, 38(5):753–756. Cited on page 33.

Mokhtar, M., Stables, M., Liu, X., and Howe, J. (2013). Intelligent multi-agent system for building heat distribution control with combined gas boilers and ground source heat pump. *Energy and Buildings*, 62:615–626. Cited on page 26.

Nordell, B. (1994). *Borehole heat store design optimization*. PhD thesis, Luleå University of Technology, Luleå, Sweden. Cited on page 30.

Olesen, B. and Kazanci, O. (2015). State of the art of HVAC technology in Europe and America. In *Proceedings of the World Engineering Conference and Convention 2015 (WECC2015)*, pages – 6pp. Cited on page 22.

Ozgener, O. and Hepbasli, A. (2005). Performance analysis of a solar-assisted ground-source heat pump system for greenhouse heating: an experimental study. *Building and Environment*, 40(8):1040–1050. Cited on page 24.

Pahud, D. and Hellström, G. (1996). The new duct ground heat model for trnsys. In *Proceedings of the Eurotherm Seminar 49, Physical Models for Thermal Energy Stores*, pages 127–136. Université de Genève. Cited on pages 29 and 41.

Pannocchia, G., Rawlings, J. B., and Wright, S. J. (2011). Conditions under which suboptimal nonlinear MPC is inherently robust. *Systems & Control Letters*, 60(9):747–755. Cited on page 33.

Peeters, L. (2009). *Water-Based Heating/Cooling in Residential Buildings: Towards Optimal Heat Emission/Absorption Elements*. PhD thesis, KU Leuven – University of Leuven, Department of Mechanical Engineering, Leuven, Belgium. D'haeseleer, W. (sup.). Cited on page 54.

Peeters, L., der Veken, J. V., Hens, H., Helsen, L., and D'haeseleer, W. (2008). Control of heating systems in residential buildings: Current practice. *Energy and Buildings*, 40(8):1446–1455. Cited on page 21.

Picard, D. and Helsen, L. (2014a). Advanced hybrid model for borefield heat exchanger performance evaluation, an implementation in Modélica. In *Proceedings of the 10th International Modélica Conference*, pages 857–866. Cited on pages 29, 31, 76, 77, 78, and 79.

Picard, D. and Helsen, L. (2014b). A new hybrid model for borefield heat exchangers performance evaluation. In *Proceedings of the 2014 ASHRAE Annual Conference*, pages – 8pp. Cited on pages 29, 31, 76, 77, 78, and 79.

Primbs, J. A. and Nevistić, V. (2000). A framework for robustness analysis of constrained finite receding horizon control. *IEEE Transactions on Automatic Control*, 45(10):1828–1838. Cited on pages 34, 35, 96, 97, 98, 99, 101, 102, 104, 107, 108, 113, 115, 128, and 130.

Rawlings, J. and Mayne, D. (2009). *Model Predictive Control: Theory and Design*. Madison, Wis. Nob Hill Pub. cop. Cited on pages 14, 16, 17, and 104.

Reuss, M., Beck, M., and Müller, J. (1997). Design of a seasonal thermal energy storage in the ground. *Solar Energy*, 59(4–6):247–257. Selected Proceedings of the ISES 1995 Solar World Congress. Part IV. Cited on pages 30, 31, 71, and 72.

Sagia, Z. and Rakopoulos, C. (2012). New control strategy for a hybrid ground source heat pump system coupled to a closed circuit cooling tower. *Journal of Applied Mechanical Engineering*, 1(2):8pp. Cited on page 24.

Sanner, B. (2001). Shallow geothermal energy. *Geo-Heat Center Bulletin*, 22(2):19–25. Cited on page 44.

Santos, L. O. and Biegler, L. T. (1999). A tool to analyze robust stability for model predictive controllers. *Journal of Process Control*, 9(3):233–246. Cited on page 33.

Sarbu, I. and Sebarchievici, C. (2014). General review of ground-source heat pump systems for heating and cooling of buildings. *Energy and Buildings*, 70:441–454. Cited on page 23.

Scokaert, P., Mayne, D., and Rawlings, J. (1999). Suboptimal model predictive control (feasibility implies stability). *IEEE Transactions on Automatic Control*, 44(3):648–654. Cited on page 33.

Scokaert, P., Rawlings, J., and Meadows, E. (1997). Discrete-time stability with perturbations: application to model predictive control. *Automatica*, 33(3):463–470. Cited on page 33.

Sourbron, M. (2012). *Dynamic thermal behaviour of buildings with Concrete Core Activation*. PhD thesis, KU Leuven – University of Leuven, Department of Mechanical Engineering, Leuven, Belgium. Helsen, L. (sup.), Baelmans, M. (co-sup.). Cited on pages xxxi, 46, 48, and 49.

Sourbron, M., Antonov, S., and Helsen, L. (2013a). Potential and parameter sensitivity of model based predictive control for concrete core activation and air handling unit. In *Proceedings of BS2013: 13th Conference of International Building Performance Simulation Association (online)*, pages 2474–2480. Cited on pages 31 and 96.

Sourbron, M. and Helsen, L. (2014). Sensitivity analysis of feedback control for concrete core activation and impact on installed thermal production power. *Journal of Building Performance Simulation*, 7(5):309–325. Cited on page 54.

Sourbron, M., Verhelst, C., and Helsen, L. (2013b). Building models for model predictive control of office buildings with concrete core activation. *Journal of Building Performance Simulation*, 6(3):175–198. Cited on page 39.

Spitler, J. D. (2000). Glhepro—a design tool for commercial building ground loop heat exchangers. In *Proceedings of the Fourth International Heat Pumps in Cold Climates Conference*. Cited on page 44.

Stojanović, B. and Akander, J. (2010). Build-up and long-term performance test of a full-scale solar-assisted heat pump system for residential heating in nordic climatic conditions. *Applied Thermal Engineering*, 30(2–3):188–195. Cited on page 24.

TESS (2006). *TRNSYS, version 16.01*. Thermal Energy System Specialists, LLC, Madison, WI, USA. Cited on pages 29, 41, 48, 54, and 79.

van Rossum, G. (1995). Python tutorial. *Technical Report CS-R9526*. Centrum voor Wiskunde en Informatica (CWI), Amsterdam, The Netherlands. Cited on page 80.

Vána, Z., Cigler, J., Široký, J., Žáceková, E., and Ferkl, L. (2014). Model-based energy efficient control applied to an office building. *Journal of Process Control*, 24(6):790–797. Energy Efficient Buildings Special Issue. Cited on page 40.

Vanhoudt, D., De Ridder, F., Desmedt, J., and Van Bael, J. (2010). Controller for optimal cost operation of a borehole thermal energy storage system. In *Proceedings of the Clima 2010, REHVA World Congress Conference*. Cited on page 27.

Verhelst, C. (2012). *Model Predictive Control of Ground Coupled Heat Pump Systems for Office Buildings*. PhD thesis, KU Leuven – University of Leuven, Department of Mechanical Engineering, Leuven, Belgium. Helsen, L. (sup.), D'haeseleer, W. (sup.). Cited on pages 7, 28, 31, 39, 40, and 42.

Verhelst, C. and Helsen, L. (2011). Low-order state space models for borehole heat exchangers. *HVAC&R Research*, 17(6):928–947. Cited on pages 29, 40, 41, 76, and 83.

Wächter, A. and Biegler, T. L. (2006). On the implementation of an interior-point filter line-search algorithm for large-scale nonlinear programming. *Mathematical Programming*, 106(1):25–57. Cited on page 81.

Wang, L., Zhang, J., Min, H., and Xu, L. (2015). Optimal control of cooling tower in hybrid ground-source heat pump system for hotel buildings. In *Proceedings of the 5th International Conference on Advanced Design and Manufacturing Engineering (ICADME 2015)*, pages 1749–1756. Atlantis Press. Cited on page 25.

Wetter, M. (2001). GenOpt® – A generic optimization program. In *Proceedings of the 7th International IBPSA Conference*, pages 601–608. Cited on page 24.

Wetter, M., Zuo, W., Nouidui, T. S., and Pang, X. (2014). Modelica buildings library. *Journal of Building Performance Simulation*, 7(4):253–270. Cited on pages 78 and 79.

Xu, X., Wang, S., and Huang, G. (2010). Robust MPC for temperature control of air-conditioning systems concerning on constraints and multitype uncertainties. *Building Services Engineering Research and Technology*, 31(1):39–55. Cited on page 33.

Yakubovich, V. A. (1971). S-procedure in nonlinear control theory. *Vestnik Leningrad University*, 1:62–77. (English translation in *Vestnik Leningrad University*, 4:73–93, 1977). Cited on page 115.

Yang, R. and Wang, L. (2012). Efficient control of a solar assisted ground-source heat pump system based on evaluation of building thermal load demand. In *Proceedings of the North American Power Symposium (NAPS), 2012*, pages – 6pp. Cited on page 25.

Yavuzturk, C. and Spitler, J. D. (2000). Comparative study of operating and control strategies for hybrid ground-source heat pump systems using a short time step simulation model. *ASHRAE Transactions*, 106:192–209. Cited on page 24.

Zafiriou, E. (1990). Robust model predictive control of processes with hard constraints. *Computers & Chemical Engineering*, 14(4/5):359–371. Cited on page 32.

Zhang, Q., Lv, N., Chen, S., Shi, H., and Chen, Z. (2015). Study on operating and control strategies for hybrid ground source heat pump system. *Procedia Engineering*, 121:1894–1901. Cited on page 25.

Curriculum

Stefan Antonov

Born 21 June, 1985 in Sofia, Bulgaria

stefan.antonov@gmail.com

Education

2010–2016	PhD program KU Leuven, Mechanical Engineering Department Supervisor: *Prof. dr. ir. Lieve Helsen*
2008–2010	Master of Engineering Technical University of Sofia, Bulgaria Subject: *Automation, Information and Control Engineering* Thesis: *Investigation of an Inertial Navigation System*
2008 May–July	ERASMUS program (Bachelor thesis work) Linköping University, Sweden Thesis: *Modeling and Implementation of a Signal Processing System (Implementation of a GPS signal search acquisition algorithm)*
2004–2008	Bachelor of Engineering Technical University of Sofia, Bulgaria Subject: *Automation, Information and Control Engineering*
1999–2004	National High School of Mathematics and Science, Sofia, Bulgaria Extensive studies in physics and mathematics

Experience

2009–2010	R&D Engineer Visteon Corporation, Sofia, Bulgaria (Company site is former property of Johnson Controls) Design, implementation and execution of model-based tests for automotive software
2007 Aug–Nov	Automation Engineer LogiSoft, Ltd, Sofia, Bulgaria Constructing industrial automation systems and preparing electrical documentation

Hobbies and sports

Dancing,
Skiing, ice skating, jogging, horseback riding,
Adventure motorcycling, rally driving, carting,
Kayaking, rafting, diving,
Yachting,
Board games

List of publications

Articles in International Journals

Antonov, S. and Helsen, L. (2016). Robustness analysis of a hybrid ground coupled heat pump system with model predictive control. *Under review with minor changes*.

Atam, E., Patteeuw, D., **Antonov, S.** and Helsen, L. (2015). Optimal control approaches for analysis of energy use minimization of hybrid ground-coupled heat pump systems. *IEEE Transactions on Control Systems Technology*, 24(2):525–540.

Antonov, S., Verhelst, C. and Helsen, L. (2014). Should the optimization horizon in optimal control of ground coupled heat pump systems cover the inter-seasonal time scale?. *ASHRAE Transactions*, 120(2):346–356.

Articles in International Conference Proceedings

Sourbron, M., **Antonov, S.** and Helsen, L. (2013). Potential and parameter sensitivity of model based predictive control for concrete core activation and air handling unit. In *Proceedings of the 13th International Conference of the International Building Performance Simulation Association*, Chambéry, France, 25–28 August, 2013.

Antonov, S., Verhelst, C. and Helsen, L. (2013). Optimal operation of ground coupled heat pump systems: Should we take the seasonal time scale into account?. In *Proceedings of Clima 2013, 11th REHVA World Congress & 8th International Conference on IAQVEC*, Prague, Czech Republic, 16–19 June, 2013.

Antonov, S., Verhelst, C. and Helsen, L. (2012). Control of ground coupled heat pump systems in offices to optimally exploit ground thermal storage on the long term. In *Proceedings of Innostock 2012*, Lleida, Spain, 16–18 May, 2012.

"Everything will be all right in the end.
If it's not all right, it is not yet the end."
Deborah Moggach

FACULTY OF ENGINEERING SCIENCE
DEPARTMENT OF MECHANICAL ENGINEERING
APPLIED MECHANICS AND ENERGY CONVERSION
Celestijnenlaan 300A box 2421
B-3001 Leuven